NOTICE

The quality of this microform is heavily dependent upon the quality of the original thesis submitted for microfilming. Every effort has been made to ensure the highest quality of reproduction possible.

If pages are missing, contact the university which granted the degree.

Some pages may have indistinct print especially if the original pages were typed with a poor typewriter ribbon or if the university sent us an inferior photocopy.

Reproduction in full or in part of this microform is governed by the Canadian Copyright Act, R.S.C. 1970, c. C-30, and subsequent amendments.

AVIS

La qualité de cette microforme dépend grandement de la qualité de la thèse soumise au microfilmage Nous avons tout fait pour assurer une qualité supérieure de reproduction.

S'il manque des pages, veuillez communiquer avec l'université qui a conféré le grade.

La qualité d'impression de certaines pages peut laisser à désirer, surtout si les pages originales ont été dactylographiées à l'aide d'un ruban usé ou si l'université nous a fait parvenir une photocopie de qualité inférieure.

La reproduction, même partielle, de cette microforme est soumise à la Loi canadienne sur le droit d'auteur, SRC 1970, c. C-30, et ses amendements subséquents.

Canada

Mapping the Substrate for Brain Stimulation Reward By Means of Current-Number Trade-Off Functions

Margaret L. Forgie

A Thesis

in

The Department

of

Psychology

Presented in Partial Fulfillment of the Requirements
for the Degree of Master of Arts at
Concordia University
Montréal, Québec, Canada

September 1989

ISBN 0-315-51347-0

ABSTRACT

Mapping the Substrate for Brain Stimulation Reward By Means of Current-Number Trade-Off Functions

Margaret L. Forgie

The most powerful methods currently employed for anatomical mapping of the neural substrate subserving brain stimulation reward assess the effectiveness of the stimulation at each site by taking a single estimate of either the frequency or current required to support a criterion level of performance. The present experiment was undertaken to evaluate and extend these methods.

Male rats were implanted with a monopolar moveable electrode aimed at the ventral tegmental area. At each site, rate-intensity functions were determined at each of several different pulse frequencies, at two different values of pulse duration. The current required to support 50% of maximum response rate was calculated by interpolation from these functions, and trade-off curves were then derived by plotting the required current against the frequency at which it was determined.

The results of this experiment make two main contributions. First, trade-off data collected with the aid of moveable electrodes place tighter constraints upon the possible anatomical configuration of the reward

substrate within the region examined than do single estimates of either the required current or frequency. Second, it was demonstrated that anatomical conclusions that are based on estimates of substrate sensitivity obtained with fixed, small stimulation fields cannot always be generalized to the results that are obtained with the larger stimulation fields used in many self-stimulation studies.

Acknowledgements

I would like to thank my thesis supervisor, Peter Shizgal, for the support he has given me during this project. Through patience and well-chosen words of encouragement he has managed to help me understand even the most complex of issues involved. His enthusiasm for the field and for this project has made the more frustrating aspects of the work much easier to bear.

I would also like to thank Pierre-Paul Rompré for his advice at all stages of the project, especially in sorting out the histology, and for allowing me to use his data for comparative purposes. His willingness to lend a hand whenever asked has contributed greatly to this thesis.

I thank Dwayne Schindler for writing most of the data analysis programs I used and who taught me the ins and outs of programming my own. His help was invaluable and I thank him for never being too busy to help me untangle a particularly thorny problem. I would also like to thank other members of the lab (Sandra Boye, Bev Murray, Barry Robinson, and Meagan Smith) who made it such an enjoyable place to work over the last two years. In particular, my gratitude goes to Bev for her patience and good-humour in teaching me the techniques I needed to carry out this project, and to Sandra for always answering my seemingly endless stream of questions. I would also like to thank

Bev and Sandra for their help and advice on putting this thesis together, for keeping me calm, and for always knowing when it was time for a break.

Most of all I would like to thank Dic for keeping me sane during this project, for knowing when I needed his support, and for believing that I could accomplish the task even when I didn't. I thank him for putting up with the long hours and the endless Saturdays I spent in the lab collecting the data and writing this thesis, and for his help with the editing and production process. Above all, I thank him for the never-ending supply of love and bad jokes.

Finally, I would like to thank the Natural Sciences and Engineering Research Council of Canada and Concordia University for supporting my graduate studies over the last two years.

Dedication

This thesis is dedicated to my parents, William and Joyce Forgie, for their love and support throughout my education. Without their continued encouragement (and the care packages from home), the road to finishing this thesis would have been a much longer one.

Table of Contents

Page

Abstract.....iii

Acknowledgements.....v

Dedication.....vii

Table of Contents.....viii

List of Figures.....xi

List of Appendices.....xv

Introduction.....1

The Psychophysical Approach.....6

A Model of the Substrate for BSR.....10

Topographical Studies of the BSR Substrate.....15

A Psychophysical Approach to Mapping.....22

The Present Experiment.....30

Method.....36

Subjects.....36

Electrodes and Surgery.....36

Apparatus.....39

Manually-controlled apparatus.....39

Computer-controlled apparatus.....41

Procedure.....42

Screening.....42

Training.....43

Stabilization.....44

Page

Mapping.....45
Histology.....51
Data Analysis and Curve-Fitting.....52
Estimating the locus of rise.....53
Estimating I_{min} 61
Depth profiles.....67
Effects of varying pulse duration.....68
Results.....73
Topographical Data.....73
The Minimum Required Current.....104
Evaluation of the Use of Fixed Stimulation Parameters.....120
Effects of Varying the Pulse Duration.....137
Comparing current-number trade-off functions.....137
Effects of varying pulse duration within sites...147
Effects of varying pulse duration between sites..150
Comparing Behavioural Criteria.....160
Discussion.....171
Current-Number Trade-Off Data.....172
Choice of behavioural criterion.....172
Topographical data.....173
Evaluating Fixed Parameter Methodologies.....180
The Minimum Required Current.....195
Practical Considerations of Using the Trade-Off Function.....198
The Effects of Varying Pulse Duration.....199

Page

Conclusions.....204

References.....206

Appendix A.....219

List of Figures

Page

Figure 1 Schematic of deriving a strength-duration function.....9

Figure 2 Example of two different relationships between trade-off functions derived at two stimulation sites.....29

Figure 3 Example of the two- and three-segment functions fit to the rate-intensity curves to estimate locus of rise.....58

Figure 4 Example of estimating the locus of rise from two subsets of the rate-intensity data.....60

Figure 5 Example of the polynomial functions fit to the current-number trade-off curves.....66

Figure 6 Example of calculating the required number or current by interpolation from the trade-off curve.....70

Figure 7 Current-number trade-off data and histological reconstruction for subject PM10 (100 μs pulse duration).....76

Figure 8 Current-number trade-off data and histological reconstruction for subject PM1 (100 μs pulse duration).....79

Figure 9 Current-number trade-off data and histological reconstruction for subject F1 (100 μs pulse duration).....82

Figure 10 Current-number trade-off data and histological reconstruction for subject F3 (100 μs pulse duration).....85

Figure 11 Current-number trade-off data and histological reconstruction for subject R1 (100 μs pulse duration).....88

Page

Figure 12 Current-number trade-off data and histological reconstruction for subject PM8 (100 µs pulse duration).....91

Figure 13 Current-number trade-off data and histological reconstruction for subject PM11 (100 µs pulse duration).....94

Figure 14 Current-number trade-off data and histological reconstruction for subject F4 (100 µs pulse duration).....97

Figure 15 Histological profile for subject PM6.....100

Figure 16 Histological profile for subject PM9.....103

Figure 17 Comparison of depth profiles using I_{min} and $Log_{10}(I)$ at 1.0 for subject PM11.....107

Figure 18 Comparison of depth profiles using I_{min} and $Log_{10}(I)$ at 1.0 for subject F3.....109

Figure 19 Comparison of depth profiles using I_{min} and $Log_{10}(I)$ at 1.0 for subject PM8.....111

Figure 20 Comparison of depth profiles using I_{min} and $Log_{10}(I)$ at 1.0 for subject PM1.....114

Figure 21 Comparison of depth profiles using I_{min} and $Log_{10}(I)$ at 1.0 for subject PM10.....117

Figure 22 Comparison of depth profiles using I_{min} and $Log_{10}(I)$ at 1.0 for subject R1.....119

Figure 23 Comparison of depth profiles using arbitrary values of current intensity or pulse number for subject PM11.....123

Figure 24 Comparison of depth profiles using arbitrary values of current intensity or pulse number for subject F3.....125

Page

Figure 25 Comparison of depth profiles using arbitrary values of current intensity or pulse number for subject PM8.....128

Figure 26 Comparison of depth profiles using arbitrary values of current intensity or pulse number for subject PM1.....131

Figure 27 Comparison of depth profiles using arbitrary values of current intensity or pulse number for subject F1.....134

Figure 28 Comparison of depth profiles using arbitrary values of current intensity or pulse number for subject F4.....136

Figure 29 Comparison of current-number trade-off data collected at two pulse durations (100 μs and 1000 μs) for subject PM10.....140

Figure 30 Comparison of current-number trade-off data collected at two pulse durations (100 μs and 1000 μs) for subject PM11.....142

Figure 31 Comparison of current-number trade-off data collected at two pulse durations (100 μs and 1000 μs) for subject PM8.....144

Figure 32 Comparison of current-number trade-off data collected at two pulse durations (100 μs and 1000 μs) for subject PM1.....146

Figure 33 Comparing the effect of pulse duration on the trade-off data gathered from a single site.....149

Figure 34 Comparison of profiles of changes to the required current intensity with depth, at different values of pulse number, for subject PM10.....153

Figure 35 Comparison of profiles of changes to the required current intensity with depth, at different values of pulse number, for subject PM11.....155

Figure 36 Comparison of profiles of changes to the required current intensity with depth, at different values of pulse number, for subject PM8.....157

Page

Figure 37 Comparison of profiles of changes to the required current intensity with depth, at different values of pulse number, for subject PM1.....159

Figure 38 Comparison of trade-off data calculated using 50% of maximum responding or locus of rise as the constant behavioural criterion for subject F3.....163

Figure 39 Comparison of trade-off data calculated using 50% of maximum responding or locus of rise as the constant behavioural criterion for subject F3.....165

Figure 40 Comparison of trade-off data calculated using 50% of maximum responding or locus of rise as the constant behavioural criterion for subject PM8.....168

Figure 41 Comparison of trade-off data calculated using 50% of maximum responding or locus of rise as the constant behavioural criterion for subject PM8.....170

Figure 42 Comparison of the depth profile obtained at 200 μA for Subject F3 with that obtained by Rompré and Miliaressis (1985) from subject 824 (medial placement).....185

Figure 43 Comparison of the depth profile obtained at 200 μA for Subject PM11 with that obtained by Rompré and Miliaressis (1985) from subject 826 (medial placement).....188

Figure 44 Comparison of the depth profile obtained at 200 μA for Subject R1 with that obtained by Rompré and Miliaressis (1985) from subject 824 (lateral placement).....192

Figure 45 Comparison of the depth profile obtained at 200 μA for Subject F4 with that obtained by Rompré and Miliaressis (1985) from subject 826 (lateral placement).....194

List of Appendices

Page

Appendix A.....219

Introduction

When observing the behaviour of a rat receiving electrical brain stimulation one cannot help but be impressed by the tenacious manner in which the animal seeks out this stimulus. At many sites in the brain the stimulation induces sniffing and exploration, and with little effort the animal can be trained to perform a variety of responses to receive this reinforcement. That the self-stimulating rat is in a highly motivated state, and exhibiting appetitive behaviour is certainly evident from the vigour with which these responses are performed and are directed towards a goal object.

This phenomenon, referred to as brain stimulation reward (BSR), has attracted the interest of students of appetitive motivation for many years. Part of the attraction of the BSR paradigm is that among the phenomena of goal-directed behaviour, BSR is one of the most amenable to experimental control. For example, BSR can be elicited very reliably from many different brain regions, and the intensity of the appetitive state can be manipulated quite precisely by changing the frequency and intensity of the stimulation offered. However, the most exciting and attractive aspect of this phenomenon is that the rat works to receive direct activation of specific neural elements (those located at the tip of the electrode).

The discovery of the neural circuit the self-stimulating animal seeks to activate is viewed as the first step in building a model of the central mechanisms involved in goal-directed behaviour (Shizgal, Bielajew, & Rompré, 1988). Once the elements that are directly excited by the electrical stimulation are known, their trajectory can be traced, and the targets to which they project identified. From this starting point, one could begin to investigate how aspects of the rewarding signal are encoded into memory, and how properties of the goal object (e.g. the magnitude of the reward), influence future decision-making behaviour. In the same way as the function of simple neural systems have been deduced from knowledge of their structural arrangement (Wine & Krasne, 1972), the existence of a diagram of the architecture of the BSR circuit can only aid the study of goal-directed behaviour.

The complexity of the neural substrate at sites where self-stimulation is elicited makes identifying the specific neurons that carry the BSR signal a difficult task. Many fibre pathways course past the electrode tip, and are activated during electrical stimulation, but it is unlikely that all are involved in the rewarding effect. For example, electrical stimulation of certain neural structures that reliably support BSR (e.g. the medial forebrain bundle) has also been shown to affect autonomic (Hess, 1957) and endocrine functions (Harris, 1948).

In order to build a neural circuit diagram of the reward-relevant neurons we must have a way of distinguishing between them and those neurons which are irrelevant to the phenomenon. The psychophysical approach (described by Gallistel, 1975) provides a method by which we can build a profile of the neurophysiological characteristics of the reward-relevant neurons from the behavioural level. Any cell that is proposed to be part of the BSR substrate (e.g. by electrophysiological means) must then match this profile in order to be considered as a "candidate neuron".

In the search for the directly stimulated neurons, mapping studies of the BSR substrate constitute the most basic of experiments employing the psychophysical approach. At the simplest level such studies contribute clues as to the location of sites where the phenomenon can be elicited. However, topographical studies also have the potential to generate data about the sensitivity of the directly stimulated substrate at these sites (e.g. by the amount of electrical stimulation needed to produce a criterion level of behaviour). Therefore, such data can be correlated with the trajectory of known anatomical pathways, and these pathways can then be investigated by more powerful psychophysical techniques.

Under one set of simple assumptions, the sites at which the sensitivity of the substrate is the highest are

those sites at which the reward-relevant neurons are the most densely packed (see Miliaressis, Rompré, & Durivage, 1982). However, several factors other than the density of the neurons can contribute to differences in stimulation efficacy between sites (e.g. the excitability of the reward-relevant neurons and/or their ability to follow high-frequency stimulation). Because of this, the more general term sensitivity is used throughout this thesis; the more sensitive the substrate at a given site, the lower the amount of stimulation required to elicit a criterion level of performance. Moreover, differences in sensitivity between sites are not presumed to represent a change in any specific substrate characteristic (e.g. density).

The usefulness of topographical data in making a contribution to the characterization of the BSR substrate depends upon the methodology used to collect them, and in the past, this methodology has often been inadequate. The interpretation of early studies is hindered mostly because behavioural output was used as the scaling variable for stimulation effectiveness. This was made necessary by the use of fixed, arbitrarily chosen values of both stimulation current and frequency. It was not until the work of Miliaressis and his colleagues (Rompré & Miliaressis, 1985; Miliaressis et al., 1982; Rompré, 1984; Rompré & Boye, in press) that consistent data (which could be replicated in the hands of different experimenters) were yielded by

mapping studies. The crux of their success lies in the application of psychophysical scaling techniques to assess the effectiveness of the stimulation. In addition, they improved upon previous techniques by using moveable stimulation electrodes and by using square-wave, cathodal stimulation rather than sine-wave stimulation. However, despite the fact that the methodology developed by Rompré and Miliaressis represents a major improvement over that used by previous researchers, it is not clear to what degree their results can be generalized to values of the stimulation parameters other than the ones they used in their study. As I argue below, this has important implications for the anatomical interpretation of mapping data and for the usefulness of such data as a guide to the application of other psychophysical techniques.

The present experiment is aimed at evaluating and extending the methodology developed by Rompré and Miliaressis by employing a procedure in which both current and frequency are manipulated in a systematic manner at many different sites, again using a moveable electrode. Not only will this method extend the amount of data that are currently gathered during topographical studies, but it will allow an evaluation of the how bias might be introduced if generalizations about the distribution of the reward substrate were based on single estimates of either the required current or frequency.

Before undertaking a presentation of the historical and theoretical considerations involved in carrying out topographical studies of the BSR substrate, the rationale for using the psychophysical approach to measure the physiological characteristics of the reward substrate is discussed. Following this, the rationale for the psychophysical techniques used in this thesis is presented.

The Psychophysical Approach

At the heart of the psychophysical approach is the use of trade-off functions (Gallistel, 1975). A trade-off function is an equivalent-stimuli function which allows one to determine combinations of two input parameters that produce a constant level of output, for example, the intensity and duration required to elicit a given level of behavioural response. Because the activity of the directly stimulated substrate in response to the input parameters is a function of its anatomical and physiological characteristics, the trade-off function allows us to draw inferences about these physiological characteristics from behavioural data (Edmonds, Stellar, & Gallistel, 1974). The same behavioural output is presumed to reflect the same level of some parameter of activity in the directly stimulated substrate. However, in order for this latter conclusion to be true, the system must behave in a strictly monotonic fashion. For a system to be monotonic, every

input must yield one and only one output. A system composed of a series of any number of concatenated, monotonic stages will behave monotonically as a whole (Gallistel, Shizgal, & Yeomans, 1981).

The system responsible for BSR has been shown to behave monotonically over a wide range of all the commonly tested input parameters (Gallistel, 1978; Gallistel et al., 1981). Therefore, if we hold the final output constant (by requiring some constant, criterion level of behavioural response), and we hold constant all other parameters that affect the level of behavioural output, we hold constant the output of the stage that combines the effects of the input parameters. If so, combinations of stimulation parameters that elicit equivalent output from the final stage, also elicit equivalent reward.

An example of a trade-off function which can be used to infer neurophysiological characteristics of the directly stimulated substrate from the behavioural data is the strength-duration function which relates the intensity of a stimulation pulse to its duration in achieving equivalent activation of the system. In order to build this trade-off function, rate-intensity curves are obtained at each of a series of pulse durations. The pulse duration is set and current is decreased in sequential steps such that rate of responding goes from maximum to zero (shown schematically in Figure 1a). The current required to support a criterion

Figure 1.

Schematic illustration of the derivation of the strength-duration trade-off function: (a) rate-intensity functions are determined at each of several pulse durations, and the current required to sustain a criterion level of behaviour at each pulse duration is calculated by interpolation from these functions. The required current is then plotted against the pulse duration at which it was determined (b) to give the strength-duration curve, which shows the combinations of the two variables that produce equivalent activation of the system.

a

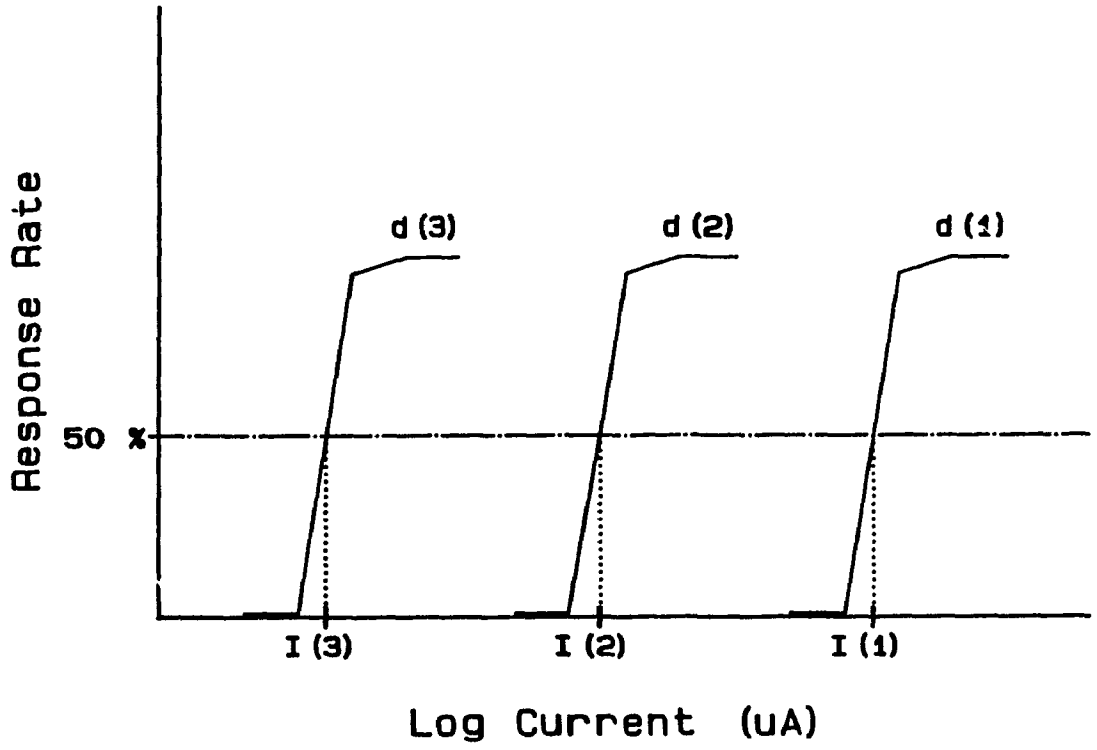
Response Rate
50 %
d (3)
d (2)
d (1)
I (3)
I (2)
I (1)
Log Current (uA)

b

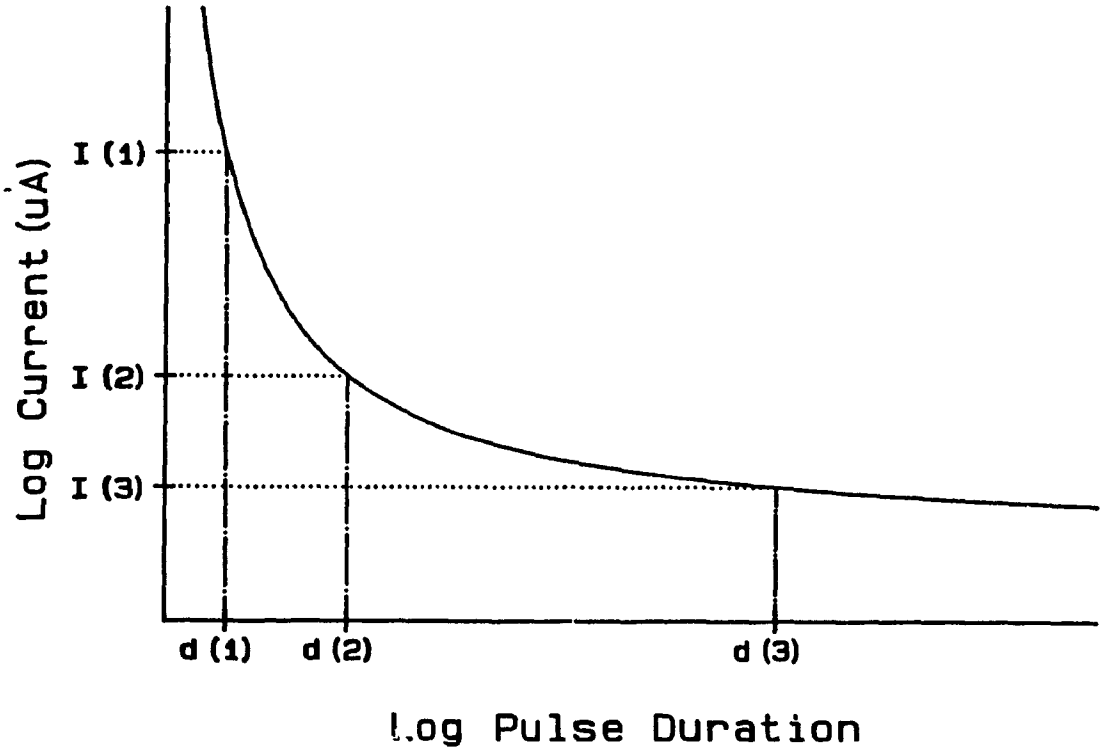
Log Current (uA)
I (1)
I (2)
I (3)
d (1)
d (2)
d (3)
Log Pulse Duration

level of responding is then calculated from each rate-intensity function by interpolation. In this example, 50% of maximum is the criterion, and the dotted lines show the required value of current along the abscissa. The value of required current is then plotted against the pulse duration at which it was obtained. The resulting trade-off function (Figure 1b) is thus composed of the combinations of pulse duration and intensity which elicit equivalent performance, and presumably, equivalent reward.

In the above discussion, and throughout this thesis, the term psychophysical is used to denote an experimental approach whereby one determines combinations of input parameters that yield a constant level of behavioural output. Such a procedure is commonly used in sensory psychophysics.

A Model of the Substrate for BSR

Gallistel (1978) and his co-workers (Shizgal, 1975/1976) have developed a minimal model of the constituent components of the BSR substrate, based on the body of behavioural data that has accumulated from application of the psychophysical approach. The model is termed minimal in that it makes only the most fundamental and parsimonious assumptions about the reward substrate and the process by which the electrical stimuli are transduced into a rewarding effect. In the Gallistel model (detailed

evidence for which is presented by Gallistel et al., 1981) the reward substrate can be represented by a chain of three components.

The "cable" or first-stage of the system consists of those reward-relevant neurons that are directly activated at the tip of the stimulating electrode. The only assumption made is that these are the elements of the reward circuitry which are directly excited by the application of the electrical stimulation.

The second-stage of the system consists of an "integrator" that performs both spatial and temporal summation of the impulses arriving via the cable from the site of stimulation. This integrator is presumed to receive trans-synaptic activation from the cable, but no assumption is made about its component parts. That is, it may consist of an elaborate network or it may consist solely of a single locus where the cable terminates and the rewarding effect is produced. Regardless of the specific architecture, its function is the spatiotemporal integration of the action potentials elicited in the first stage.

Finally, the third stage of the system consists of a "conversion process" whereby the magnitude of the reward received (taken to be the peak output of the integrator) on a previous trial is stored in memory. To postulate the existence of a memory stage is made necessary by empirical

evidence (Gallistel, Stellar, & Bubis, 1974) demonstrating that behaviour on subsequent trials is influenced by the magnitude of the reward received on previous ones. Again, no assumptions are made about the architecture of the mnemonic stage.

The majority of psychophysical experiments have focused on applying trade-off functions aimed at the characterization and identification of the cable or first-stage neurons. The reason for this is that these elements are the most accessible. The reward substrate of the medial forebrain bundle (MFB) has received the most attention in this regard, (see Shizgal & Murray, 1989 for a review), but investigation of the directly stimulated BSR substrate has also been undertaken for the prefrontal cortex (Schenk & Shizgal, 1982, 1985), and the brainstem (Bielajew, Jordan, Ferme-Enright, & Shizgal, 1981; Boye, 1988; Rompré & Boye, in press; Rompré & Miliaressis, 1987).

A review of all the psychophysical experiments that have been carried out in the various brain regions is beyond the scope of this thesis. However, an example of the neurophysiological data yielded by experiments employing trade-off functions is worthwhile. Through the application of the psychophysical approach, it has been inferred that the reward-relevant neurons include cells with myelinated axons; with diameters of 0.3 to 1.5 μm (Bielajew & Shizgal, 1982, 1986); with conduction

velocities of 1 to 8 m/s (Bielajew & Shizgal, 1982, 1986; Gratton & Wise, 1988; Shizgal, Bielajew, Corbett, Skelton, & Yeomans, 1980); and having absolute refractory periods in the range of 0.5 to 1.2 ms (Bielajew & Shizgal, 1982; Bielajew, Lapointe, Kiss, & Shizgal, 1982; Yeomans, 1979). Furthermore, at least some of these neurons are thought to give rise to long fibres that descend in a rostro-caudal direction (Bielajew & Shizgal, 1986) and extend between the lateral hypothalamus and the ventral tegmental area (Murray, 1988; Shizgal et al., 1980), perhaps continuing as far as the brainstem (Boye, 1988).

Gallistel (1975) and his colleagues (Gallistel et al., 1981) have proposed that the function of the integrator is to perform spatial and temporal summation of the action potentials generated in the first-stage neurons. Despite the fact that little is known or assumed about the neural network that comprises the second stage of the system, its interaction with the directly stimulated neurons has also been investigated through the use of psychophysical trade-off experiments. By trading-off a spatial variable (current) with a temporal variable (frequency), the spatiotemporal properties of the BSR system have been investigated for stimulation sites in the MFB (Gallistel, 1978; Schindler, 1983) and in the prefrontal cortex (Schenk, Prince & Shizgal, 1985).

It has also been proposed that this trade-off function can be used to gather information about the characteristics of the directly stimulated substrate (Yeomans, Pearce, Wen, & Hawkins, 1984), because the function reflects not only how the integrator processes output from the cable, but also how the characteristics of the directly stimulated neurons themselves determine the input to the integrator. For example, the spatial characteristics of the directly stimulated neurons will be reflected in the current required at a particular frequency. Therefore, because the unique characteristics of the substrate in any one region will effect the form of the current-number trade-off function, it is an attractive tool for topographical studies where the goal is to gather as much information as possible about the spatial distribution and sensitivity of the reward substrate surrounding the electrode tip. Moreover, because both current and pulse frequency are varied in order to derive the trade-off function, it can be used as a tool to evaluate mapping methods in which the value of one of these parameters is fixed at some arbitrarily-chosen level. In the following sections, the rationale for undertaking topographical studies and the methodological considerations involved are explored in more detail.

Topographical Studies of the BSR Substrate

One of the most fundamental steps in the investigation of BSR is to delineate the topography of the directly stimulated substrate. The rationale for this step is simple: topographical information provides clues to the location and distribution of the first-stage neurons, and aids the application of more powerful techniques to identify and characterize them. As a brief example of how mapping information can be useful in this regard, consider the collision experiment. This is one of the most powerful of the psychophysical trade-off techniques because it can reveal direct axonal linkage between two stimulation sites, as well as providing estimates of the conduction velocity of the directly-stimulated neurons involved (Bielajew & Shizgal, 1982; Shizgal et al., 1980; Shizgal & Murray, 1989; Shizgal, in press). This technique relies on the precise alignment of two electrode tips separated in space. Because employing the technique is time consuming, the existence of a detailed and accurate map of the region to which it is being applied can greatly facilitate the planning and execution of such experiments. Furthermore, from topographical data, profiles of zones of peak sensitivity of the BSR substrate can be constructed, and these can then be compared to the trajectory of known neural pathways. These profiles can then provide clues to candidate areas for further investigation.

In order to fulfil such goals, topographical studies must employ methodology that is capable of generating an unbiased, detailed data set that is also sufficiently general in its scope to contribute information relevant to the research approaches of many different investigators.

The concept of mapping various brain regions for the occurrence of stimulation-induced behaviours and then relating the performance of such behaviours to certain anatomical features is not a new one (Olds & Milner, 1954; Olds, 1956), and has not been restricted to the study of self-stimulation (von Holst & von Saint Paul, 1962; Wise, 1971, 1972). It was not until quite recently however, that the methodology used in such experiments evolved to allow the gathering of data that meet the criteria outlined above. Unfortunately, with a few important exceptions (e.g. Corbett & Wise, 1979, 1980; Gratton & Wise, 1983; Rompré & Miliaressis, 1985), the data from most early work on the BSR substrate have not been amenable to straightforward interpretation, mainly because the methodology employed did not make use of psychophysical scaling techniques. Data collected from the same brain region have often seemed contradictory, and in several cases, different investigators have reported opposite results for the same neural structure. For example, although Routtenberg and Malsbury (1969) have reported that the median raphe does not support self-stimulation,

Miliaressis (1977) and Rompré and Miliaressis (1985) have demonstrated that very low-threshold self-stimulation can be obtained from this structure.

Three main problem areas can be identified within these studies that can account for the introduction of bias: (a) the use of fixed stimulation electrodes which introduce unnecessary histological error, (b) the use of inadequate techniques to measure the stimulation efficacy, and (c) the selection of arbitrary, fixed stimulation parameters at which to collect the data. Each of these factors can influence the anatomical conclusions that are drawn from the resulting data.

The use of a fixed electrode means that only one site can be tested in each animal (per penetration). Therefore, in order to construct an overall map of the region investigated, each electrode placement (from each individual animal) must be assigned a set of coordinates according to an atlas of the rat brain and then placed on some summary figure (e.g. Routtenberg & Malsbury, 1969; Routtenberg, 1971; Crow, 1972; Liebman, Mayer, & Liebeskind, 1973). Each time one attempts to determine the position of an electrode tip histologically there is always some error involved. The cumulative error associated with creating a summary map from many different animals could severely hinder one's ability to interpret the resulting data and to characterize the relationship between

stimulation sites. Much of the contradictory information generated by previous mapping experiments can be attributed to reliance on fixed stimulating electrodes.

In order to combat this problem, moveable electrodes of several types have been developed (Wise, 1976; Miliaressis, 1981), and they provide a distinct advantage to topographical studies. The construction of these electrodes allows one to lower the electrode in roughly equal increments and many successive dorso-ventral sites can be examined for each penetration. Although there is still error associated with identifying the precise location of the electrode tip and in knowing the exact increment moved, the overall histological error is considerably reduced. Because the axis of movement is fixed, it is possible to more accurately determine the relationship between data gathered from adjacent sites.

The second problem with interpreting the results of previous studies arises from the use of inadequate techniques for the measurement of the rewarding value of the stimulation at a particular site. With relatively few exceptions the sensitivity of a site or the efficacy of the stimulation has been measured by the maximal behavioural output observed. There are many problems with this approach. It has been demonstrated that the rate of the instrumental response is not a valid indicator of the rewarding value of the stimulation. Hodos and Valenstein

(1962) have shown that rats always preferred a stronger stimulus when it was presented in a choice situation with one of lower intensity. This occurred even when the animal had responded at a faster rate for the low intensity stimulus when the animal was allowed free access to it.

Further support for the notion that response rate is not a valid indicator of the rewarding value of the stimulation comes from a series of studies conducted by Miliaressis, Rompré and their colleagues (Miliaressis et al., 1982; Miliaressis, Rompré, Laviolette, Philipe, & Coulombe, 1986; Miliaressis & Rompré, 1987). In one of these studies they demonstrated that a depression of asymptotic responding for lateral hypothalamic (LH) stimulation could be produced by the simultaneous stimulation of the reticular formation (RF). Stimulation delivered to the RF electrode produced movements of the head and body (thus decreasing response rate), but did not itself support self-stimulation. By comparing the rate-frequency functions obtained when pulses were delivered to the LH electrode alone with those obtained when each pulse delivered to the LH electrode was followed by one delivered to the RF electrode, it was observed that the amount of stimulation needed to reach the behavioural criterion (for the LH site) did not change (Miliaressis & Rompré, 1987). Because the presence of stimulation-induced movements can affect the estimate of stimulation effectiveness when rate

of response is used as the scaling variable, an alternative to this indicator has been developed to assess the efficacy of the stimulation.

In this method, known as the curve-shift paradigm, the rate of the instrumental response (e.g. lever-pressing or speed in the runway) is measured over a range of values of the scaling variable (e.g. frequency) such that this rate changes from zero to a maximal level. The resulting function (known generally as a reward-summation function) is roughly sigmoid in shape and usually rises very steeply from zero to maximum. The placement of the curve along the abscissa is seen as reflecting the rewarding impact of the stimulation. For example, if one makes a manipulation that decreases the rewarding value of the stimulation, such as decreasing the current, a higher frequency will be needed to produce the same behavioural output, and the function will be shifted to the right towards these higher frequencies.

The results of several validational studies demonstrate that manipulations to performance variables do not cause large changes to the lateral position of the reward-summation function (as compared to manipulations to the current, for example), but may cause a decrease in maximum rate (Edmonds & Gallistel, 1974; Miliaressis et al., 1986, but see Fouriezos & Emdin, 1988). Furthermore, the assertion that the rewarding impact of the stimulation

is reflected by the lateral position of the reward-summation function along the abscissa has received validation from two groups of researchers, both using a preference paradigm (Miliaressis & Malette, 1987; Waraczynski, Stellar, & Gallistel, 1987). Unlike the use of behavioural output as the scaling variable, the use of the curve-shift method allows a clearer comparison of two stimulation sites regardless of the presence of performance differences, and allows one to evaluate the full range of the behavioural response within a site.

A second factor related to the use of behavioural output as the scaling variable involves the arbitrary choice of stimulation parameters (e.g. current and frequency) at which to assess the sensitivity of the substrate at each site. In an elegant demonstration of how bias can be introduced by the use of such a procedure, Miliaressis et al. (1982) demonstrate that selecting fixed values of both of these parameters can influence the anatomical conclusions drawn from the behavioural data. When single values of current and frequency are chosen, and are kept constant for the testing of all stimulation sites, there is no way of assessing the true range of behaviour at a site, nor the true value of the rewarding impact of the stimulation. For example, the combination of stimulation frequency and current chosen may be too low to elicit self-stimulation behaviour because they cannot produce enough

excitation in the first-stage neurons to reach the integrator criterion. If neither of the parameters are varied there is no way of determining if the site would have supported self-stimulation had slightly higher values been chosen. Such floor effects increase the number of false negative sites reported and can thus distort the resulting conclusions.

On the other hand, ceiling effects can occur if the choice of values elicits responding in the asymptotic range. In this case there is no way of determining whether the site would have supported self-stimulation at lower values of either parameter. This makes it difficult to compare the relative sensitivity of the reward substrate at a site where high levels of responding are elicited, to other, related stimulation loci. Without varying the parameters, the contribution of these biases cannot be accurately assessed.

A Psychophysical Approach to Mapping

Methods which provide a solution to such problems have been used by Corbett and Wise (1979, 1980), Wise (1981), Gratton and Wise (1983), Rompré and Miliaressis (1985), and Rompré and Boye (in press). In these studies, one of the stimulation parameters is varied, behavioural output is measured at each level of this parameter (a reward-summation function is determined) and the curve-shift

paradigm is employed. Thus, a shift in the position of the reward-summation function determined at two different sites would reflect that one site was relatively more sensitive than the other, while a change in asymptotic responding would be consistent with the interpretation that there was a change in some performance variable, for example in stimulation-induced movements.

The mapping studies of Wise and his colleagues greatly improved upon the previous methodologies by manipulating current and by using moveable electrodes. They determined a rate-intensity function at each site by varying the current at a fixed value of frequency (60 Hz). However, they employed sine wave stimulation which does not allow one to manipulate the number of times each neuron fires, independently of the number of neurons that are fired by each pulse. Increasing the frequency of the stimulation decreases the duration of each cycle of current flow and thus decreases the number of neurons which are stimulated by each cycle.

Rompré and Miliaressis improved upon these studies by using cathodal square-wave pulses rather than sine wave stimulation. With this wave-form, the frequency of the pulses is independent of their duration, and therefore one can independently control both the number of times each neuron fires and the number of neurons that are fired. Like Wise and his colleagues they also used moveable

electrodes, but chose to manipulate frequency at a fixed low value of current (rate-frequency functions). Because the major goal of the present study is to extend and evaluate the mapping methodology developed by Miliaressis et al. (1982) and Rompré (1984) the rationale for their method will be treated in some detail.

Miliaressis et al. (1982) advocate the use of a fixed current in mapping studies for two main reasons. First, they propose that by holding the value of current constant from site to site, the radius of excitation produced will be of a constant size, and therefore, the same number of neurons will be stimulated at each site. In order for this to be true, several assumptions about the homogeneity of the reward substrate in the region of the electrode tip must be made. They hypothesize that if the neurons of the cable are homogeneously arranged in space, if all are equal in their ability to be fired by each stimulation pulse, if current flow is isotropic, and if all stimulated neurons carry the same behavioural weight at the integrator then the same level of current will yield a stimulation field of roughly constant size. Given these assumptions, determining the number of times the neurons have to fire to produce a constant level of behavioural output (by manipulating the number of pulses in a train of fixed duration), yields a reasonable estimate of the density of the neural substrate at each site. For example, if

the stimulation frequency needed to produce a criterion level of behaviour at 200 μA is 10 pulses per train at one site, the neural substrate would be considered to be twice as dense as one at which such a criterion was achieved at 200 μA and 20 pulses per train.

Second, they propose that the use of variable current and fixed frequency will produce more bias than the converse. Their reasoning is that the former would be more in danger of being biased by floor effects. For example, if the neural substrate were not very dense at a particular site, then it is possible that given the choice of a low fixed value for frequency, there would be no current at which a sufficient number of neurons could be recruited to produce enough action potentials in the cable to meet the integrator criterion, and thus the site would be erroneously reported as one which did not support self-stimulation (Rompré, 1984).

Using the arguments that a fixed current allows one to estimate the density of reward neurons at a stimulation site, and that the use of variable current at a fixed frequency biases the results towards finding "false negatives", Miliaressis et al. (1982) propose that the best way to gather mapping data is to use variable frequency at a fixed value of current. Furthermore, they also conclude that the value of current should be relatively small

because this will result in the maximum spatial resolution between sites.

The rationale for fixed parameter methods relies on the assumption that a single estimate of the required frequency or current taken at a fixed value of the independent parameter is representative of the trade-off function of which it is a member. Moreover, if one is to generalize to effects obtained with other values of the fixed parameter then the only difference between two trade-off functions derived at two different sites must be a change in position with respect to the scaling variable. In other words, the trade-off functions gathered at successive sites must maintain a constant relationship to each other over their entire range.

This situation is schematically illustrated in Figure 2a. If the curves taken at two successive sites are parallel, then a single reward-summation function determined at a fixed value of the independent parameter at two sites will be representative of the relationship between the two trade-off curves. Because the trade-off function obtained at one site (e.g. the narrow solid line in Figure 2a) always lies above that obtained at the second site (e.g. the wide solid line) then any point taken at the same place from each curve will also reflect this relationship. This conclusion is supported by considering the dotted lines numbered 1 to 3 in Figure 2a. The

intersection of these lines with the trade-off curves represents the required number that might be obtained at each of three different fixed values of current. Note that regardless of where the curves are sectioned, similar results are obtained. Moreover, note that the lowest value of current (line 3) does not intersect one of the functions. This represents one of the dangers of using fixed stimulation parameters, some information may be missed if the chosen value of the fixed parameter is below the minimum necessary to elicit the criterion behaviour.

It is possible however, for the relationship between trade-off functions gathered from successive sites to be much more complex than that shown in Figure 2a; for example, if the functional form of the curve changes as the electrode is moved. Such a situation is schematically illustrated in Figure 2b. In this case, the relationship between the trade-off function depends on which part of the curves are considered. It is not true that a single value taken at the same point on each curve will be representative of the relationship between the two functions over their entire range. Depending on where the curves were sectioned, a different result is obtained. This conclusion is supported by considering the dotted lines numbered 1 to 3 in Figure 2b. The intersection of these lines with the trade-off curves again represents the required number that might be obtained at each of three

Figure 2.

Schematic illustration of two relationships that could exist between current-number trade-off functions derived at two different self-stimulation sites. (See text for explanation).

a

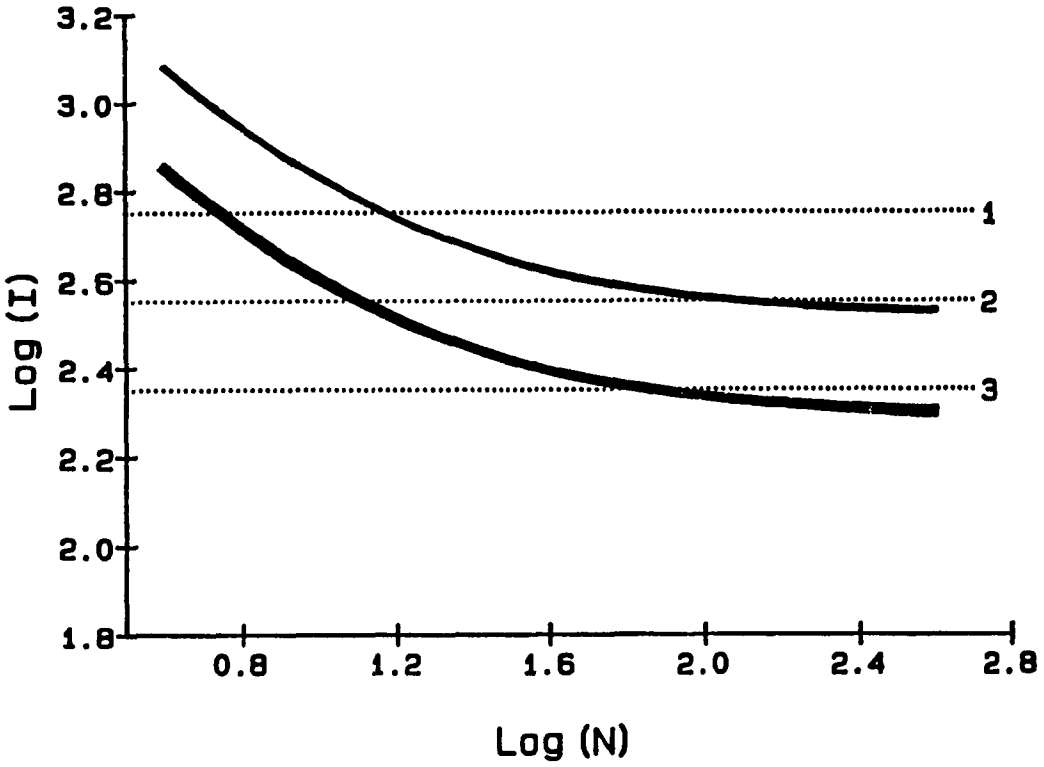
3.2
3.0
2.8
2.6
2.4
2.2
2.0
1.8
Log (I)
1
2
3
0.8
1.2
1.6
2.0
2.4
2.8
Log (N)

b

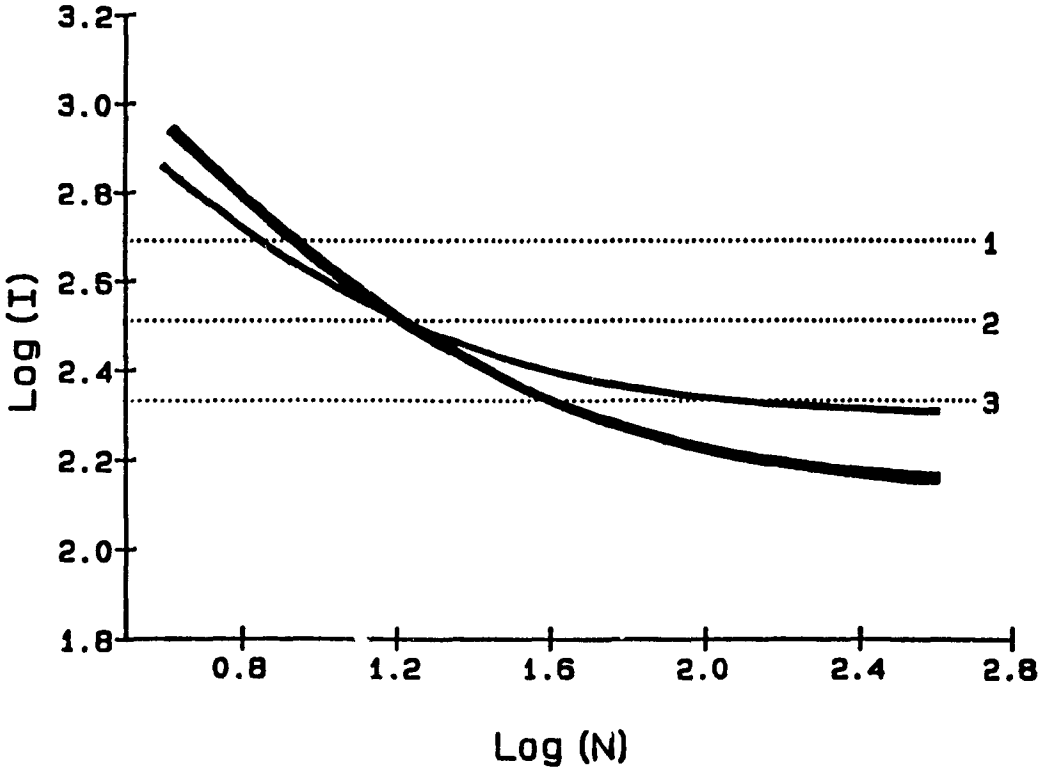
3.2
3.0
2.8
2.6
2.4
2.2
2.0
1.8
Log (I)
1
2
3
0.8
1.2
1.6
2.0
2.4
2.8
Log (N)

different fixed values of current. Note that three different conclusions would be yielded depending on which value of current was chosen. For this reason, generalizations based on a single estimate of required frequency or current could be misleading when the functional form of the trade-off curves derived from different sites changes.

The Present Experiment

As discussed previously, because the current-number function represents both the spatial and temporal characteristics of the directly stimulated neurons at a particular locus, these characteristics will influence the form of the function derived. Furthermore, because methods which determine a single reward-summation function can be viewed as collapsing the trade-off function into one point, the goals of extending the amount of information gathered, and of evaluating the use of fixed stimulation parameters, can both be accomplished by determining the current-number trade-off function at multiple sites along the trajectory of a moveable electrode.

This trade-off function can be determined in two ways, either by setting the current at several different values and varying the frequency at each one (as was done by Gallistel, 1978; Schenk et al., 1985; and Schindler, 1983), or by setting the frequency at many different values and

varying the current at each one (as was done by Schenk et al., 1985; and Schindler, 1983). Rather than extending the Miliaressis and Rompré method by taking rate-frequency functions at many different current intensities, I chose to determine the function by the converse method.

The main reason for this decision was my interest in deriving an empirical estimate of the minimum current required at each site (I_{min}). Miliaressis et al. (1982), and others (Schenk et al., 1985), have suggested that spatial resolution will be the highest when the stimulation field is very small and is recruiting only the neurons nearest the electrode tip. Because, I_{min} is defined as the minimum current required to recruit enough neurons to produce a criterion level of behaviour when those neurons are firing at their maximum rate, this measure should theoretically have the highest spatial resolution.

In order to measure I_{min}, the trade-off function must be determined by manipulating current at different levels of frequency. If the converse method is used, once a value of current is chosen that is less than I_{min}, behaviour will not be observed. Therefore the point at which the actual value occurs cannot be estimated. By manipulating current as the dependent variable, a point will be reached where the rate-intensity function is not shifted to the left by further increases in frequency. That is, further increases to stimulation frequency do not cause an increase in the

rewarding impact of the stimulation, the current cannot be further reduced, and the trade-off function will approach asymptote. This asymptote of the current-number function at high frequencies allows one to estimate the minimum current necessary to recruit enough neurons to maintain the criterion behaviour.

In conducting the present topographical study, I also chose to manipulate a third variable, pulse duration. This manipulation affects the number of neurons which are stimulated by a given current, and may also affect the proportion of neurons of different classes that are stimulated in a given region.

Increases in the pulse duration over a certain range permit a reduction in the required current; as the pulse duration is lengthened, the current required to achieve a given radius of excitation will be smaller. Eventually, a minimum value of current is reached beyond which further increases to the pulse duration do not permit further reductions to the current. The function that relates current to pulse duration (the strength-duration function) will thus approach asymptote. This minimum current is known as the rheobase. The time that is takes for the function to approach asymptote can be described by a second parameter, chronaxie. This is the pulse duration at which the required current is twice the rheobasic value. The importance of chronaxie to the present experiment is that

the choice of pulse duration will affect the relative proportions of neurons with short and long chronaxies that are stimulated by a given current.

Assume that the neurons in the region surrounding the electrode tip have the same chronaxie. If trade-off functions are obtained at two values of pulse duration, the trade-off function obtained at the longer pulse duration will be shifted down the ordinate, towards lower values of current. Furthermore, the two trade-off functions will be parallel on logarithmic coordinates. That is, the curve taken at the longer pulse duration will be shifted down the ordinate by the same proportion at all values of frequency.

It has been suggested, however, that the reward substrate is comprised of several sub-classes of neurons having different chronaxies (Matthews, 1977; Schenk & Shizgal, 1982; Shizgal & Schindler, 1982; Schindler, 1983). Differences in the chronaxies of the fibres surrounding the electrode tip may influence the current-number trade-off function determined at two different values of pulse duration. If neurons with long and short chronaxies are equally distributed in the region surrounding the electrode tip, then increasing the pulse duration may alter the relative proportion of neurons of each class that are stimulated. In this case, the trade-off function determined at the longer pulse duration will again be parallel to that determined at the short pulse duration and

will again be shifted down the ordinate. However, the magnitude of this shift may be different than that obtained where the substrate is homogeneous, reflecting the change in proportion of neurons of long and short chronaxie that are fired.

If, however, neurons of different fibre classes are not evenly distributed in the region surrounding the electrode tip (e.g. long-chronaxie neurons are clustered in a sub-region), then the trade-off function determined at a longer pulse duration may be different in shape to one taken at a short pulse duration (in addition to being shifted down the ordinate). This would occur if the proportion of stimulated neurons with long and short chronaxies varied with the current as well as with the pulse duration.

The manipulation of pulse duration may also reveal interesting differences as the electrode is moved. For example, if the ratio of long- and short-chronaxie fibres varies across the area traversed by the electrode (that is the distribution of different fibre classes is not uniform), then the longer duration pulse will be relatively more effective at producing action potentials at sites where neurons with long chronaxies are more common. This will be reflected in the distance the function is moved down the ordinate. By determining the current-number trade-off function at a second, longer pulse duration it is

hoped that a preliminary assessment of such factors can be made.

In order to compare the data generated by this method with the results of previous experiments, I chose to apply the method to the study of the ventral tegmental area of the midbrain (VTA). Part of this region was included in Rompré and Miliaressis' (1985) thorough topographical investigation of the pontine and mesencephalic substrates for BSR, and in the earlier studies of Corbett and Wise (1980) and Wise (1981).

Method

Subjects

Subjects were 16 male "old colony" Long Evans rats from Charles River Breeding Farms, weighing between 325 and 425 grams at the time of surgery. Each subject was individually housed in plastic, wire-topped cages in a room maintained on a 12 h lights on/lights off schedule. All testing took place during the dark period of the cycle. Standard lab chow and water were available *ad libitum* throughout the course of the experiment.

Electrodes and Surgery

Subjects were implanted with either one or two fixed, monopolar stimulating electrodes which were of two types depending on the stimulation cable to be used. Type A electrodes were constructed from 0.25 mm stainless steel wire, with a male amphenol pin crimped to one end. The length of the wire was then insulated with Formvar to within 0.1 mm of the rounded tip. Type B electrodes were again constructed from 0.25 mm stainless steel wire, but a second, insulated flexible wire was soldered 1.0 cm from the rounded tip. The shaft of the rigid wire was then insulated with Formvar from the solder joint to within 0.1 mm of the tip. A male amphenol pin was crimped to the other end of the flexible wire.

Each subject was also implanted with a single, monopolar moveable electrode, of the type described by Miliaressis (1981). The upper portion of the moveable electrode was inserted into a snugly fitted nylon receptacle, and was held there by a small set screw. Once implanted, movement of the electrode was accomplished by attaching a calibrated driver to the externally threaded top of the receptacle, loosening the set screw, and turning the threaded, internal shaft of the driver in 0.80 mm increments.

The indifferent electrode consisted of a male amphenol pin crimped to one end of a flexible stainless steel wire which was then wrapped around the four to five jeweller's screws imbedded in the skull as anchors for the electrode assembly.

Subjects were food-deprived approximately 18 hours before surgery was undertaken. Twenty minutes prior to anaesthetization, an intraperitoneal (i.p.) injection of atropine sulphate (0.6 mg/kg) was administered to reduce mucous secretions. Anaesthesia was then induced with 65 mg/kg sodium pentobarbitol (Somnitol) injected i.p. Supplemental injections were administered as necessary throughout the surgery. Following induction of deep anaesthesia, subjects were mounted in a stereotaxic instrument, with their skulls held level between bregma and lambda. Fixed electrodes were aimed at the LH using the

following coordinates: -2.8 mm posterior to bregma, 1.7 mm lateral to the mid-sagittal suture, and -7.8 mm ventral to the dural surface. In those animals for which only one fixed electrode was implanted, this was aimed at the right LH. The moveable electrode was aimed at the left VTA using the following coordinates: -4.8 mm posterior to bregma, 1.0 mm lateral to the mid-sagittal suture, and -6.0 mm ventral to the dural surface. White petroleum jelly was applied to the shaft of the moveable electrode at the base of the plastic sleeve to prevent dental acrylic from adhering to the electrode.

Once the electrodes were implanted, dental acrylic was used to cement them to the skull and to the anchoring screws. For type A electrodes, the male amphenol pins attached to the fixed electrodes and to the current return protruded from the acrylic and were attached separately to the stimulation cable. For type B electrodes, the amphenol pins of each electrode and the current return were inserted into a nine-pin connector constructed from an externally threaded nylon rod (1.0 cm in length), which was then cemented to the skull. By means of an internally threaded ring, this connector was attached to a matching socket mounted on the end of the stimulation cable.

Following surgery, subjects received a 0.1 cc injection of ampicillin (i.m.) to reduce the likelihood of

infection, and a 5.0 mg/kg injection (i.p.) of morphine sulphate to reduce post-operative pain.

Subjects were allowed 5 to 7 days post-operative recovery before initial testing was undertaken.

Apparatus

Two different testing facilities were used in this experiment. Initial screening and training procedures were carried out in a manually-controlled set-up. This testing facility was also used for preliminary assessment of the subjects' behaviour at each new stimulation site as the moveable electrode was lowered. A computer-controlled testing facility was used to stabilize self-stimulation performance, and to collect the current number trade-off data at each position of the moveable electrode.

Manually-controlled apparatus. Testing boxes were constructed of plywood and measured 25 cm (width) x 25 cm (depth) x 70 cm (height). The front panel of each box was constructed of clear Plexiglas and floors were of wire mesh. A Lehigh Valley rodent lever protruded from the centre of the left wall of each box approximately 5 cm from the floor. A yellow "jewel" light was located above the lever and was illuminated whenever the lever was armed (i.e. when stimulation could be obtained).

The stimulation cable was attached to the subject's electrode assembly by either direct connection to the protruding amphenol pins, or by the nine-pin connector described above. The moveable electrode connector was of a design similar to that described by Miliaressis (1981), with electrical connection achieved by inserting a stainless steel wire into the end of the electrode/cannula assembly. The other end of the stimulation lead was connected to the stimulator via a seven-channel, slip-ring commutator (Airflyte CAY-652-7) located in the centre of the test box ceiling. This allowed for free movement of the animal without twisting of the cable.

Electrical stimulation delivered upon depression of the lever consisted of 400 ms trains of 100 µs, cathodal, rectangular pulses. Train duration remained constant throughout all phases of the experiment and therefore the number of pulses per train covaried with the frequency. Pulse duration remained constant at 100 µs for all screening and training periods, while trade-off functions were collected at two pulse durations, 100 and 1000 µs. Stimulation was delivered on a continuous reinforcement schedule, that is, each depression of the lever resulted in the delivery of a train of stimulation.

The temporal parameters of the stimulation were controlled by manually-operated, integrated-circuit, pulse generators. The current was determined by dual constant-

current amplifiers (Mundl, 1980) and controlled by a potentiometer, and monitored by measuring the voltage drop across a 1 kohm resistor in series with the rat. Charge accumulation at the brain-electrode interface was minimized by a circuit that shorted the stimulator outputs through a 1 kohm resistor when no pulse was present.

Computer-controlled apparatus. The computer facility used to stabilize performance and to collect trade-off functions was similar in many respects to the manually-operated facility. Parameters of the stimulation such as train duration and schedule of reinforcement were also the same. Only those components that differed will be described below.

Testing boxes were constructed wholly of Plexiglas with hinged doors on the upper half of the front panel and removable trays serving as floors. Each testing box was equipped with two Lehigh Valley rodent levers, one located 5 cm from the floor and 5 cm from the back wall on the left hand side, and the other located similarly, but diagonally across the cage on the right wall. A yellow "jewel" light was located above the rear lever, and a red one above the other. Only the rear lever was used during this experiment.

Each test box was placed inside a larger plywood enclosure measuring 50 cm x 50 cm x 90 cm, and insulated

with a 2.5 cm thick layer of Styrofoam. Plexiglas windows in the removable, wooden front panels allowed remote viewing via a video camera during testing sessions. A 40 watt house light bulb was placed in the centre of the ceiling of the plywood enclosure over the test cage. This light was briefly turned off and then on again at the beginning of each trial to signal the onset of priming stimulation.

The temporal parameters of the stimulation were controlled by a dedicated microprocessor with a custom-built interface. The cathode and anode were selected by banks of relays controlled by the parallel port of the dedicated microprocessor. Pulse amplitude was determined by a constant current amplifier of similar design to that described by Mundl (1982), except that the reference voltage was supplied by a digital to analog converter. Range selection of the reference voltage was digitally controlled by the parallel port of the microprocessor.

Procedure

Screening. Subjects were first screened for self-stimulation at the LH placement(s) that were to serve as "training sites" in order to familiarize the animal with the task, testing environment and experimental protocol before starting the mapping phase of the experiment.

Initial testing parameters were 15 pulses per train at a current of 400 μA. If the animal showed interest by approaching the lever and/or sniffing, or if the stimulation elicited no observable response, the stimulation intensity and frequency were systematically varied and conventional shaping procedures were employed to try to induce the animal to press the lever. If the stimulation appeared to be aversive (e.g. the subject attempted to escape the box), if seizure activity was elicited, or if the animal could not be shaped to press the lever within three one-hour testing sessions (on consecutive days) testing was terminated and the animal was screened at the implantation site of the moveable electrode the following day. If the animal learned the lever-press response then a period of training ensued.

Training. Once the animal acquired the lever-pressing response, the frequency and intensity of the stimulation were adjusted to a level that produced consistent and vigorous behaviour, and the animal was allowed free access to the lever for approximately ½ hour. This was repeated over the next two testing sessions until the animal reliably maintained the response. Once the behaviour was established, animals were trained to respond within the parameters (e.g. trial duration) of the mapping experiment.

First, five trains of priming stimulation were administered and the light above the lever illuminated, signalling that the lever was operative. This was followed by a 30 second period during which the subject, by pressing the lever, could obtain trains of the same stimulation previously given as priming. At th end of this period stimulation was withdrawn until the animal extinguished lever-pressing. When the animal had stopped responding and moved away from the area of the lever, another trial was started, beginning with the priming stimulation. This phase was continued until the animal reliably returned to the lever following the priming trains, and reliably stopped lever-pressing upon cessation of the stimulation. Once the animal's performance met these requirements, stabilization procedures were begun in the computer-controlled facility.

Stabilization. Stabilization consisted of repeated determinations of the function relating lever-pressing rate to current. In order to obtain this function, the subject was presented with several 30 second trials (each preceded by five identical priming trains) in which the pulse number was held constant while the current was decreased in 0.05 $\log_{10}$ unit steps on each consecutive trial. This continued until the animal made fewer than five responses for two consecutive trials (quitting criterion). The rate of

response was recorded for each trial, and the current corresponding to half maximal response rate (the required current) was calculated by interpolation from this function. Stabilization sessions consisted of 15 repetitions of these determinations, with each session lasting approximately one hour. Animals were tested for 2 hours in the morning followed by a 3 hour rest in their home cage, and then tested for 2 more hours in the afternoon.

Performance was considered stable when it met at least one of the following criteria. First, the required current did not vary by more than 0.10 $\log_{10}$ units within a session for four consecutive sessions; and second, the standard error of the mean of the logarithms of the required current was less than or equal to $\log_{10}(1.03)$ for four consecutive sessions (equivalent to ± 3.00% of the geometric mean).

Mapping. This phase was begun when subjects' performance for LH stimulation was considered stable, or when no self-stimulation behaviour could be elicited from the LH placements. Screening of the first site at the VTA placement (moveable electrode) proceeded in the same way as outlined above, except that sessions lasted approximately 1½ to 2 hours. If by the end of this time the animal could not be taught to approach the lever, or if the stimulation elicited an aversive reaction, the electrode was lowered

0.32 mm and a new site was tested 18 to 24 hours later. If sniffing or other signs of interest were elicited but the animal could not be taught to press the lever, the animals were retested at the same site following a three hour rest period in the home cage. If the animal could not be taught to perform the response after this second session, the electrode was lowered 0.16 mm and a new site tested 18 to 24 hours later. Each time the electrode was lowered, the animal was immobilized briefly with a short-acting inhalant anaesthetic (Metofane).

Once self-stimulation was elicited, training and stabilization proceeded as outlined above. When performance was considered stable, collection of the trade-off functions commenced. The first testing session, lasting approximately 3 to 4 hours, was carried out in the manual testing facility and its purpose was to screen the new site and to estimate the parameters of the stimulation to be used in collecting data in the computer-controlled facility. Data collected in the manual facility were not included in any subsequent analyses.

Prior to starting the current-number tests, the impedance of the electrode-brain interface was measured by calculating the voltage drop across the electrode for a current of 200 μA. A low impedance (< 5 kohms) can be indicative of a break in the electrode insulation. In no

case was an impedance of less than 10 kohms recorded at any site.

Once the impedance test was completed, two determinations of the rate-intensity function at the pulse number and starting current used for the stabilization sessions were taken as a "warm-up" for the animal. Next, rate-intensity functions were obtained at each of a series of 17 different pulse numbers ranging from 8 to 201 pulses per train and separated by increments of roughly 0.10 $\log_{10}$ unit. At each pulse number, current was again decreased in 0.05 $\log_{10}$ unit steps on consecutive 30 second trials (each preceded by five priming trains of stimulation), until the quitting criterion was reached. Pulse duration for this phase remained at 100 µs.

Following a 10 to 20 minute rest period the pulse duration was set to 1000 µs and the process was repeated. For this longer pulse duration, the range of pulse numbers that could be tested was determined by the building up of charge at the brain-electrode interface. This build-up was inferred by the failure of the oscilloscope trace to return to baseline between pulses. This problem occurred when the pulse duration was long relative to the inter-pulse interval, as was the case when testing higher frequencies with the pulse duration set at 1000 µs.

Testing was immediately terminated whenever it was determined that charge build-up was occurring. The

specific frequency at which this occurred varied from site to site and animal to animal. Because the range of testable frequencies was always more narrow in the 1000 μs condition, several additional points were added to the trade-off functions in approximately 0.05 $\log_{10}$ unit increments, with the number of pulses ranging from 7 to between 37 and 64 pulses per train. The specific pulse numbers tested in the 1000 μs condition were changed slightly for animals later in the experiment (F1, F3, F4, and R1) in order to make the values coincide more closely with those tested in the 100 μs condition. Prior to this, many of the pulse numbers tested at the longer pulse duration were different from those tested in the 100 μs condition. This occurred because the basic schedule was formed by incrementing in 0.10 $\log_{10}$ units from 7 pulses rather than 8 pulses, and therefore, many of the values tested fell between those used in the 100 μs condition.

Following the manual testing animals were allowed a 3 hour rest in their home cage and then data collection began in the computer-controlled facility. Computer-controlled testing sessions were run in a similar fashion to the manually-controlled sessions. The two pulse duration conditions were run consecutively separated by a rest period of 10 to 20 minutes, and the entire session lasted 3 to 3½ hours. The sequence of pulse numbers at which the rate-intensity functions were collected was reversed from

session to session. To create the first sequence, the pulse numbers to be tested were arranged in ascending numerical order and assigned a rank based on their position on the list. Starting with the lowest value (assigned a rank of 1) each odd ranked position on the list was assigned a new consecutive ranking (e.g. the third member of the list would be assigned a rank of 2, the fifth a rank of 3, and so forth). Upon reaching the highest value, the ranks continued to be assigned to the values which had been previously skipped over in descending fashion. The schedule was then formed by putting the ranks in ascending numerical order. In this way, the pulse numbers at which the rate-intensity functions were determined first increased and then decreased during a testing session. The second schedule consisted of the reverse of the first one, so that values that had been tested last using schedule one were now tested first. The two schedules for each pulse duration condition were both formed in this manner (See Appendix A for an example of the schedules used). The 1000 μs pulse duration condition always followed the 100 μs condition.

Values of the starting current used in collecting the rate-intensity functions at each frequency were chosen on the basis of the results from the manual testing sessions, so that the animal would reach the quitting criterion in five to seven trials. Required current for each pulse

number was calculated by interpolation from the individual rate-intensity functions, and the current-number trade-off was obtained by plotting the logarithm of the required current against the logarithm of the number of pulses.

Following the first day of testing, two daily computer sessions separated by a 3 hour home-cage rest period were run on subsequent days until five to seven determinations of the current-number trade-off function were obtained for each pulse duration. When testing was finished the electrode was lowered 0.16 mm and the new site was screened 12 to 18 hours later in the manual facility. While every attempt was made to maintain a schedule of 3 days testing per site (six testing sessions including the initial manual screening), occasionally additional replications were necessary or testing was precluded due to unavoidable circumstances (e.g. equipment failure).

The experiment was terminated when the electrode was deemed to be near the base of the brain by calculating the distance moved from the estimated depth of implantation. This criterion was used for only three animals however, due to extenuating circumstances. One animal (PM1) lost its electrode assembly part way through the mapping experiment, and testing of another (F1) was terminated when the wire of the moveable connector snapped off inside the moveable shaft. Testing of three animals (F3, F4, and R1) was terminated when the current-number trade-off functions

taken at a single site changed significantly after a lengthy (11 day) period of non-testing. In addition, five animals were discarded from the study during training or during collection of mapping data at the first site due to the loss of their electrode assembly, or similar circumstances which rendered the moveable electrode untestable. Testing of two animals for which no mapping data were collected was terminated when the electrode assembly was damaged (PM9), or when the animal could not be trained nor stabilized after repeated testing at several sites (PM6).

Histology

Two to five days following the last testing session, the subjects were administered an overdose of Somnitol, and a marking lesion was made at each electrode tip by passing an anodal current of 100 μA for 15 seconds through each electrode. The animals were then perfused intracardially with 0.9% physiological saline followed by a Prussian Blue solution (0.3% potassium ferracyanide, 0.3% potassium ferrocyanide, 0.5% trichloroacetic acid in 10% formalin). The brains were removed and immediately stored in 10% formalin for at least one week. Three days prior to sectioning at -20 °C, the brains were stored for consecutive 24 hour periods in each of three sucrose solutions (10%, 20%, 30%), which were all prepared with 10%

formalin. Freshly cut sections (0.40 μm thick) were placed on gelatine coated slides and examined under a microprojector. Sections were also subsequently stained with thionine and re-examined for location of the electrode tips.

Data Analysis and Curve-Fitting

In constructing the trade-off functions, some data points (mean of the required current at a particular pulse number) were discarded. These data points were discarded when less than half of the number of maximum replications of required current at the majority of pulse numbers tested were obtained. For example, if five replications of the required current had been obtained for most of the values of pulse number tested at a site, and only two replications were made for one pulse number (e.g. 8 pulses), then this point was discarded from the function. These data were discarded prior to any subsequent analyses of the data.

Apart from plotting the trade-off functions in the logarithmic domain and examining their shape and relationship to each other visually, several analyses of the trade-off data were undertaken. The method employed for each is discussed below.

Estimating the locus of rise. Miliaressis et al. (1986) have demonstrated that under certain conditions the use of a percentage of maximum response rate as the behavioural criterion can bias the estimate of the required dependent variable (e.g. the required current if rate-intensity functions are determined). For example, at sites where the stimulation induces movements that interfere with the lever-pressing response, the asymptotic rate is often decreased. This has been shown to produce small changes to the estimate of the required current or pulse number. However, if a change to the slope of the reward-summation function accompanies this change in the asymptotic rate, then significant changes to the estimate of the required dependent parameter may be artifactually produced. Under these circumstances, Miliaressis et al. have demonstrated that the use of a zero behavioural criterion (their "theta 0") is less subject to such bias, because the function "rotates" around this point. That is, although the reward-summation function may rise more slowly, the threshold for responding remains unchanged.

The data of many of the subjects tested in this experiment might be influenced by such factors. Several animals experienced some form of stimulation-induced movements at each site, and some showed large variations in maximum response rate across the range of frequencies tested within a site. Because I used the current required

to maintain 50% of maximum response rate to calculate the required current at each frequency, I was concerned that such factors may have influenced the trade-off data collected.

In order to determine whether the choice of behavioural criterion had influenced the form of the trade-off function, data from several animals that experienced stimulation-induced movements and whose rate-intensity functions showed large variations in asymptotic rate and/or slope over the range of frequencies tested at a particular site were chosen for further analysis of this problem. In this analysis, two different trade-off functions were constructed from the raw data, one using 50% of maximum response rate as the criterion, and one using a threshold criterion. The current required at threshold (zero behaviour) was defined as the locus of rise (L.O.R) of the rate-intensity function.

In order to provide a non-arbitrary estimate of the locus of rise a curve-fitting procedure was employed. Each rate-intensity curve was fit with a series of two- or three-segment functions, with each segment describing a different portion of the curve. In all cases, a horizontal segment (consisting of an average of the points in this part of the curve) was used to describe the lower asymptote. This was based on the quitting criterion which had been used in the experimental protocol. Given that the

animal was required to lever-press less than five times on two consecutive trials in order for the determination to be terminated, and regardless of the absolute value of the response rate on these trials (i.e. whether the animal pressed five times on both trials or zero times on both trials), they have satisfied the quitting criterion. Therefore, there must be at least two points at this portion of the curve.

Required current values were transformed to their logarithmic equivalents before curve-fitting was undertaken. Each rate-intensity curve was first fit with a two-segment function consisting of a lower horizontal segment and a straight-line function fit to the remaining points (Figure 3a). This function was chosen because many of the rate-intensity curves did not have a clear upper asymptote, particularly at sites where the movements were so severe as to prevent any increase to the starting value of the current. All possible forms of this function were tried, and the one yielding the least sum of squares was chosen as the best-fitting of this function type.

Two three-segment function types were also fit to each rate-intensity curve. The first consisted of two horizontal segments (an upper and a lower) that were joined together (i.e. there were no points on the slope between them--Figure 3b). The second consisted of an upper and a lower horizontal segment, with a straight line function fit

to the points on the slope between them (Figure 3c). Again, the best-fitting function of each type was determined as the one yielding the least sum of squares. The function type (i.e. two- or three-segment) that provided the best overall description of the rate-intensity curve was taken as the one yielding the least sums of squares. Locus of rise was then determined as the current corresponding to the intersection of the rising portion of the curve and the lower horizontal segment (Figure 3: a, b, and c).

If the rate-intensity function approached zero more than once, (i.e. the function crossed 25% of maximum response rate and then crossed back over 50% of maximum response rate--Figure 4) then the locus of rise could not be estimated with certainty. In order to estimate the L.O.R. for these curves the geometric mean of two estimates taken from different parts of the rate-intensity function was used. First, the values comprising the curve were divided into two subsets. Subset A consisted of the upper asymptote and all the points up to and including the first point to lie below 25% of the maximum rate (Figure 4--dotted line). Subset B included the lower asymptote and all the points up to and including the last point at which this part of the function was still rising (Figure 4--dashed line). Any points lying between the two subsets were not included in the fit.

Figure 3.

Examples of the two- and three-segment functions fit to actual rate-intensity data. Locus of rise in each case corresponds to the intersection of the rising portion of the curve with the lower horizontal segment: (a) a two-segment function consisting of a lower horizontal segment and a linear, rising segment, (b) a three-segment function consisting of an upper and a lower horizontal segment with no points on the slope (illustrated as a dotted line joining the two segments), and (c) a three-segment function consisting of an upper and a lower horizontal segment with a linear segment fit to the intervening points.

a

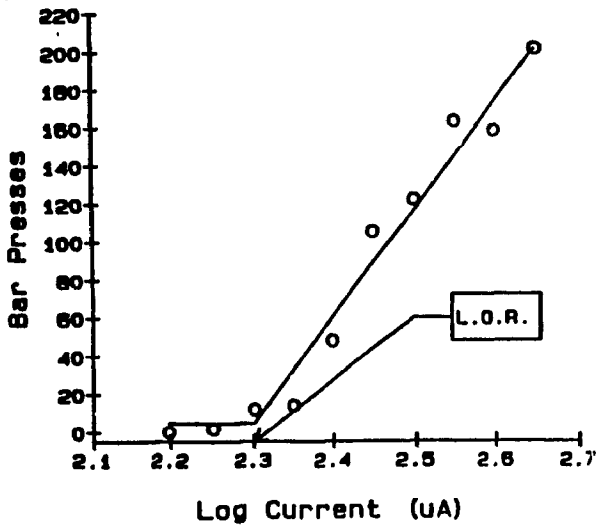
Bar Presses
220
200
180
160
140
120
100
80
60
40
20
0
2.1
2.2
2.3
2.4
2.5
2.6
2.7
L.O.R.
Log Current (uA)

b

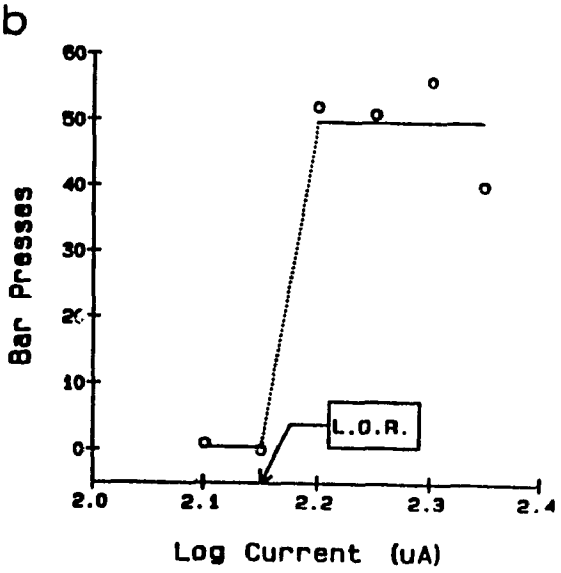
Bar Presses
60
50
40
30
20
10
0
2.0
2.1
2.2
2.3
2.4
L.O.R.
Log Current (uA)

c

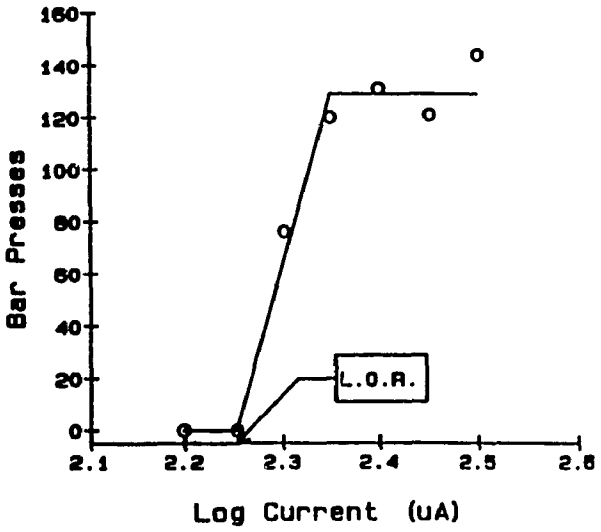
Bar Presses
160
140
120
100
80
60
40
20
0
2.1
2.2
2.3
2.4
2.5
2.6
L.O.R.
Log Current (uA)

Figure 4.

An example of a rate-intensity function fit as two subsets of data with locus of rise calculated as the geometric mean of the estimates from the two subsets (See text for explanation).

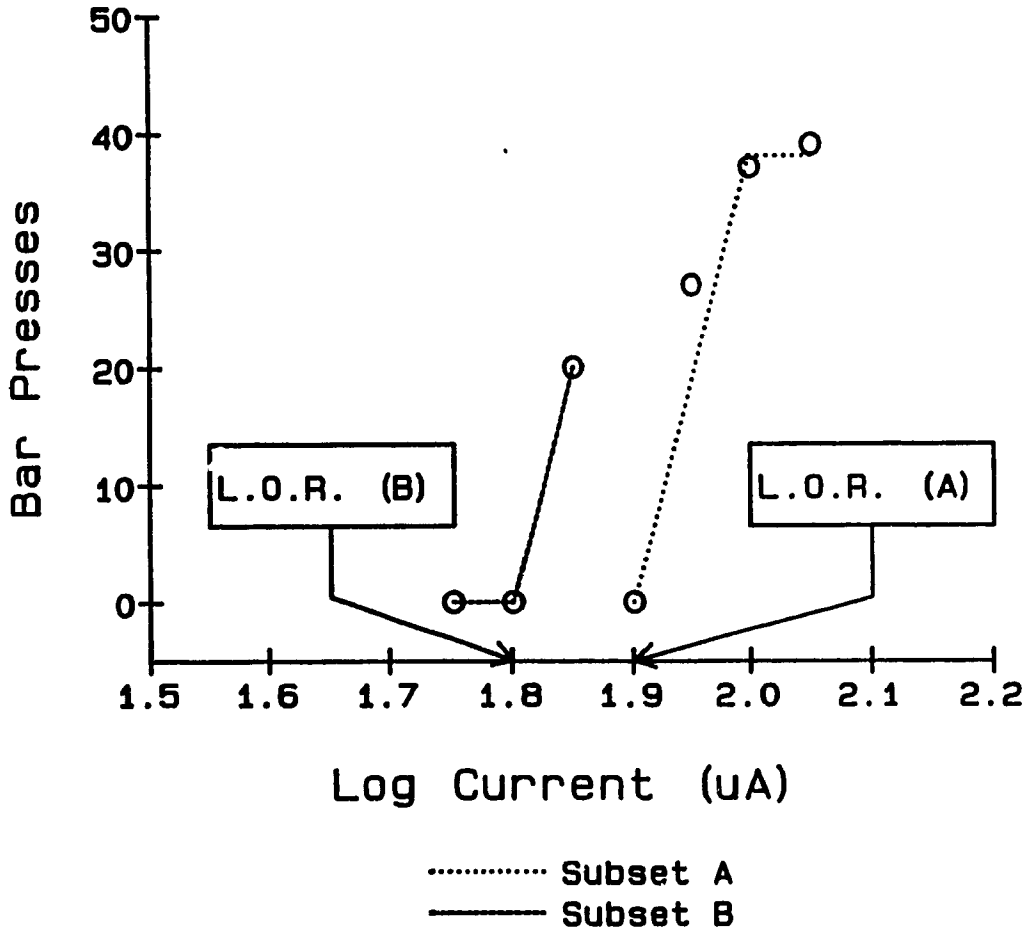
50
40
30
20
10
0
Bar Presses
L.O.R. (B)
L.O.R. (A)
1.5
1.6
1.7
1.8
1.9
2.0
2.1
2.2
Log Current (uA)
Subset A
Subset B

Once these subsets were determined, each was separately fit with the three function types described above using the same procedure. In addition, subset A was fit with one additional two-segment function type consisting of an upper horizontal segment and then a linear function fit to the remaining points (illustrated in Figure 4). This function was not fit to the other rate-intensity curves, nor to subset B because of the quitting criterion dictated by the experimental protocol.

Again, the function type which yielded the least sum of squares was chosen as the one that best described each subset, and L.O.R. was estimated as the current corresponding to either the intersection of the horizontal segment with the rising portion of the curve, or to the lowest y-value, depending on which function was chosen. In the case where the y-value corresponding to L.O.R calculated on subset A differed from that of subset B, the L.O.R for subset A was calculated by extrapolation using the y-value of subset B. The overall L.O.R was then taken as the geometric mean of the estimate from subset A and subset B.

Estimating I_{min}. I_{min}, the minimum current required to elicit responding at a site, is defined as the current at which the trade-off function approaches its horizontal asymptote. In order to provide a non-arbitrary estimate of

this current, a composite function was fit to each current number trade-off curve using the Derivative-Free Non-Linear curve fitting option (AR) in the Biomedical Data Package (BMDP). This composite function consisted of two segments: (a) a linear or higher order polynomial function that was used to describe the descending portion of the trade-off curve, and (b) a horizontal line segment that was used to describe the horizontal asymptote. The purpose of using different functional forms for the descending segment was to determine which points lay along the adjacent horizontal segment, and thus which points were to be included in the estimate of I_{min}. No a priori prediction about which functional form should best fit the trade-off curves was made.

In the course of searching for the function which would best describe the shape of the trade-off curve, several composite functions of increasingly higher order were tried until the improvement to the fit (based on the magnitude of the residual variance and visual inspection of the pattern of residuals) was very small. Because a higher order function will always produce a better fit to the data than a lower order function, the lower order function was chosen in the case where fitting one of higher order did not change the value of the estimate of I_{min}, and where it did not yield a meaningful reduction in the magnitude of the residual error variance. Functions that did not

converge or converged beyond the maximum value of pulse number tested were rejected. No polynomial of higher than fourth-order was required to achieve a good description of the shape of the curve based on these criteria.

Estimates of the parameters of this two-segment function were found by systematically varying the initial values supplied by the experimenter and calculating the residual sum of squares. The parameters yielding the smallest residual sum of squares were then fit to the data. Regardless of which function type yielded the best fit, I_{min} was always estimated from the parameter set yielding the smallest residual sums of squares. The values of both current and pulse number were converted to their logarithmic equivalents before curve-fitting.

The procedure for finding the function that best described the shape of the descending portion of each trade-off function, and thus I_{min} was undertaken as follows. First, a two-segment function composed of two straight lines was tried (e.g. Figure 5a). The initial values supplied were the y-intercept, and the pulse number and current at which the asymptote was estimated to begin (based on visual inspection of the curve). The parameters that yielded the smallest residual sum of squares were then plotted with the data, and used to construct a graph of the residual error terms. Visual inspection of both graphs was used to determine whether there were systematic deviations

of the points from the fitted function. If the residual error terms appeared to be reasonably unsystematic in their pattern, this function was judged to fit adequately, and the current at which the trade-off curve approached its horizontal asymptote (i.e. the intersection of the two segments) was used as the estimate of I_{min} (Figure 5a).

If the two segment straight-line function was judged to be an inadequate description of the trade-off curve (by the visual inspection criteria), a new composite function (illustrated in Figure 5b) was then tried. The two segments consisted of a second-order polynomial to describe the descending portion of the curve and a horizontal segment to describe the asymptote. Initial values supplied to the program consisted of the coefficients of each term in the polynomial, and the pulse number at which the asymptote was estimated to begin. Again, the function yielding the smallest residual sum of squares was plotted with the data curve and used to generate a plot of the residual error terms. Visual inspection of these graphs was again used to determine the presence of any systematic deviations from the fitted function. If this polynomial fit resulted in a reduction in the magnitude of the residual variance (over the linear function described above), and no systematic deviations in the residual error terms were evident, the function was judged to provide a

Figure 5.

Examples of the composite functions fit to the trade-off data for the purposes of estimating I_{min}. Each composite function consists of two segments, a linear or higher-order polynomial which describes the descending portion of the curve, and a lower horizontal segment to describe the asymptote: (a) composite function in which the descending segment consists of a straight line, (b) composite function in which the descending segment consists of a second-order polynomial, and (c) composite function in which the descending segment consists of a third-order polynomial.

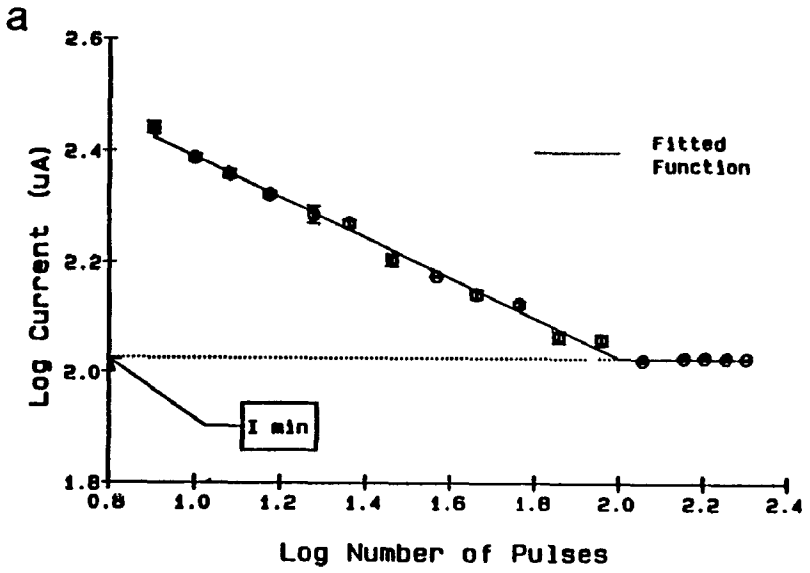
a
Log Current (uA)
2.6
2.4
2.2
2.0
1.8
0.8
1.0
1.2
1.4
1.6
1.8
2.0
2.2
2.4
Log Number of Pulses
Fitted Function
I min

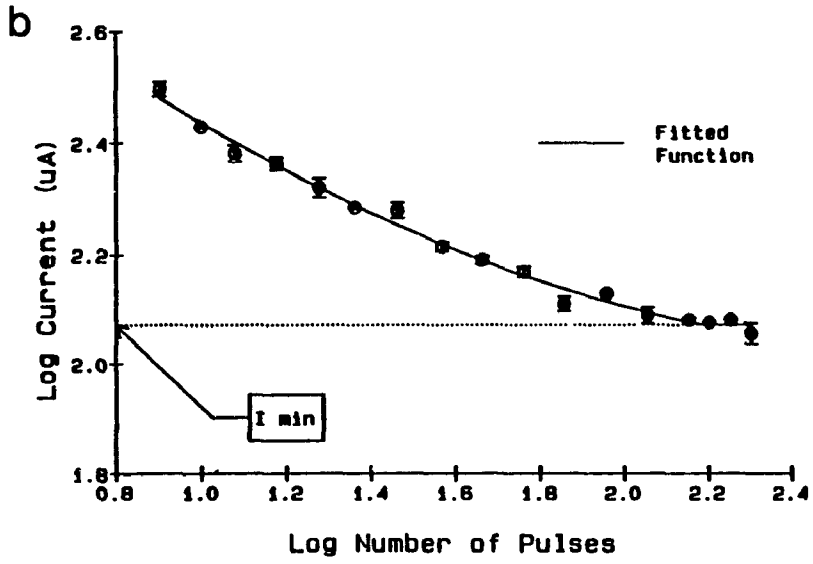
b
Log Current (uA)
2.6
2.4
2.2
2.0
1.8
0.8
1.0
1.2
1.4
1.6
1.8
2.0
2.2
2.4
Log Number of Pulses
Fitted Function
I min

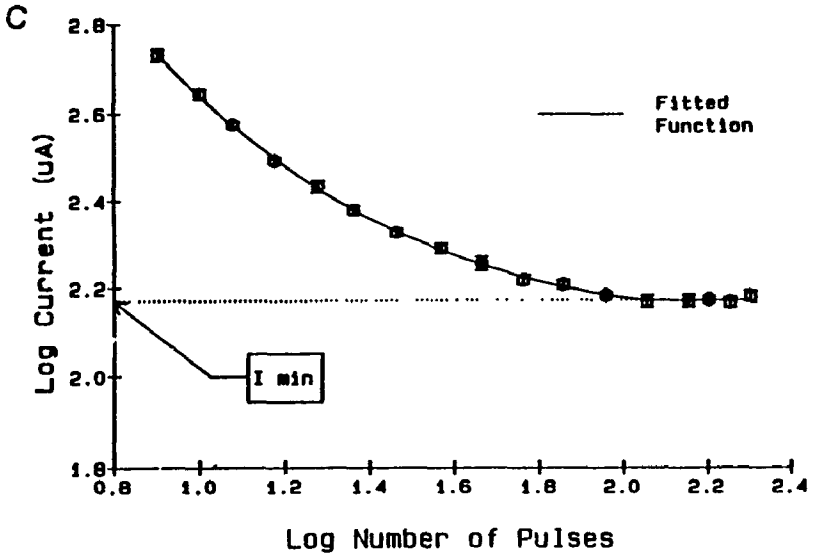
c
Log Current (uA)
2.8
2.6
2.4
2.2
2.0
1.8
0.8
1.0
1.2
1.4
1.6
1.8
2.0
2.2
2.4
Log Number of Pulses
Fitted Function
I min

"good fit". I_{min} was again taken to be the current at which the two segments intersected (Figure 5b).

If this second-order polynomial function was found to be inadequate, the process was repeated using a third-order, and if necessary, a fourth-order polynomial to describe the descending portion of the curve (Figure 5c).

Depth profiles. In order to evaluate how substrate sensitivity changed with depth of electrode penetration, and whether such profiles might depend on the selection of arbitrary values for the stimulation parameters, two related analyses were undertaken. First, a series of profiles were constructed to reflect the results which might have been obtained had the value of current been held constant at each site, and rate-frequency functions determined. Three different values of current were chosen, and the number of pulses corresponding to each was calculated by interpolation from the trade-off functions (Figure 6a). To compare the results to those of Rompré and Miliaressis (1985), I used a criterion current of approximately 200 μA ($antilog_{10}$ 2.30) and then bracketed this in equal logarithmic increments by using criterion currents of $antilog_{10}$ 2.15 (approximately 141 μA) and $antilog_{10}$ 2.45 (approximately 282 μA). For some animals, a value of $antilog_{10}$ 2.00 (100 μA) was also used.

In an analogous manner the current required to sustain half-maximal responding was estimated for five different values of criterion pulse-number (Figure 6b). For the short pulse duration, logarithmic values of 1.0 (10 pulses), 1.4 (25 pulses), 1.8 (63 pulses) and 2.2 (158 pulses) were chosen so as to span the range of the trade-off function in equal logarithmic increments. An additional logarithmic criterion number of 1.2 (16 pulses) was also used for the purposes of making a comparison between the two pulse duration conditions (see below).

Effects of varying pulse duration. In order to assess whether the trade-off functions collected at a pulse duration of 1000 μs differed from those collected at 100 μs at each site (i.e. whether the two taken at the same site were of the same functional form) another curve-fitting procedure was employed. The rationale for the procedure was as follows. First, because the required current is reduced at each frequency when the pulse duration is lengthened, the curve taken at 1000 μs will be shifted down the ordinate from that taken at 100 μs, and this makes it difficult to compare the two curves. Therefore, the amount of this shift was first estimated by determining the value of an additive constant needed to shift the 1000 μs curve along the ordinate to overlap the 100 μs curve. Once this was known, it was reasoned that if

Figure 6.

Example of calculating the required value of either current or pulse number (dependent parameter) at a fixed value of the independent parameter: (a) required number calculated by interpolation from the trade-off curve at a fixed value of criterion current, and (b) required current calculated by interpolation from the trade-off curve at a fixed value of criterion number.

a

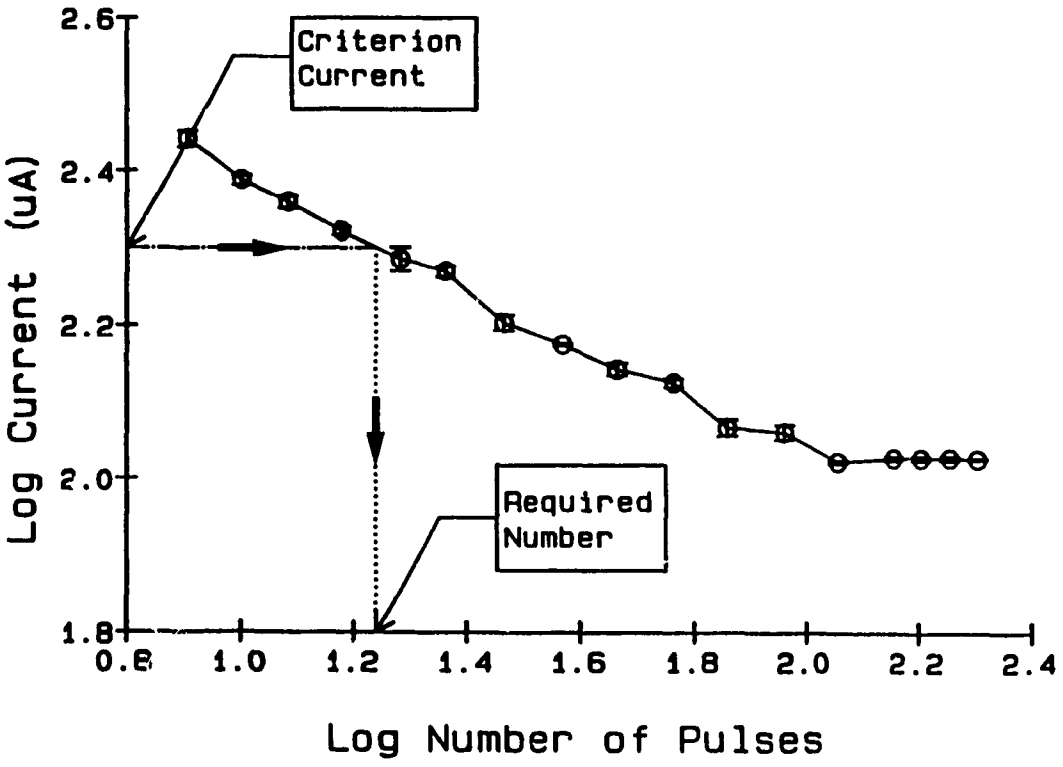
Criterion
Current
Required
Number
Log Current (uA)
2.6
2.4
2.2
2.0
1.8
0.8
1.0
1.2
1.4
1.6
1.8
2.0
2.2
2.4
Log Number of Pulses

b

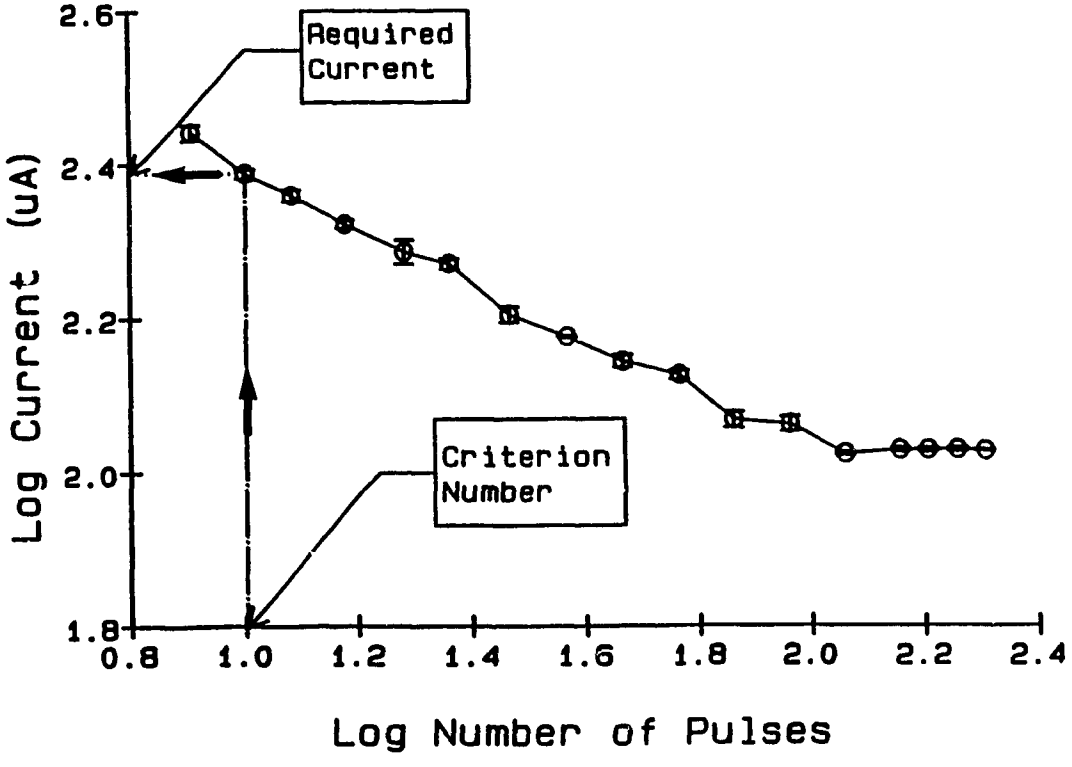
Required
Current
Criterion
Number
Log Current (uA)
2.6
2.4
2.2
2.0
1.8
0.8
1.0
1.2
1.4
1.6
1.8
2.0
2.2
2.4
Log Number of Pulses

there were no change in shape between the two curves, then the best-fitting function which describes the 100 μs data should also describe the 1000 μs data when it has been transformed by the addition of this constant.

The first step in the procedure was to select a smaller subset of the 100 μs data to use in the comparison, because the number of frequencies tested was greater than for the 1000 μs condition. Functions of progressively higher-order were then fit to this truncated 100 μs data set until the function which best described its shape was determined. The criteria for selecting the best-fitting function were the same as those previously described for estimating I_{min}. That is, the best-fitting function was the one for which the magnitude of the residual error variance was small, and for which visual inspection of the graph of residual error terms and the plot of the function fitted to the data, revealed no systematic deviations. As in the previous analyses, no a priori prediction was made as to the functional form which would best fit the data.

Once this function had been determined, it was transformed by adding a constant term. For example, if the function was a second order polynomial, the transformed function would be $[(a + bx + cx^2) + K]$. This transformed function was then fit to the 1000 μs data (using the same coefficients) in order to estimate the value of the additive constant. The 1000 μs data were then transformed

by adding the value of K to the required current and plotted on a graph with the 100 μs data and the fitted function. Visual inspection of both this graph, and a graph of the residual error terms was used to assess whether the 1000 μs data deviated systematically from the trade-off curve taken at 100 μs.

In order to assess the effects of varying the pulse duration between sites, depth profiles were calculated in the same way as outlined above for the 100 μs data. For the 1000 μs data, logarithmic values of the number of pulses (1.0, 1.2 and 1.4) were chosen to span the range of the trade-off function. The values differ from those used for the 100 μs condition due to the narrower range of pulse numbers tested at 1000 μs, and the variation in highest pulse number tested across subjects in this latter condition.

Results

Topographical Data

Mapping data in the form of current-number trade-off functions were collected for a total of eight animals and are presented along with histological reconstructions of the tested sites in Figures 7 through 14. The format of each figure is the same. Trade-off functions are plotted on the left hand side, with the depth of electrode penetration at which each function was determined given in the graph key to the right of this plot. The colour of each curve is matched to the colour of the corresponding circle on the histological reconstruction at the far right, with open circles referring to sites at which self-stimulation could not be elicited. The number above the enlargement refers to the distance posterior to bregma (in mm) according to the Paxinos and Watson (1986) stereotaxic atlas. All other histological measurements also refer to the scale used in this atlas. The zero reference point for the dorso-ventral scale is defined by Paxinos and Watson (1986) as "the horizontal plane passing though bregma and lambda on the surface of the skull". All depth measurements in this thesis are referenced to this plane.

Figure 7 shows the mapping profile for subject PM10. The final location of the electrode tip was 4.80 mm posterior to bregma, 1.40 mm lateral to the midline, and

8.90 mm ventral. Self-stimulation could not be elicited at three sites above the medial lemniscus, and although sniffing and exploration were observed at the next two sites in the dorsal medial lemniscus, the first site at which self-stimulation could be elicited was located at the ventral border of this structure (7.62 mm).

At sites from 7.62 to 7.94 mm ventral, severe stimulation-induced movements characterized by backward rearing occurred with high pulse numbers. These movements precluded testing of the full range of pulse numbers and thus the trade-off functions are truncated at the point beyond which it was deemed unsafe to test.

The first site at which a complete trade-off function could be collected was located at 8.10 mm ventral, at the border of the substantia nigra, pars compacta (SNC). Clockwise circling was observed during delivery of the priming stimulation at all sites along the border of the VTA and this behaviour became more rapid as the pulse number was increased. Note that with the exception of the last site tested, there is more separation between the functions at low pulse numbers than at high values.

It is possible that the electrode insulation may have been damaged in this subject as there was evidence of non-localized blue staining along the electrode track above the marking lesion made at the last site tested.

Figure 7.

Current-number trade-off data (pulse duration = 100 μs) and the histological reconstruction of tested sites for Subject PM10. Trade-off curves are plotted on the left of the figure, with the values in the graph key corresponding to the depth of electrode penetration. The colour of each curve is matched to the circles on the histological profile at the right, with open circles referring to sites where self-stimulation could not be elicited. The number above the enlarged section refers to the distance posterior to bregma (in mm) according to the Paxinos and Watson atlas (1986).

Abbreviations: VTA = ventral tegmental area; SNR = substantia nigra, pars reticulata; ml = medial lemniscus; R = red nucleus.

PM10

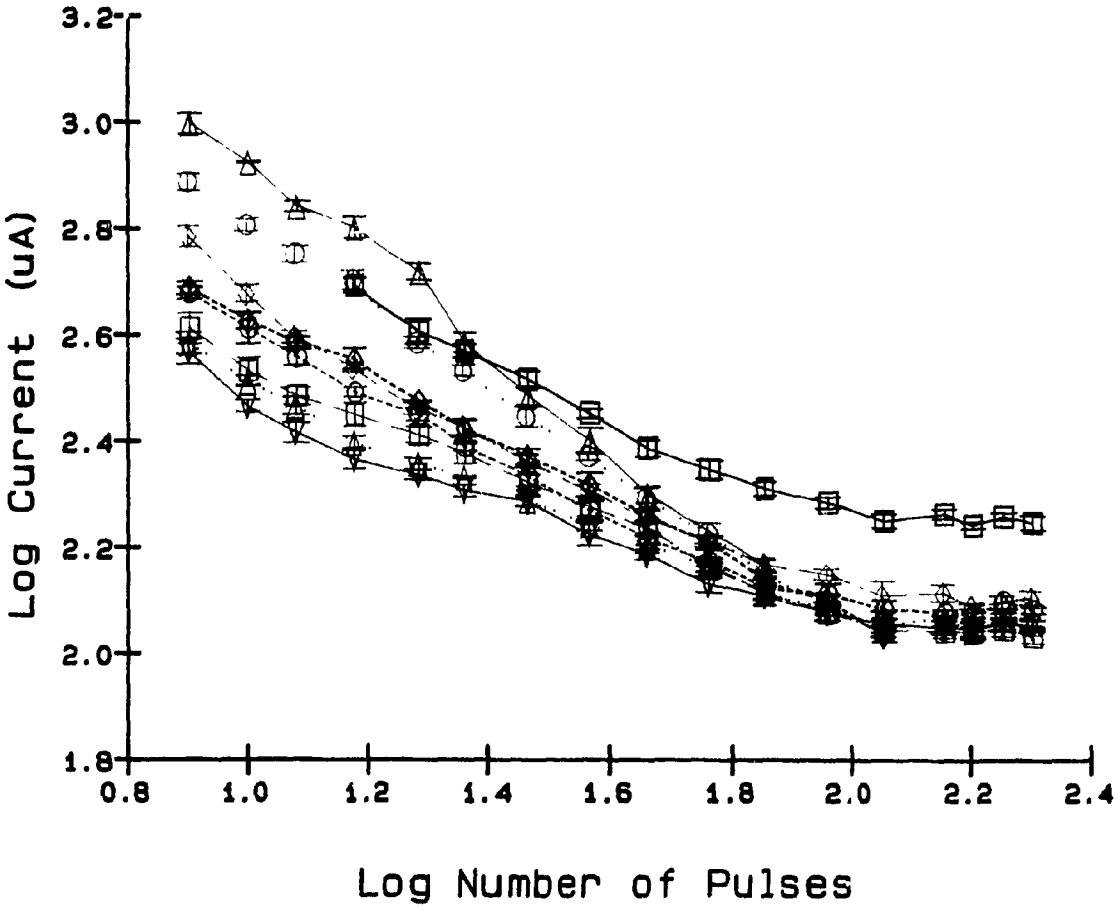
3.2
3.0
2.8
2.6
2.4
2.2
2.0
1.8
Log Current (uA)
0.8
1.0
1.2
1.4
1.6
1.8
2.0
2.2
2.4
Log Number of Pulses

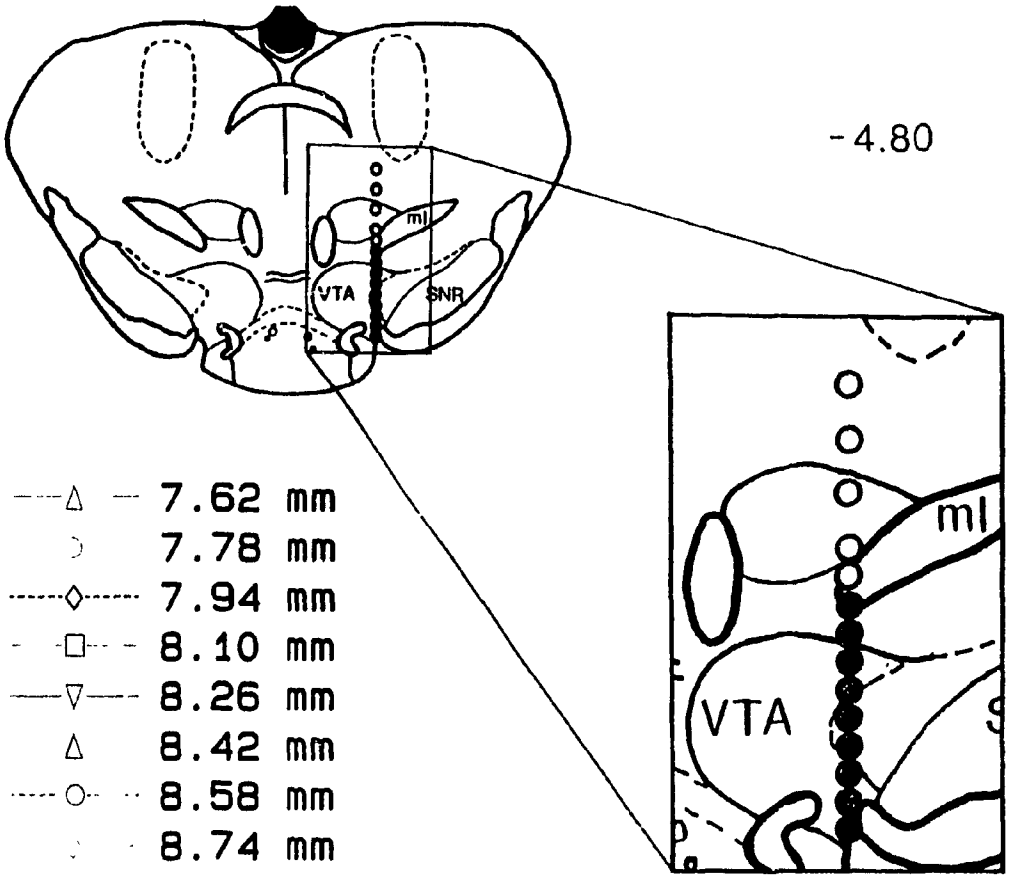
-4.80
ml
VTA
SNR
ml
VTA
7.62 mm
7.78 mm
7.94 mm
8.10 mm
8.26 mm
8.42 mm
8.58 mm
8.74 mm
8.90 mm

Unfortunately, due to an error in the perfusion and de-braining process, the electrode was not available for examination post-mortem.

Figure 8 shows the mapping data for subject PM1. The electrode track was found just lateral to that of subject PM10 at the same rostro-caudal level (1.50 mm from midline, 8.50 mm ventral). Four sites at which self-stimulation could not be elicited lay dorsal to, and within the medial lemniscus. The first positive site was located at the dorsal border of the VTA (7.86 mm). Considering the number of sites at which self-stimulation was elicited for PM10, (sites dorsal to the first site at which it was observed in this subject), and given that PM1 was the first subject tested in this study, it is possible that insufficient training may account for the negative sites recorded dorsal to the VTA.

The trade-off functions do not show a consistent relationship to each other over the range of pulse numbers tested. Depending on which part of the functions are considered, a different conclusion can be drawn concerning the relative sensitivity of the BSR substrate at the different sites. At low values of pulse number the stimulation is most effective at 8.18 mm, while at the highest values of pulse number, the most sensitive sites are dorsal to this at 7.86 and 8.02 mm. Furthermore, note that as the electrode progresses, the functions begin to

Figure 8.

Current-number trade-off data and the histological reconstruction for Subject PM1.

PM1

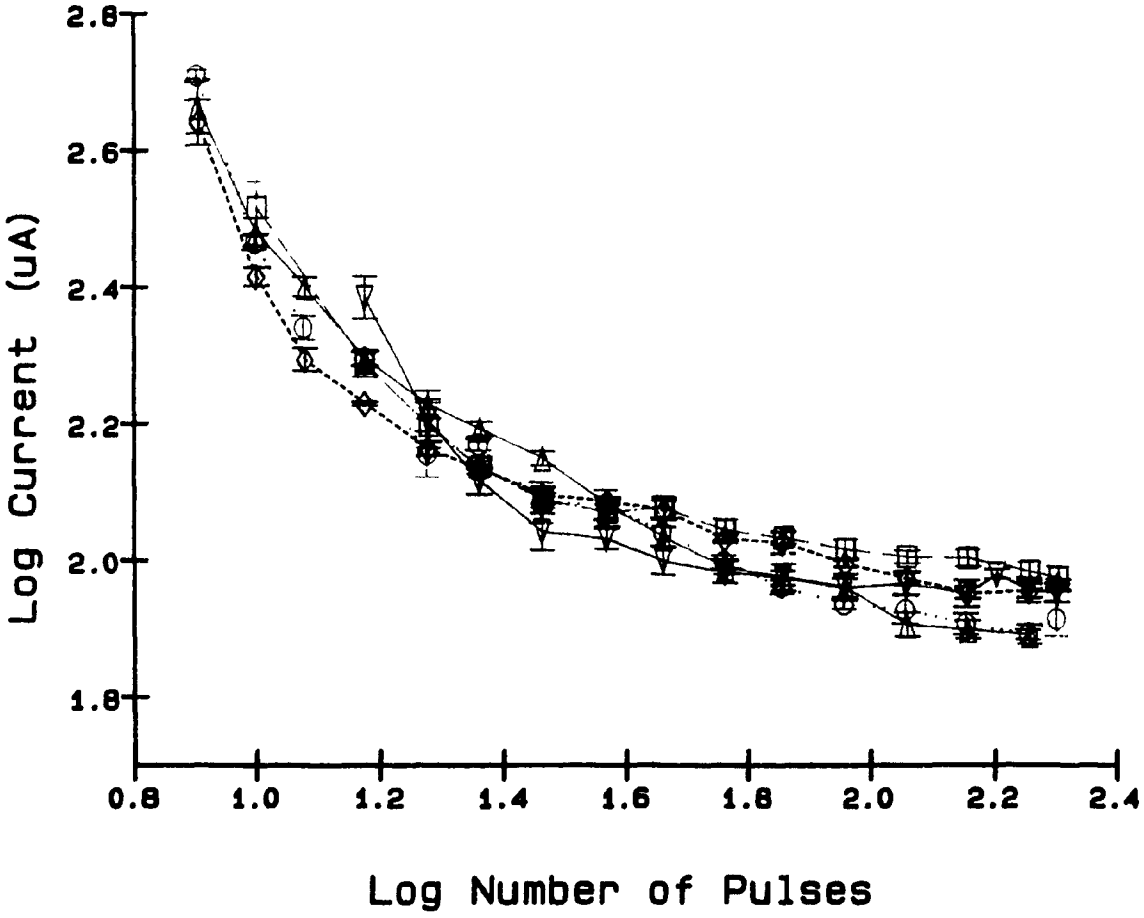
2.8
2.6
2.4
2.2
2.0
1.8
Log Current (uA)
0.8
1.0
1.2
1.4
1.6
1.8
2.0
2.2
2.4
Log Number of Pulses

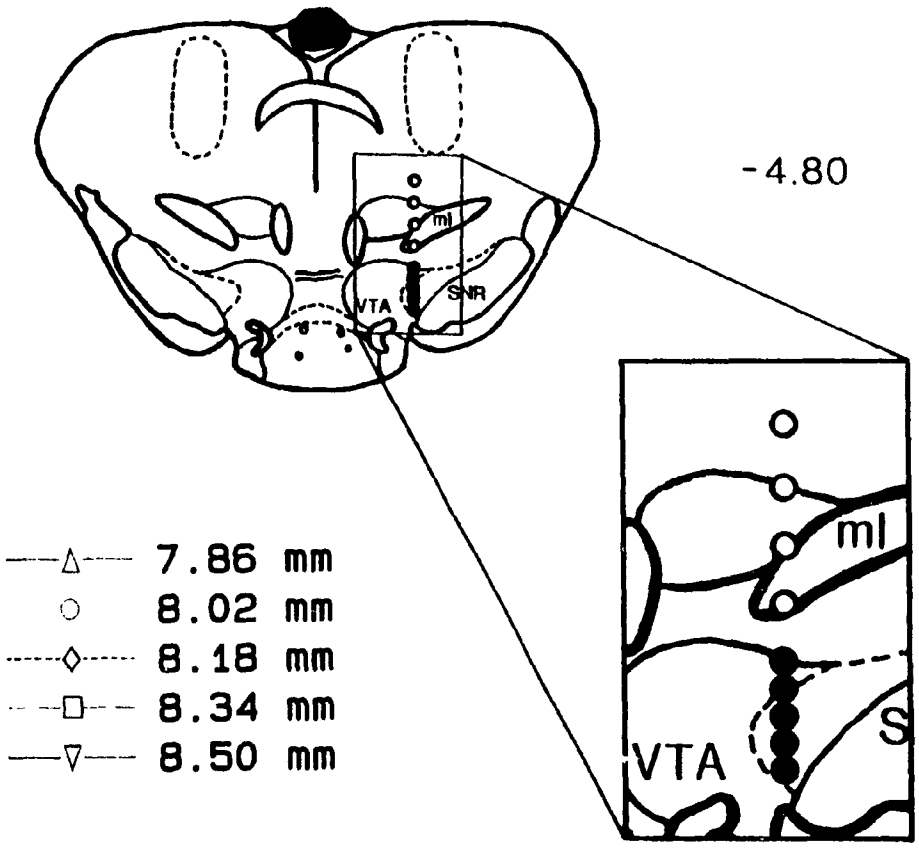
-4.80
ml
VTA
SNR
ml
VTA
S
7.86 mm
8.02 mm
8.18 mm
8.34 mm
8.50 mm

bend, indicating that the greatest sensitivity occurs over the mid-range of pulse numbers tested (See Figure 12--subject PM8). Unfortunately this animal lost its electrode assembly at 8.50 mm and could not be examined further. Because of this, location of the last site was inferred from the end of the electrode track.

Figure 9 shows the mapping data for subject F1. The final position of the electrode tip was just posterior to that of PM10 at 5.20 mm posterior to bregma, 1.00 mm lateral to the midline and 8.80 mm ventral. The first site at which self-stimulation could be elicited lies just dorsal to the pre-rubral field. Trade-off functions collected from this region (6.88 to 7.36 mm) are again truncated due to the presence of stimulation-induced movements that precluded testing the full range of pulse numbers.

Across the range of pulse numbers tested, the most sensitive sites appear to lie just ventral to the pre-rubral field, bordering the medial lemniscus. Stimulation-induced oral behaviours such as chewing were observed at these sites, and the animal exhibited clockwise circling during priming.

As the electrode passes into the VTA, there is a large decrease in stimulation effectiveness. At 8.16 mm the curves become truncated at the low pulse numbers because supra-threshold current intensities (> 1000 μA) elicited

Figure 9.

Current-number trade-off data and the histological reconstruction for Subject F1.

F1

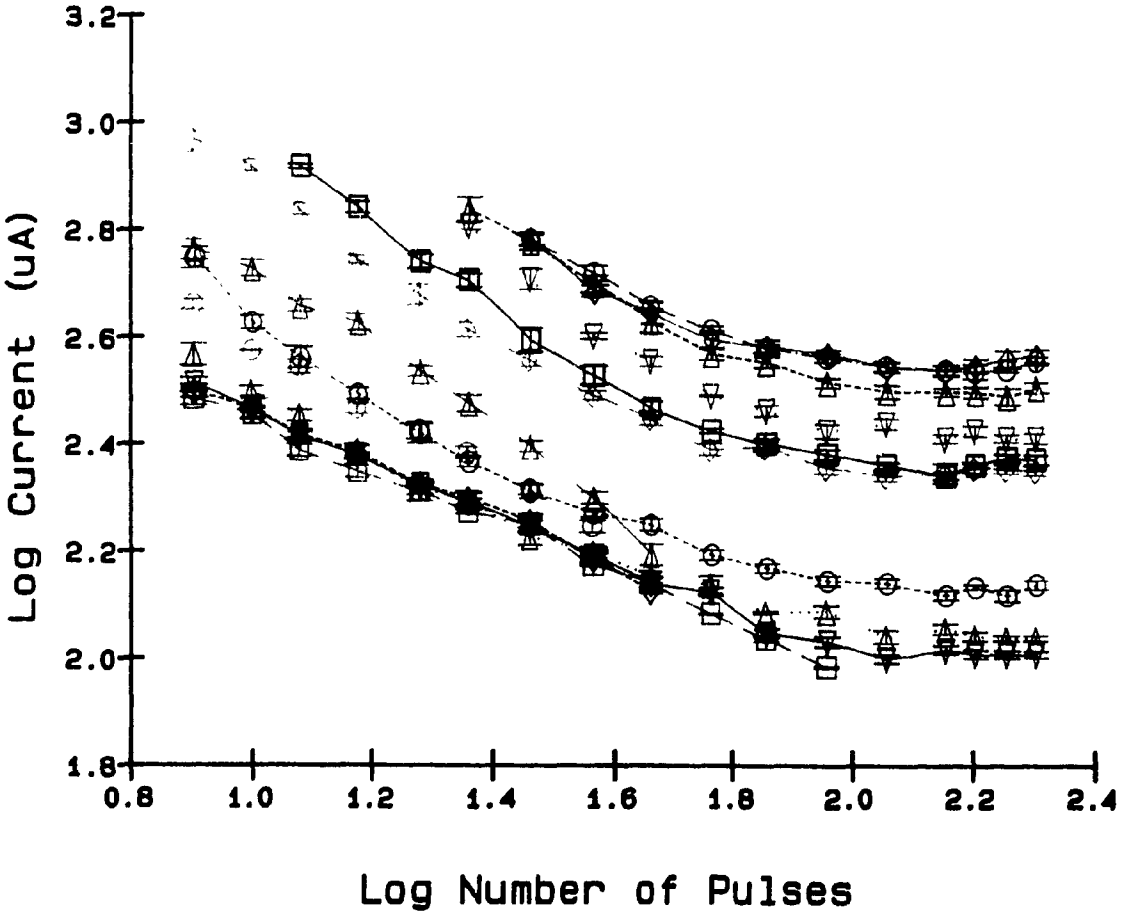
3.2
3.0
2.8
2.6
2.4
2.2
2.0
1.8
Log Current (uA)
0.8
1.0
1.2
1.4
1.6
1.8
2.0
2.2
2.4
Log Number of Pulses

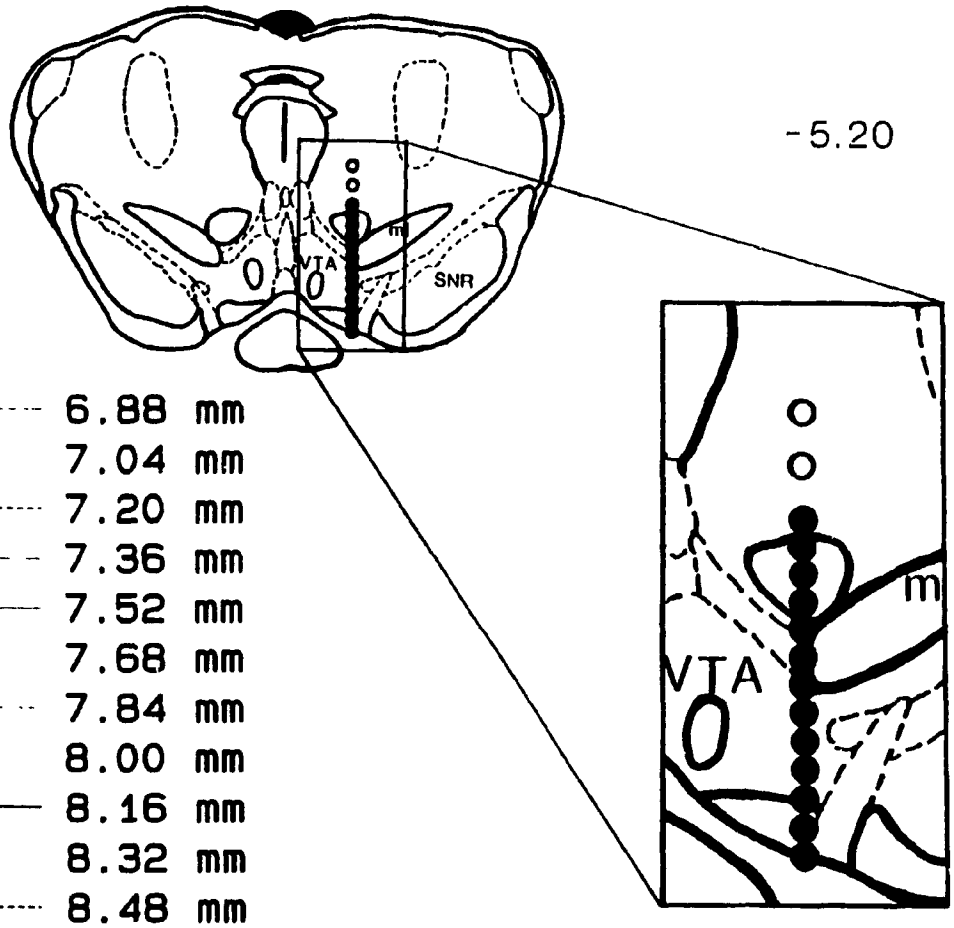

6.88 mm
7.04 mm
7.20 mm
7.36 mm
7.52 mm
7.68 mm
7.84 mm
8.00 mm
8.16 mm
8.32 mm
8.48 mm
8.64 mm
8.80 mm

aversive reactions consisting of shaking, jumping and occasional vocalization, whereas lower current did not elicit the bar-pressing response. Movements of the ipsilateral eye were also observed in this region. Interestingly, at the most ventral sites, the highest required current values recorded in this study (over the range of pulse numbers tested) were observed.

Figure 10 shows the data for subject F3. The final position of the electrode tip was in the centre of the VTA at the level of fasciculus retroflexus (5.30 mm posterior to bregma, 0.80 mm lateral to midline and 8.30 mm ventral). Self-stimulation was first elicited at sites just dorsal to the red nucleus (7.02 mm). As was the case with most subjects tested, stimulation in this region again induced vigorous movements.

The first site at which the full range of pulse numbers could be safely tested lies just at the ventral border of this structure (7.66 mm). At this, and the following site, the subject exhibited extremely high rates of lever-pressing at the lowest pulse numbers tested (e.g. > 200 presses/trial at 10 pulses ($\log_{10}(N) = 1.0$)) which diminished rapidly as the pulse number was increased. Note that as the electrode enters the VTA there is again a decrease in the effectiveness of the stimulation across the range of pulse numbers tested. Furthermore, note the change in shape of the curve taken from the last site

Figure 10.

Current-number trade-off data and the histological reconstruction for Subject F3.

F3

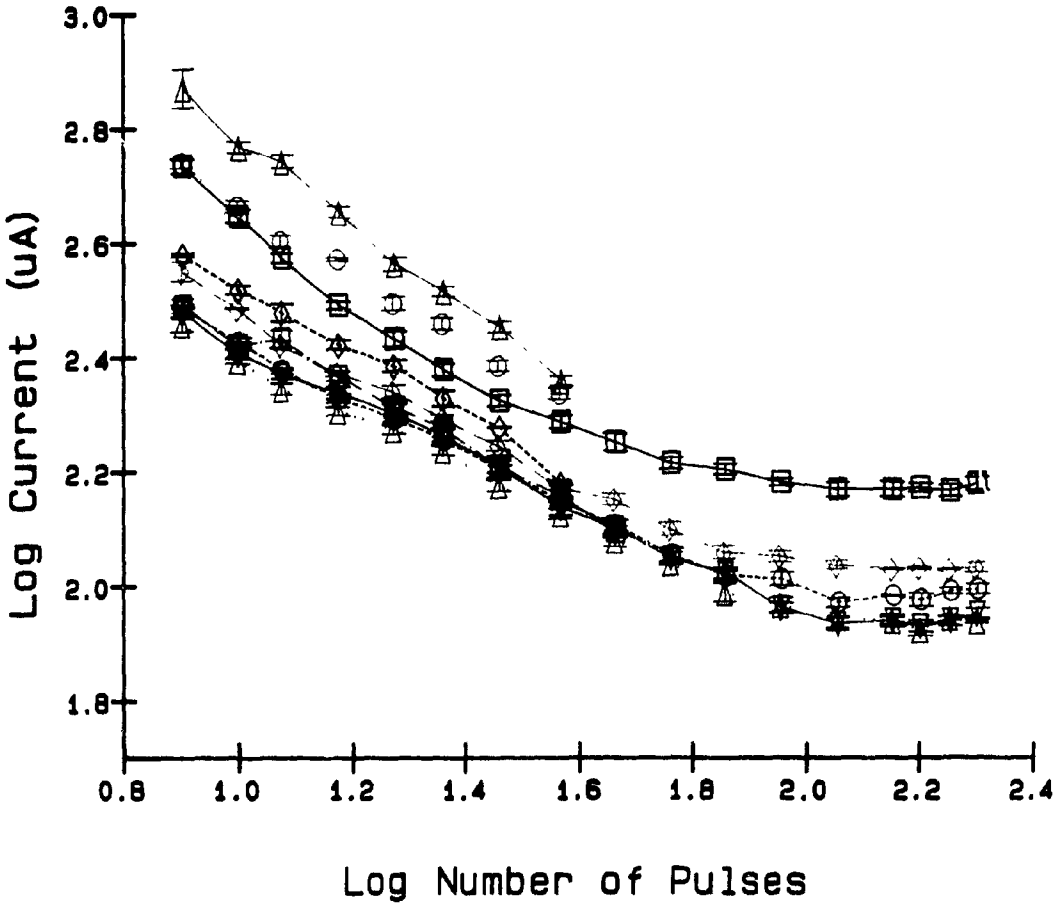
3.0
2.8
2.6
2.4
2.2
2.0
1.8
Log Current (uA)
0.8
1.0
1.2
1.4
1.6
1.8
2.0
2.2
2.4
Log Number of Pulses

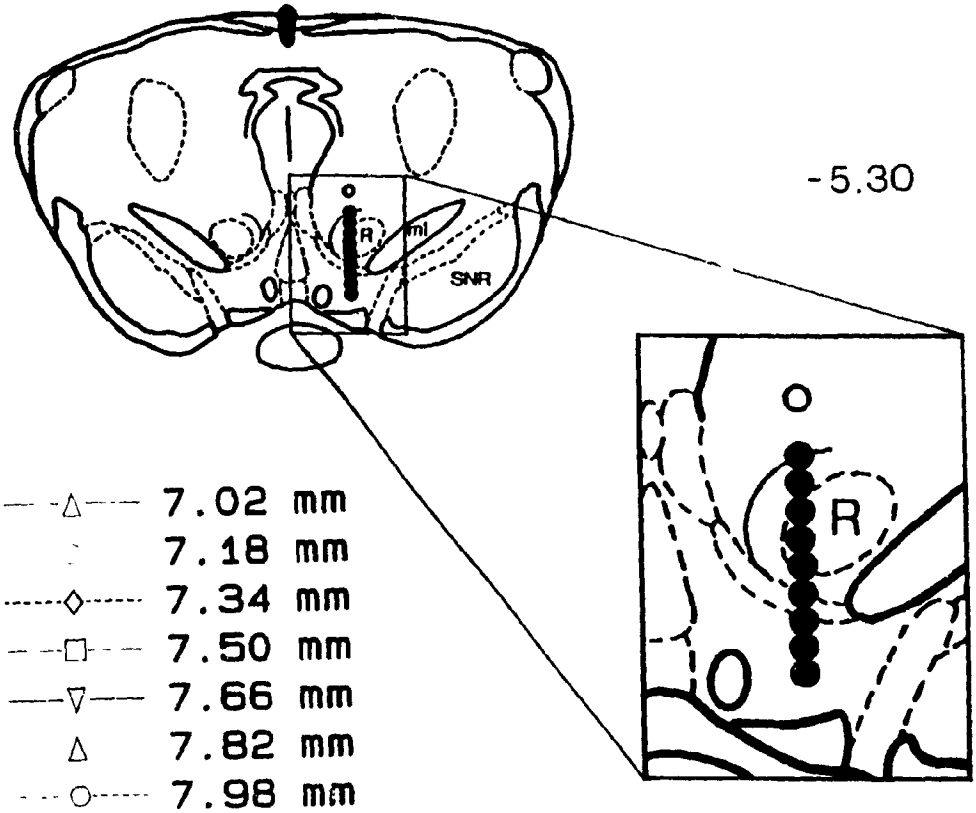

7.02 mm
7.18 mm
7.34 mm
7.50 mm
7.66 mm
7.82 mm
7.98 mm
8.14 mm
8.30 mm

tested (8.30 mm). Clockwise circling during priming stimulation was again observed at most of the sites tested.

Figure 11 shows the mapping data collected for animal R1. The electrode was found just lateral to that of subject F3 (1.15 mm from the midline) at the same rostro-caudal level. The lesion indicating the position of the electrode tip was located at the base of the brain, approximately 0.16 mm below the last site indicated on Figure 11 (8.70 mm). Data collected at the lesioned site were discarded due to an equipment failure during testing at 8.70 mm. The regression approach to analysis of variance (ANOVA) was used to determine whether data taken before and after the failure were significantly different. For subject R1, there was no significant difference in the trade-off data collected with a pulse duration of 100 µs ($p > .05$), however there was a significant difference for that collected at 1000 µs, $F(2,103) = 20.11$. $p < .05$. It was decided, based on the 1000 µs difference, that all subsequent data would be discarded. Thus, although testing continued, the data is not shown.

Self-stimulation was elicited at the first site tested (7.90 mm, within the tip of the medial lemniscus). The curves are overlapping until the electrode tip nears the base of the brain within the median terminal nucleus of the accessory optic tract (MT).

Figure 11.

Current-number trade-off data and the histological reconstruction for Subject R1.

R1

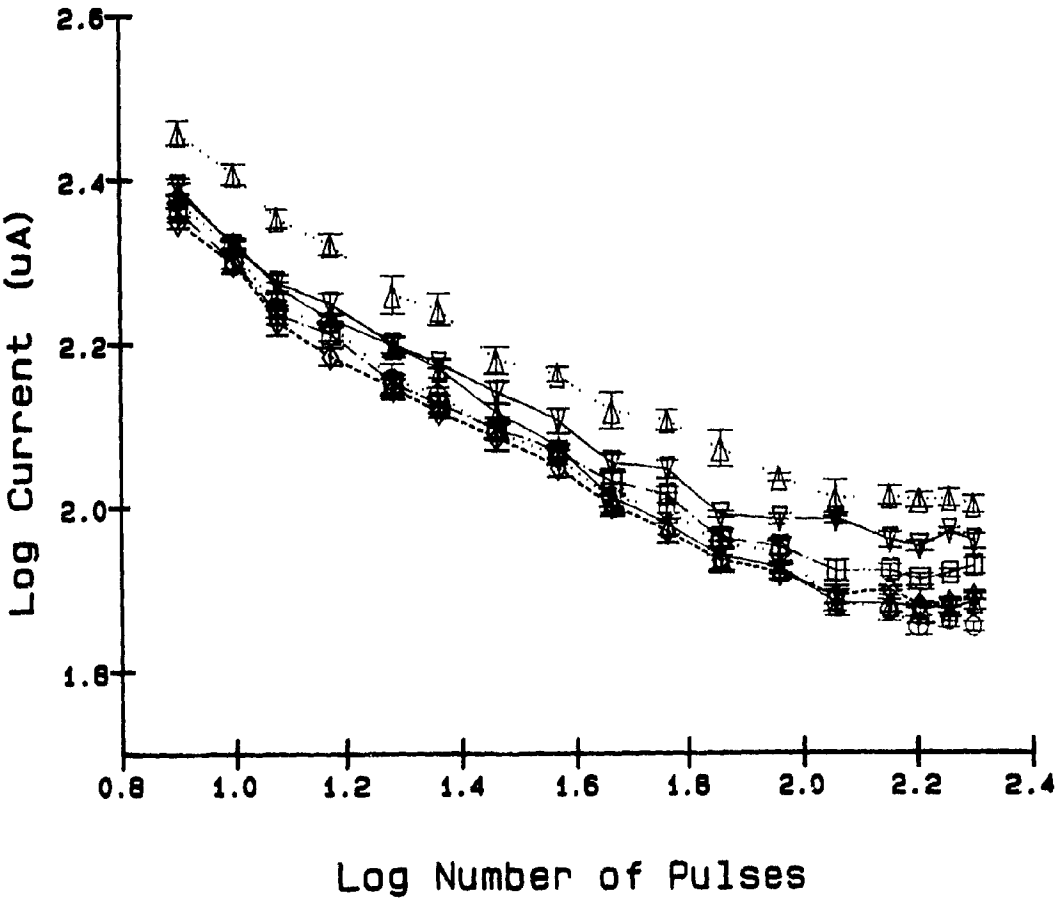
2.6
2.4
2.2
2.0
1.8
Log Current (uA)
0.8
1.0
1.2
1.4
1.6
1.8
2.0
2.2
2.4
Log Number of Pulses

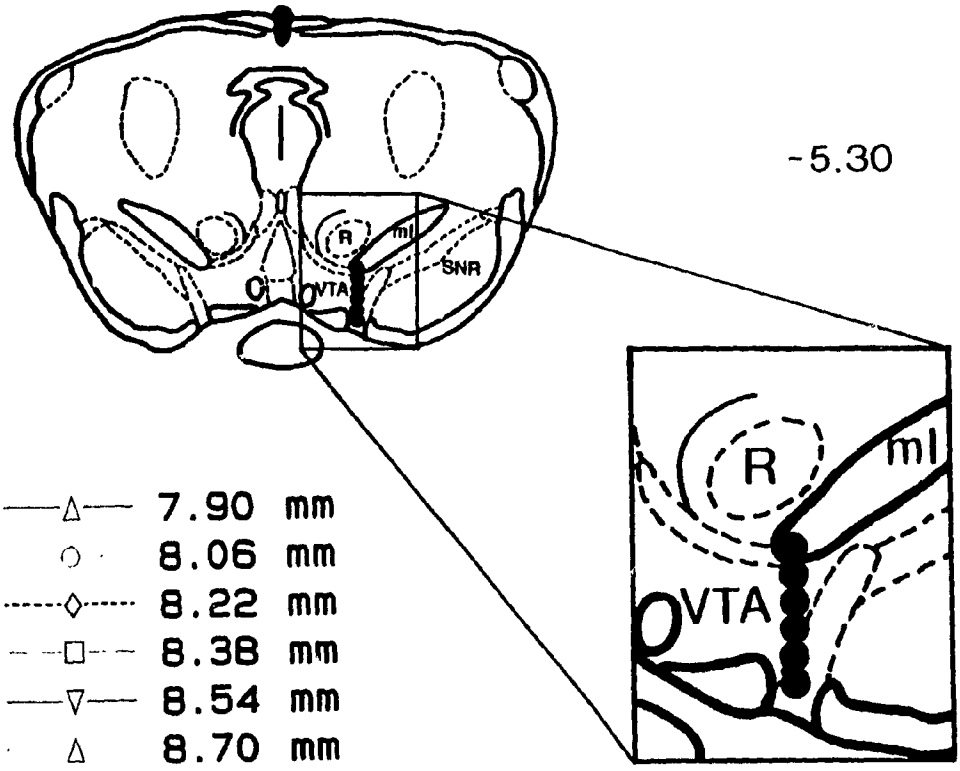
-5.30
R
ml
SNR
VTA
R
ml
VTA
7.90 mm
8.06 mm
8.22 mm
8.38 mm
8.54 mm
8.70 mm

It is interesting to compare this data set with that of the next subject, PM8, shown in Figure 12. The final position of the electrode tip was lateral to that of R1 at 1.50 mm from the midline, and 9.00 mm ventral. The electrode traversed the medial lemniscus and the medial border of the substantia nigra, pars reticulata (SNR), with the first positive site located at 8.04 mm within the tip of the MT. Although this subject also exhibited stimulation-induced movements at all sites, they were never severe enough to preclude testing of the full range of pulse numbers.

The most striking aspect of this subject's data is the crossing of the trade-off functions. As the electrode passes into and through the SNR, the descending portion of the trade-off functions changes in shape from convex to concave. This indicates that at the dorsal sites (8.04 mm to 8.36 mm), greater stimulation effectiveness is found at the highest pulse numbers tested. As the electrode is lowered, the stimulation effectiveness becomes relatively greater over the mid-range of pulse number (in particular, note the position and shape of the curve taken at 8.84 mm). It is also interesting to compare these data with those of subject PM1, where the electrode was similarly located with respect to the lateral coordinate, but was more anterior.

At the last site tested (9.00 mm), the function is truncated at the low pulse numbers. High current

Figure 12.

Current-number trade-off data and the histological reconstruction for Subject PM8.

PM8

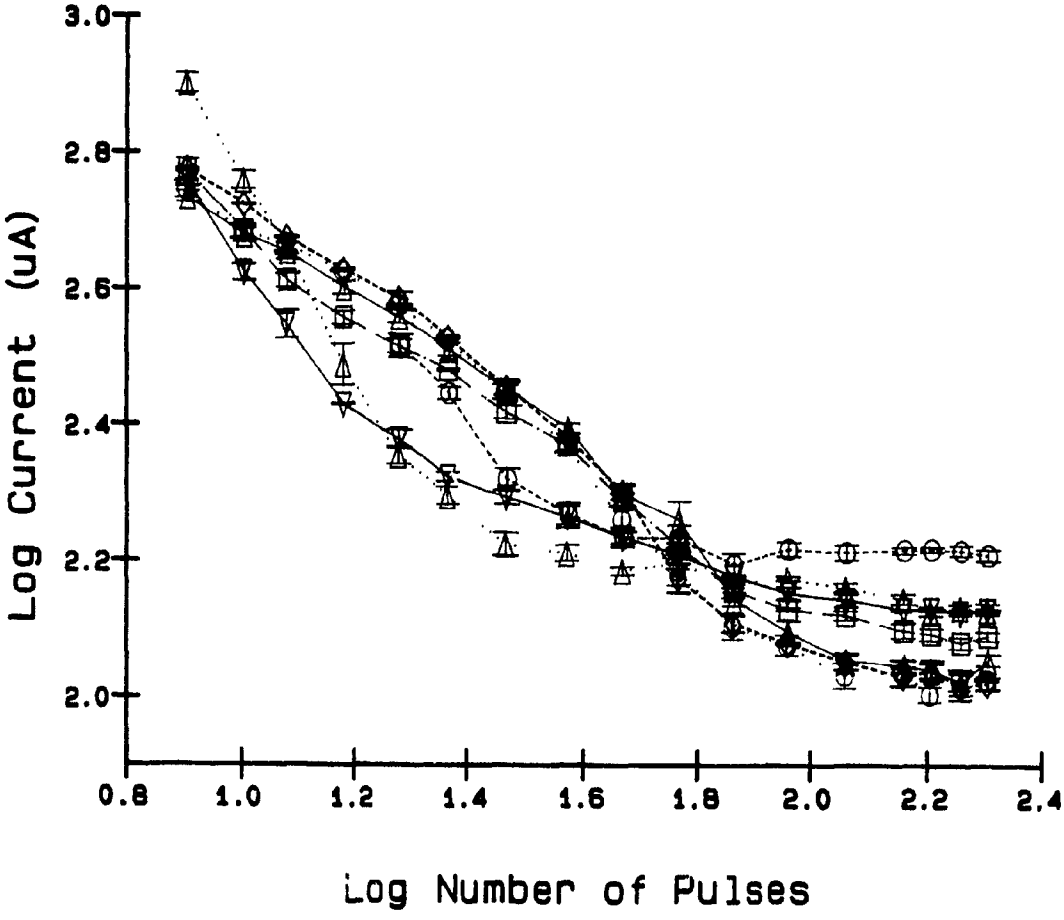
3.0
2.8
2.6
2.4
2.2
2.0
Log Current (uA)
0.8
1.0
1.2
1.4
1.6
1.8
2.0
2.2
2.4
Log Number of Pulses

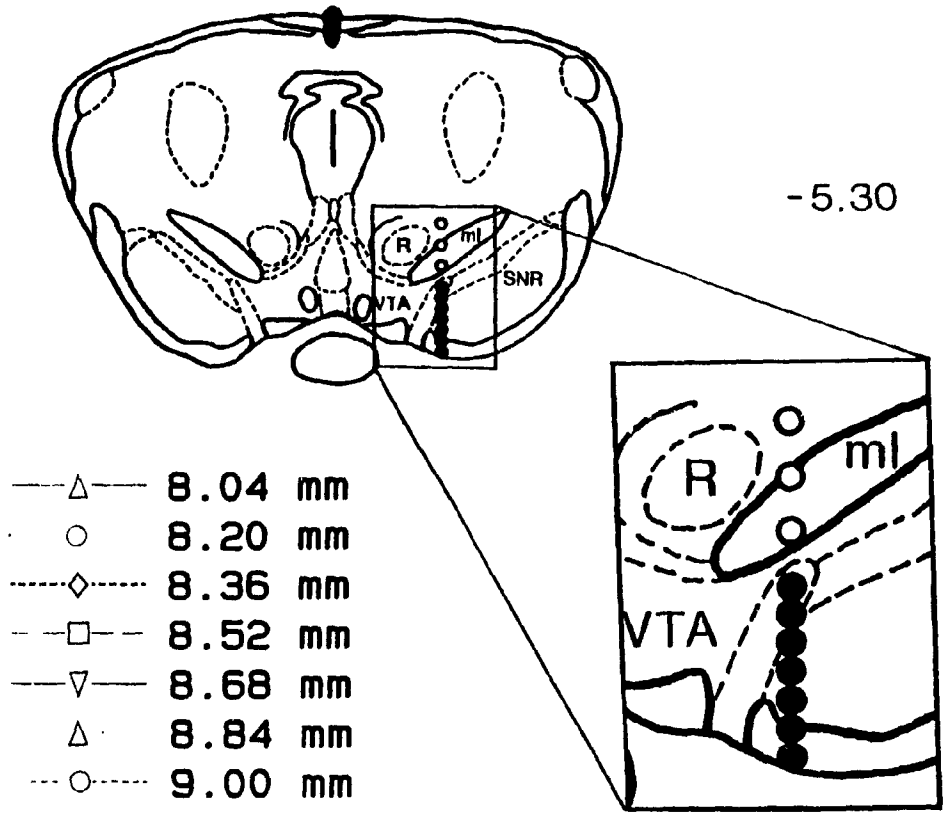
-5.30
R
ml
SNR
VTA
8.04 mm
8.20 mm
8.36 mm
8.52 mm
8.68 mm
8.84 mm
9.00 mm

(> 1000 μA) produced aversive responses and the animal could not be induced to bar-press. Whereas it was possible to collect a single determination of the required current at some pulse numbers between 8 and 15, these were discarded as it was felt that they were unrepresentative (see method section).

Figure 13 shows the mapping data for subject PM11. The electrode tip was found 5.60 mm posterior to bregma, 0.55 mm lateral to the midline, at the dorsal border of the VTA (8.40 mm ventral). The first site that supported self-stimulation was located just dorsal to the red nucleus and, as in many of the subjects, severe stimulation-induced movements characterized by backwards rearing and circling were encountered at sites throughout this region. The first site at which the full range of pulse numbers could be tested lies just within the ventral border of the red nucleus (7.76 mm). As with subjects F1 and F3, the effectiveness of the stimulation decreases as the electrode passes into the VTA (8.24 mm to 8.40 mm). Furthermore, note that the function taken at the last site (8.40 mm) is again more curved than those taken from more dorsal sites.

The most striking characteristic of these data is the extremely orderly relationship between the trade-off functions as the electrode is advanced. The functions show a consistent increase in stimulation effectiveness followed by a consistent decrease in stimulation effectiveness

Figure 13.

Current-number trade-off data and the histological reconstruction for Subject PM11.

PM11

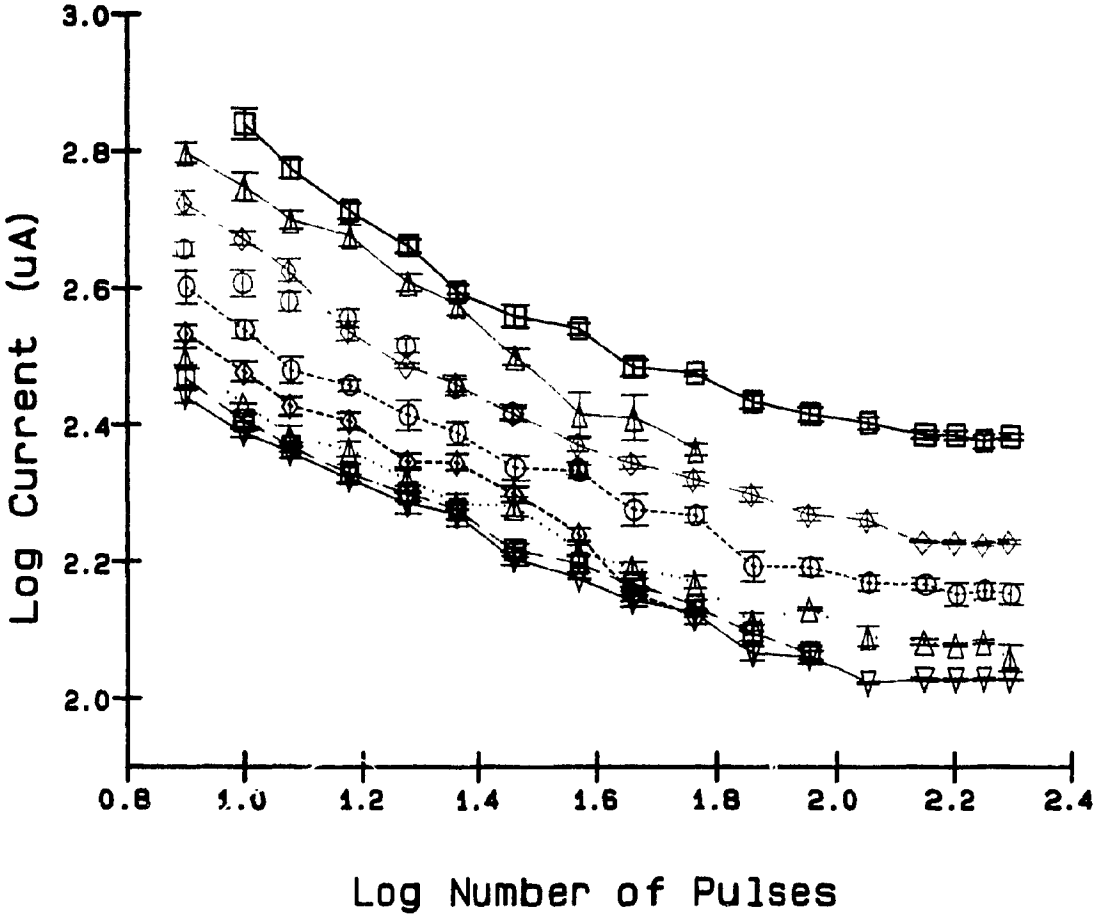
3.0
2.8
2.6
2.4
2.2
2.0
Log Current (uA)
0.8
1.0
1.2
1.4
1.6
1.8
2.0
2.2
2.4
Log Number of Pulses

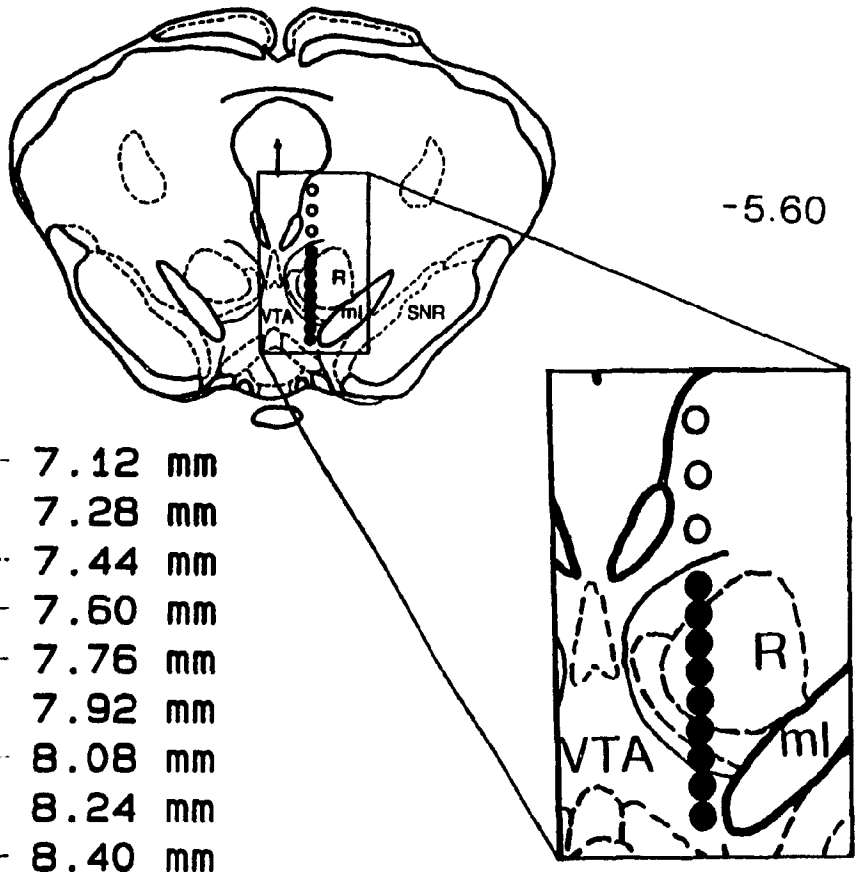

7.12 mm
7.28 mm
7.44 mm
7.60 mm
7.76 mm
7.92 mm
8.08 mm
8.24 mm
8.40 mm

(across the range of pulse numbers tested).

Figure 14 shows the mapping data for subject F4. The electrode was found to be located lateral to that of PM11 (0.90 mm from the midline) at the same rostro-caudal level. As with subject R1 the full set of data collected for this animal is not shown. The marking lesion was located at the base of the brain approximately 0.32 mm below the last site shown. Again, data collected before and after an equipment failure at 8.80 mm were deemed significantly different, (100 μs: $F(2,149)=14.58$, $p<.05$; 1000 μs: $F(2,103)=5.65$, $p<.05$), and thus functions collected at the two most ventral sites were discarded.

In contrast to the results obtained for many of the subjects, sites in the red nucleus did not support self-stimulation in this animal. The first site at which self-stimulation was elicited lay at the dorsal border of the medial lemniscus (8.00 mm). At all sites within this structure stimulation at the highest pulse numbers elicited severe movements which impaired performance. Although these movements precluded testing of the full range of pulse numbers, the point at which testing was terminated occurred at higher numbers than in other subjects (eg. F3 and F1). At the last two sites tested (8.64 and 8.80 mm), note that the functions cross the others. At the lowest pulse numbers they indicate the greatest stimulation effectiveness, while at the highest frequencies tested,

Figure 14.

Current-number trade-off data and the histological reconstruction for Subject F4.

F4

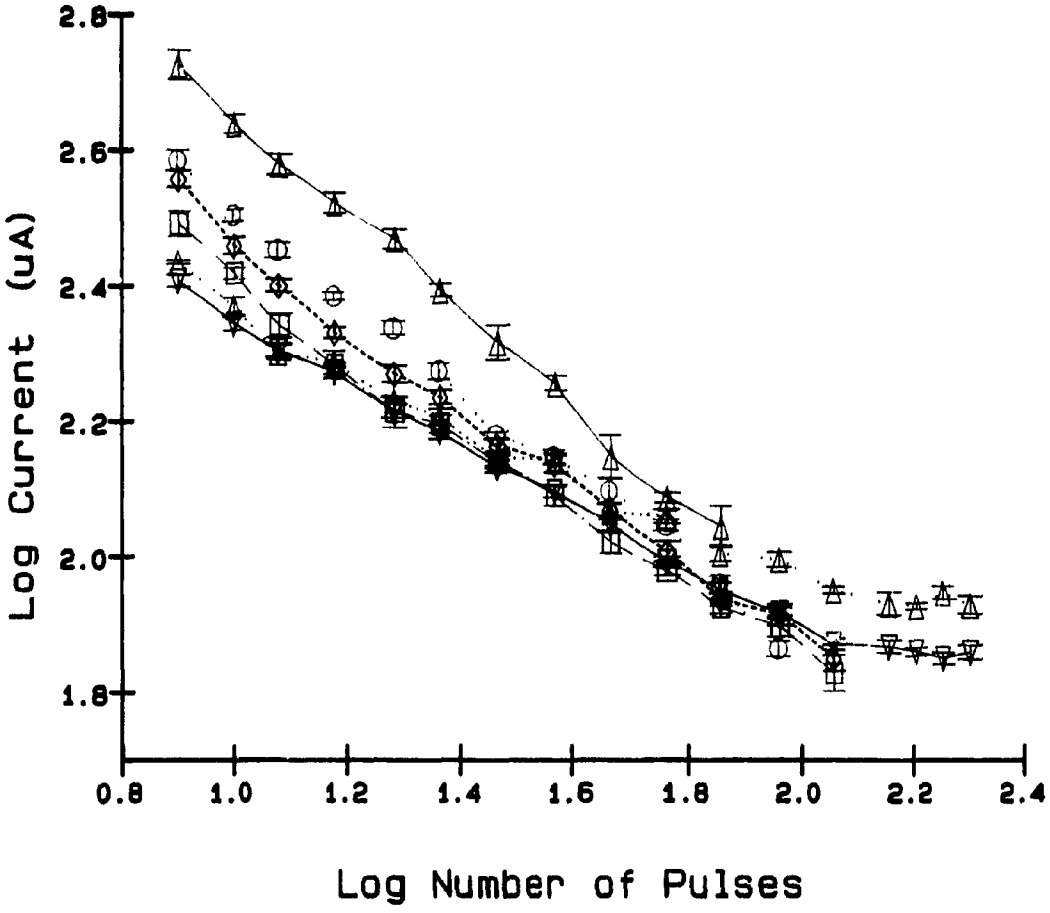
2.8
2.6
2.4
2.2
2.0
1.8
Log Current (uA)
0.8
1.0
1.2
1.4
1.6
1.8
2.0
2.2
2.4
Log Number of Pulses

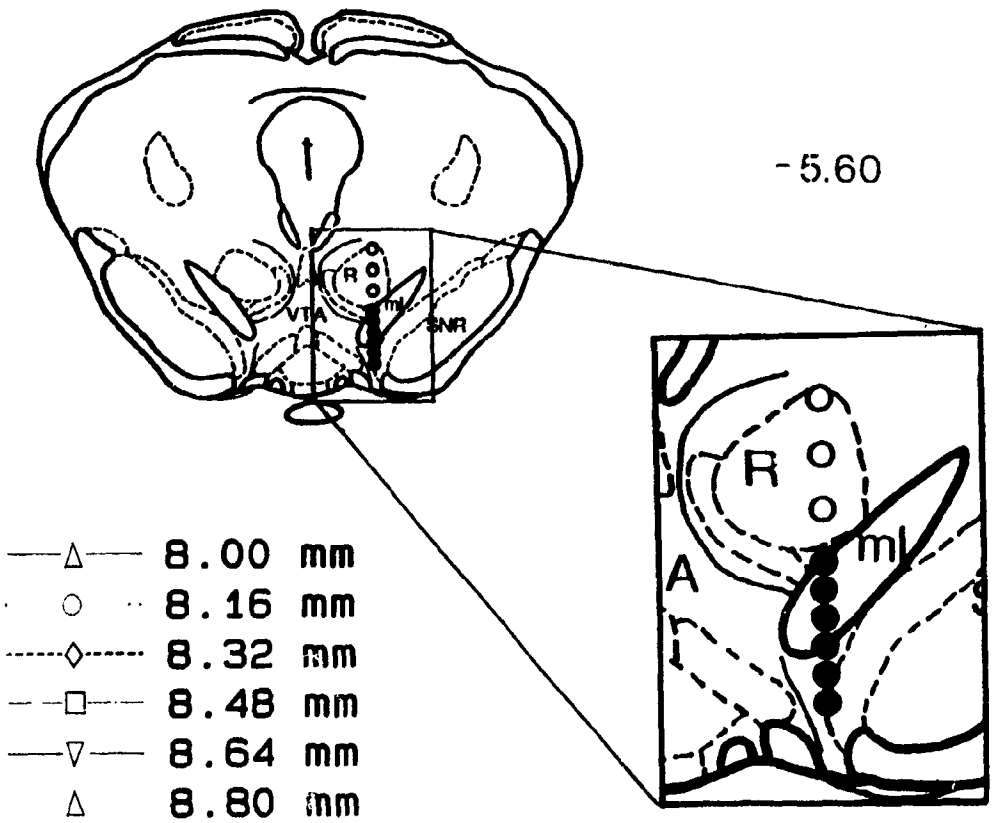
-5.60
R
VTA
ml
SNR
R
A
ml
8.00 mm
8.16 mm
8.32 mm
8.48 mm
8.64 mm
8.80 mm

they lie above the other curves.

Two additional subjects were tested at multiple sites but self-stimulation behaviour was never established. The histological profiles for these subjects are shown in Figures 15 and 16. In these figures, depth of electrode penetration is listed next to the corresponding open circle on the enlargement, and the number to the left of the full illustration indicates the distance posterior to bregma (in mm).

For subject PM6, the electrode tip was located 4.80 mm posterior to bregma, 2.30 mm lateral from the midline, and 8.70 mm ventral (Figure 15). Consistent self-stimulation behaviour could not be elicited at any of the sites tested. At 7.42 mm, just above the SNC, the animal pressed the lever but could not be trained to return following priming. Often it remained motionless at the lever after pressing once or twice. At the following sites similar behaviour was observed. The large gap between 7.42 and 8.22 mm occurred when the electrode slipped when rotating the driver.

Although lever-pressing behaviour was established at 8.38 mm the animal could not be trained and would often refuse to press the bar after 20 or 30 minutes despite repeated priming and shaping. This behaviour is similar to that observed by MacMillan et al. (1985) at sites in this region.

Figure 15.

Histological reconstruction of tested sites for Subject PM6. The numbers to the right of the enlarged section refer to the depth of the electrode position, while the number to the right of the full-size section indicates the distance posterior to bregma (in mm).

PM6

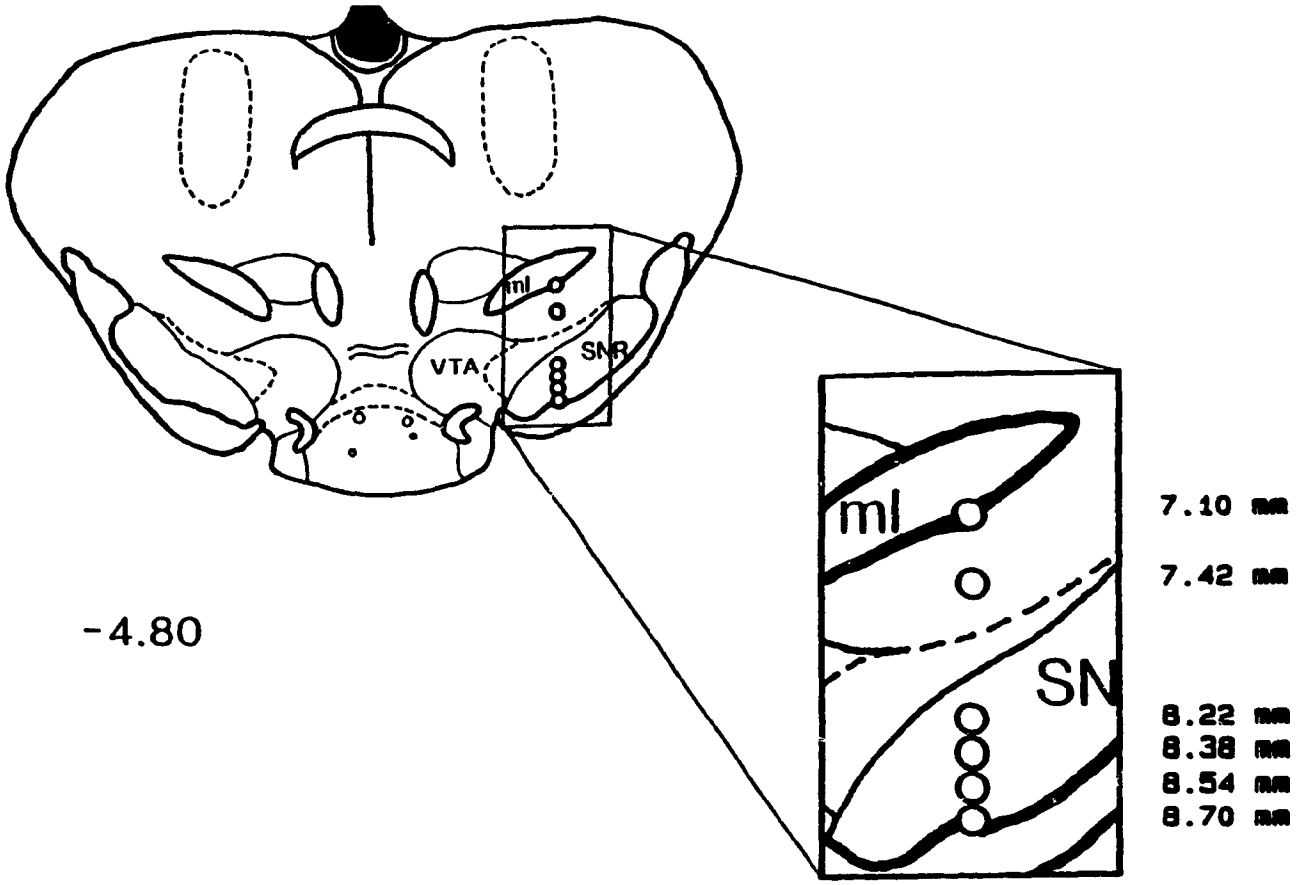

-4.80

Self-stimulation could not be elicited at any of several sites for another subject, PM9. The histological profile for this animal is shown in Figure 16. The final position of the electrode tip was located 5.20 mm posterior to bregma, 2.30 mm lateral to the midline, and 8.00 mm ventral. Stimulation at sites dorsal to the medial lemniscus produced movements of the head and neck, and high current elicited aversive reactions. Some exploration and sniffing were observed at sites within the medial lemniscus, but the subject seemed for the most part uninterested and spent the greater part of the time in the corner of the cage. Stimulation elicited escape responses (e.g. jumping) at higher values of pulse number and current. At sites in the SNC (7.68 mm) the subject pressed the lever but like PM6 would not sustain the behaviour over time. This subject also seemed to "freeze" after making a response. Often it retreated from the lever and could not be induced back even with repeated priming (i.e. 20 trains).

Figure 16.

Histological reconstruction of tested sites for Subject PM9.

PM9

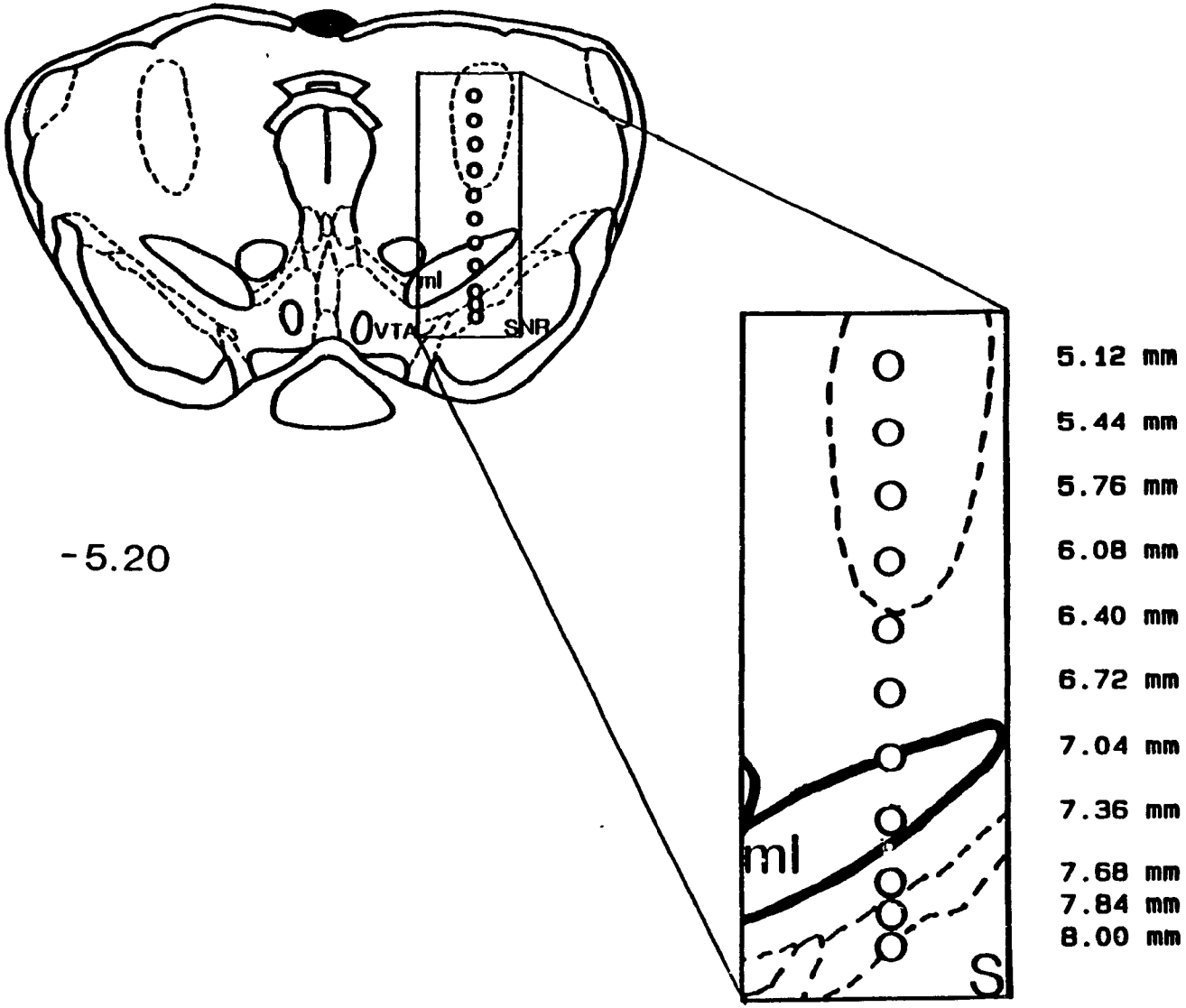
ml
VTA
SNR
ml
S
5.12 mm
5.44 mm
5.76 mm
6.08 mm
6.40 mm
6.72 mm
7.04 mm
7.36 mm
7.68 mm
7.84 mm
8.00 mm

-5.20

The Minimum Required Current

The minimum current required to elicit behaviour (I_{min}) represents one way of measuring the sensitivity of the reward substrate at a particular site, and theoretically, should yield the optimal measure of spatial resolution. In order to determine whether the results obtained using a low current can be generalized to other, higher values of current a comparison of I_{min} to the required current calculated at a low value of pulse number was undertaken at each site.

Figures 17 through 22 show this comparison for six subjects. The current required to sustain a half-maximum response rate at 10 pulses per train (logarithmic value of 1.0) was calculated by interpolation (in the logarithmic domain) from the trade-off function taken at each site. I_{min}, the value of current at which the trade-off function approaches its horizontal asymptote, was determined by the previously described curve-fitting procedure. Because the two measures have a different range of values, a transformation was performed in order to render them comparable. For each data set, (I_{min} or $Log_{10}(I)$ at $log_{10}(N) = 1.0$), the minimum value obtained was subtracted from each of the other values. This has the effect of setting the minimum value equal to zero, with the other values representing deviations from the minimum. Therefore, the two quantities now have the same unit of measurement. The

histological profile to the right of each figure illustrates the tested sites. Sites for which self-stimulation could not be elicited (open circles) are not shown on the graph.

The data for subject PM11 is shown in Figure 17. A complete set of I_{min} values could not be obtained due to the motor interference at higher frequencies at the first four sites. At sites where both measures could be calculated, they agree with respect to the site of maximum stimulation effectiveness. Furthermore, the similarity in the shape of both profiles reflects the relatively parallel nature of the trade-off functions they represent.

Figure 18 shows the data for subject F3, and again the two measures yield very similar results. Both give 7.82 mm as the most sensitive site, and the two profiles are overlapping.

The generally close agreement that these two measures give for these two subjects can be inferred by considering the form and relationship between the trade-off functions from which they were calculated. The shape of the portions involved in these calculations is independent of the depth of electrode penetration. This was not true of all subjects.

Figure 19 shows this comparison for subject PM8. Note that the two measures do not give a similar picture of the area traversed by the electrode. The maximally sensitive

Figure 17.

Comparison of two measures of substrate sensitivity, I_{min} and $Log_{10}(I)$ at $log_{10}(N) = 1.0$, for subject PM11. Depth of electrode penetration (in mm) is plotted on the ordinate. Units on the abscissa reflect the deviation of the calculated value from the minimum (which has been set equal to zero--See text for further explanation of this transformation). The histological reconstruction to the right of the graph shows the stimulation sites tested (filled circles), with the number below the profile referring to the distance posterior to bregma (in mm). Open circles refer to sites where self-stimulation could not be elicited, and are not shown on the graph.

PM11

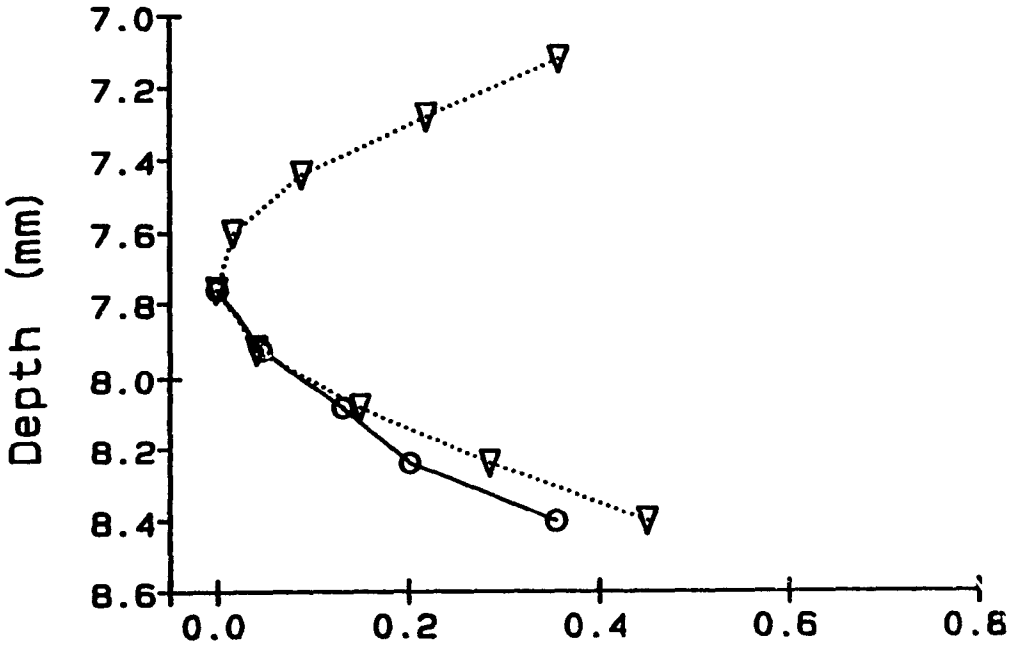
Depth (mm)
7.0
7.2
7.4
7.6
7.8
8.0
8.2
8.4
8.6
0.0
0.2
0.4
0.6
0.8
Deviation from Minimum
(log units)
I min
Log(I) at N = 1.0

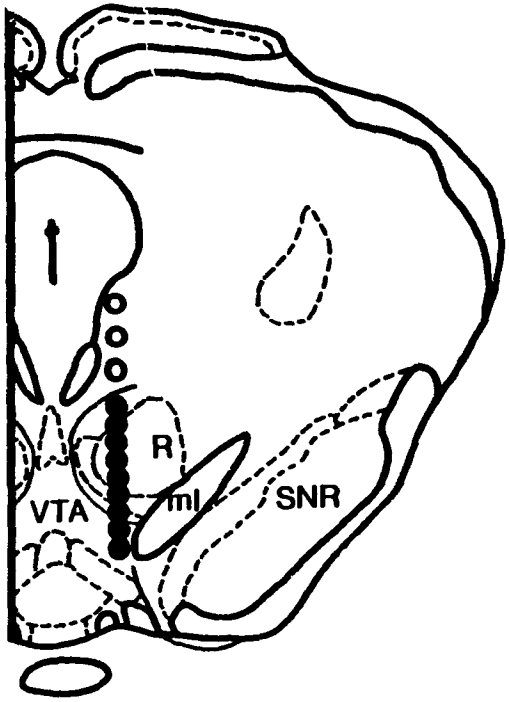
R
VTA
ml
SNR

-5.60

Figure 18.

Comparison of two measures of substrate sensitivity, I_{min} and $Log_{10}(I)$ at $log_{10}(N) = 1.0$, for Subject F3.

F3

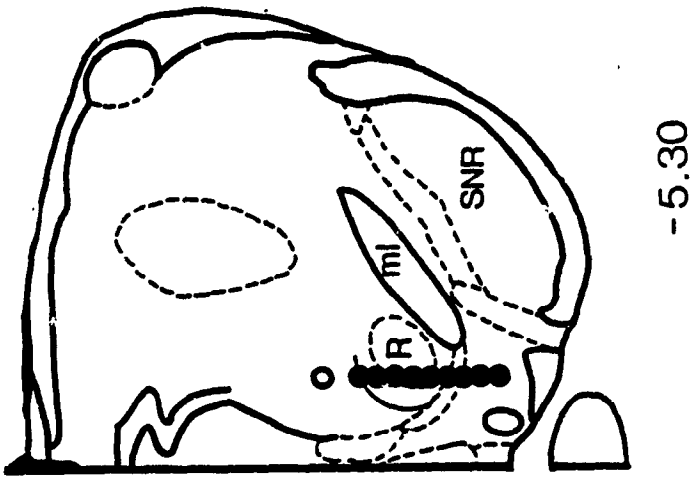
SNR
ml
R
O
-5.30

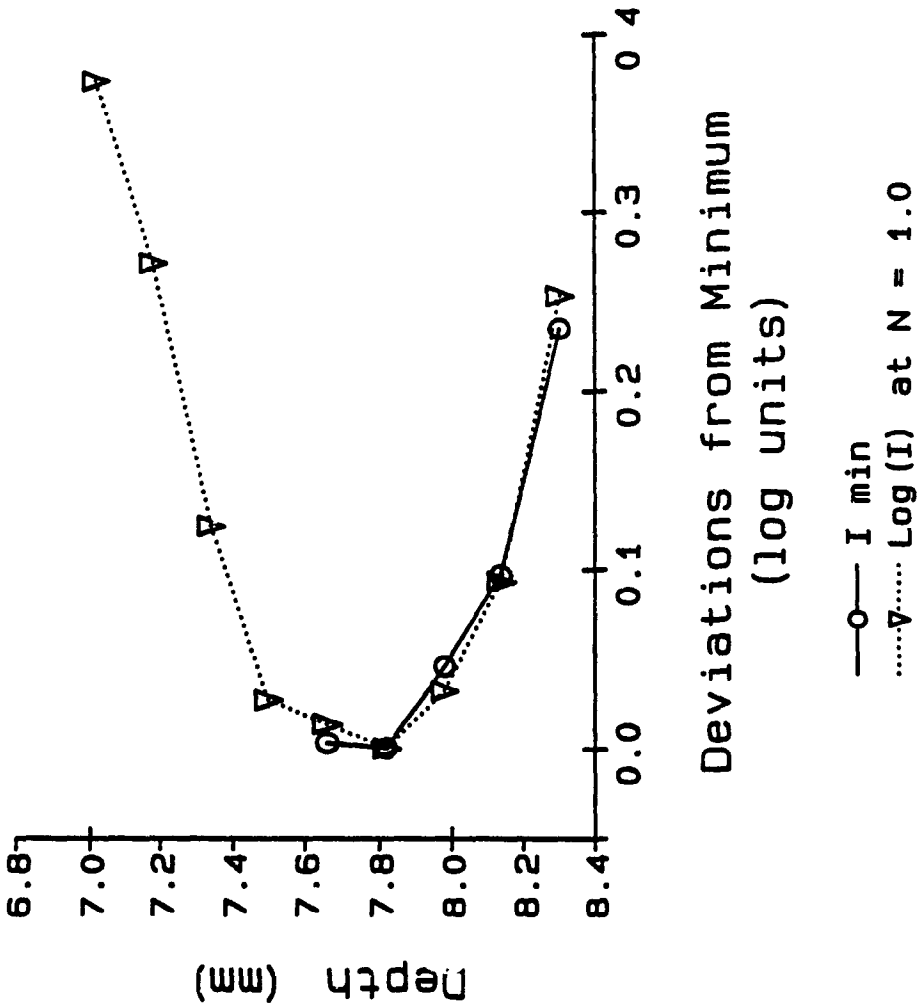
Depth (mm)
6.8
7.0
7.2
7.4
7.6
7.8
8.0
8.2
8.4
0.0
0.1
0.2
0.3
0.4
Deviations from Minimum
(log units)
I min
Log(I) at N = 1.0

Figure 19.

Comparison of two measures of substrate sensitivity, I_{min} and $Log_{10}(I)$ at $log_{10}(N) = 1.0$, for Subject PM8.

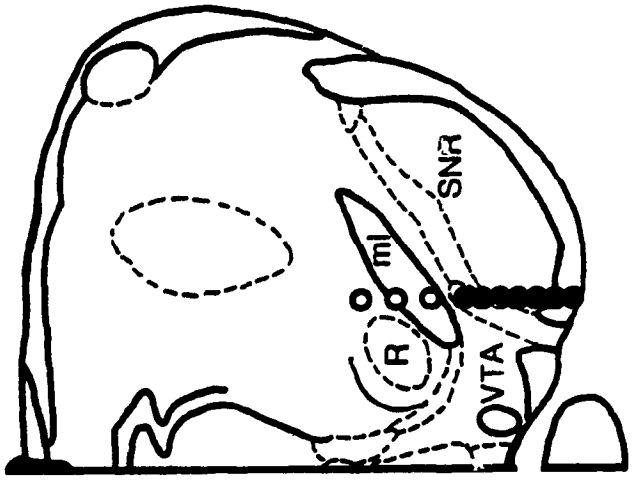
SNR
ml
R
VTA

-5.30

PM8

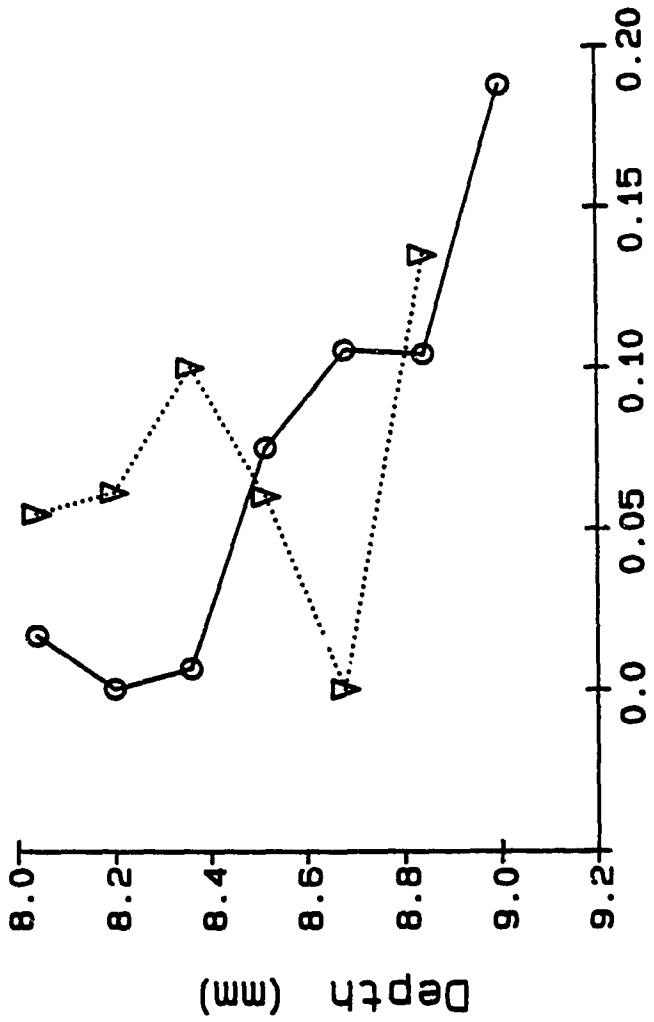
Depth (mm)
8.0
8.2
8.4
8.6
8.8
9.0
9.2
0.0
0.05
0.10
0.15
0.20
Deviation from Minimum
(log units)
I min
Log(I) at N = 1.0

site is 8.20 mm when I_{min} is measured, but at 10 pulses, the smallest $Log_{10}(I)$ value is recorded from 8.72 mm. Furthermore, the sites for which the smallest minimum current is required to support the criterion behaviour tend to be those for which the highest values of current are required at a low pulse number (with the exception of the site at 8.84 mm). Note that $Log_{10}(I)$ could not be calculated for the last site tested because the trade-off curve is truncated at the low pulse numbers.

A similar result can be seen wher considering the data from subject PM1 (Figure 20). The two measures give different pictures of the changes in substrate sensitivity with depth of electrode penetration, and both yield different estimates of the site of maximum sensitivity.

That neither of the two measures can adequately summarize the data set collected for these two subjects can again be inferred by considering the relationship between the trade-off functions which they represent. Due to their crossing, the trade-off functions do not maintain a consistent relationship over the two parts of curve from which these measures were calculated. In other words, the relationship between the parts of the curve from which they are calculated is dependent on the depth of electrode penetration (in contrast to subjects PM11 and F3, where the relationship is independent of depth).

Figure 20.

Comparison of two measures of substrate sensitivity, I_{min} and $Log_{10}(I)$ at $log_{10}(N) = 1.0$, for Subject PM1.

PM1

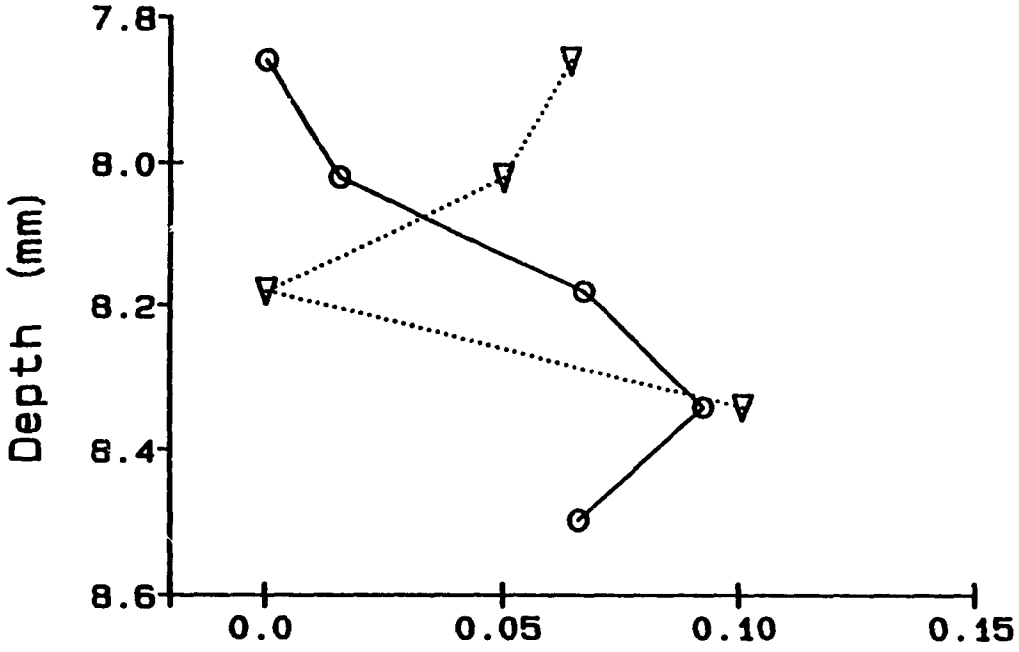
7.8
8.0
8.2
8.4
8.6
Depth (mm)
0.0
0.05
0.10
0.15
Deviation from Minimum
(log units)
I min
Log(I) at N = 1.0

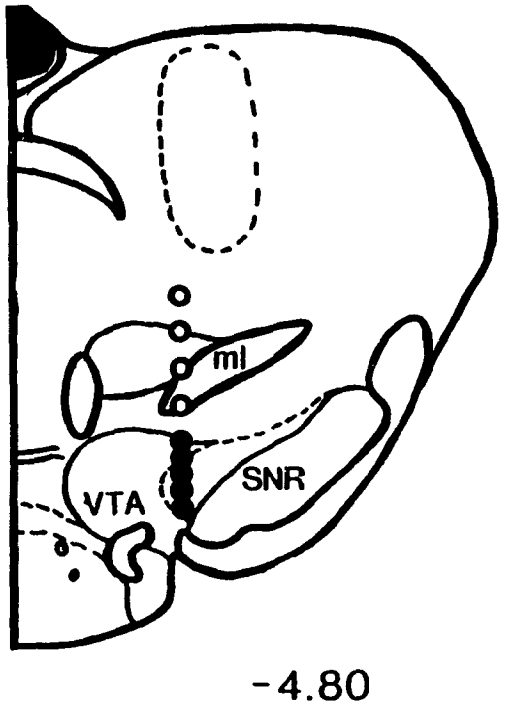
ml
VTA
SNR

-4.80

Figures 21 and 22 show the data for two additional subjects, PM10 and R1. Note that these two measures again give a different estimate of the site of maximum sensitivity. This is because, with the exception of the last site tested in each case, the trade-off functions converge (at high frequencies for PM10, and at low frequencies for R1), and some crossing is evident (see Figures 7 and 11, respectively).

An interesting phenomenon was encountered in trying to apply the curve-fitting procedure to estimate I_{min} for one subject's data (F1), a problem of a mathematical nature that I as yet do not understand. For the curves taken from 8.16 mm and 8.64 mm, although a clear asymptote is evident from visual inspection of the curves (See Figure 9), lower-order functions converged beyond the maximum frequency tested (and were thus discarded). A fourth-order function converged, but yielded a parameter set in which one of the coefficients of the polynomial was locally highly correlated with the other terms. This may indicate that the order of the coefficient in question does not contribute to improving the fit. However, because lower-order functions did not converge, the precise mathematical relationship which describes these curves cannot be determined. Work is under way to attempt to describe the relationship that does exist.

Figure 21.

Comparison of two measures of substrate sensitivity, I_{min} and $Log_{10}(I)$ at $log_{10}(N) = 1.0$, for Subject PM10.

PM10

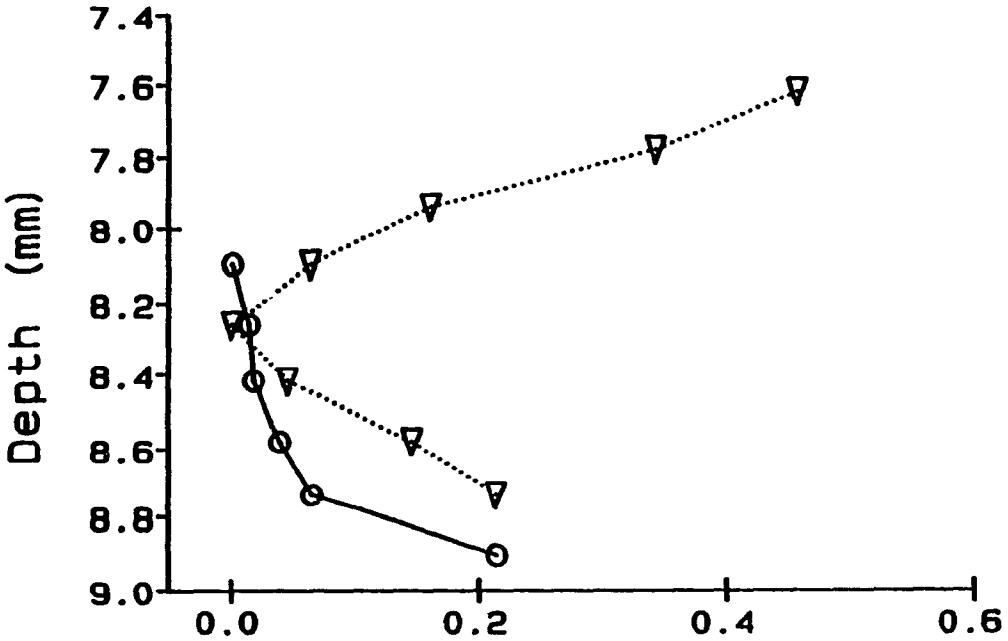
7.4
7.6
7.8
8.0
8.2
8.4
8.6
8.8
9.0
Depth (mm)
0.0
0.2
0.4
0.6
Deviation from Minimum
(log units)
I min
Log (I) at N = 1.0

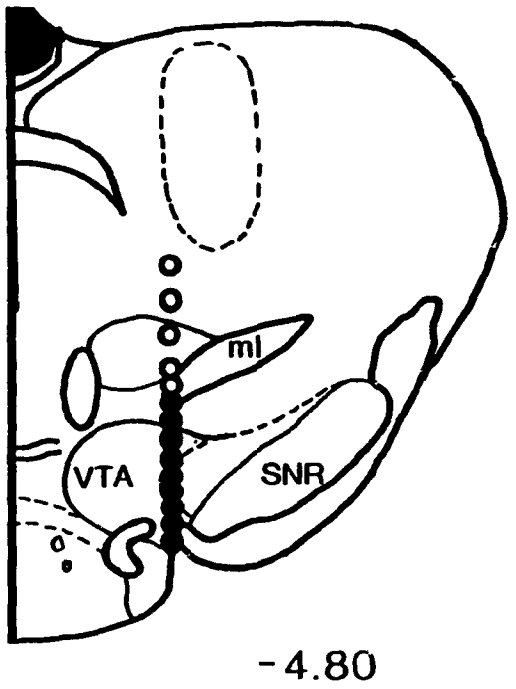
ml
VTA
SNR
-4.80

Figure 22.

Comparison of two measures of substrate sensitivity, I_{min} and $Log_{10}(I)$ at $log_{10}(N) = 1.0$, for Subject R1.

R1

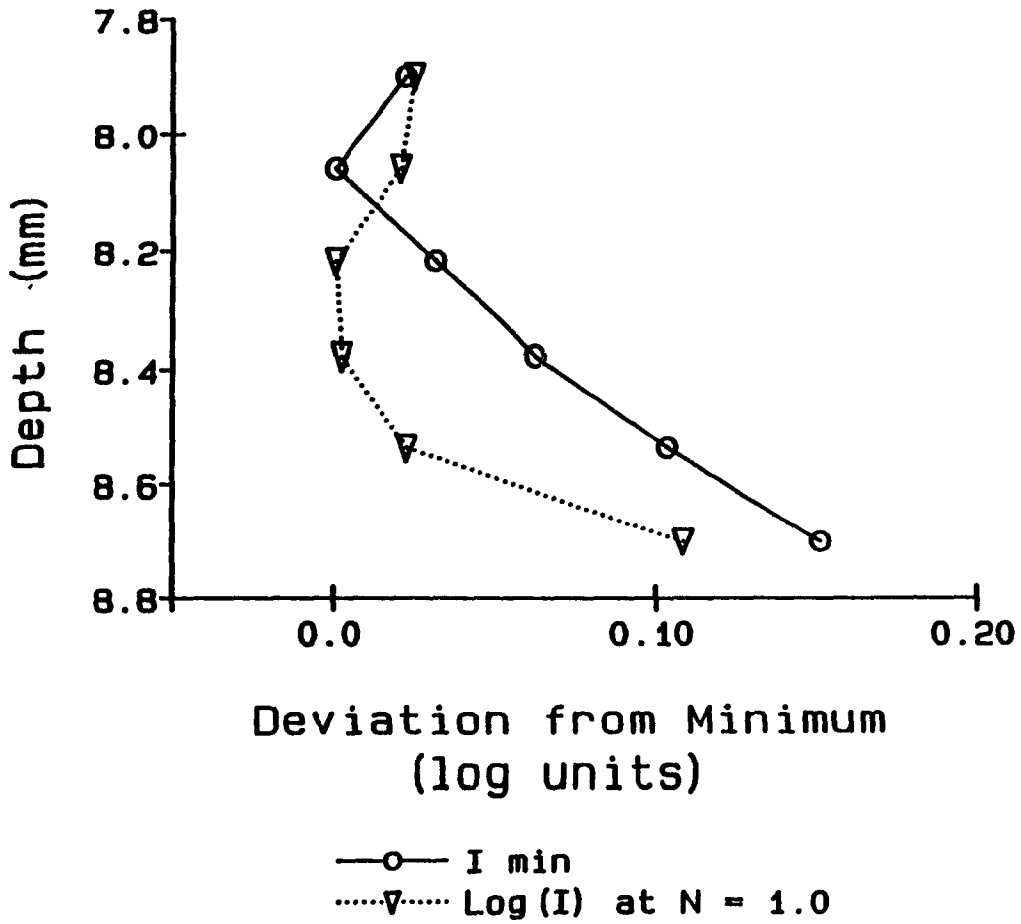
7.8
8.0
8.2
8.4
8.6
8.8
Depth (mm)
0.0
0.10
0.20
Deviation from Minimum
(log units)
I min
Log (I) at N = 1.0

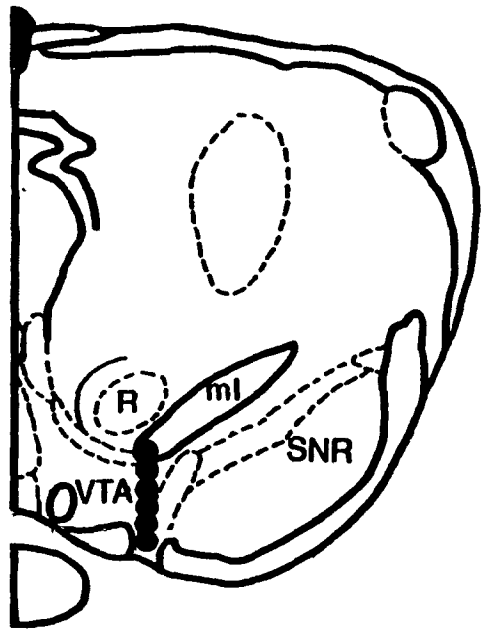
R
ml
SNR
VTA

-5.30

Evaluation of the Use of Fixed Stimulation Parameters

By collecting trade-off data at each depth examined, current and pulse number were both varied. Therefore, profiles of changing substrate sensitivity can be generated to simulate the results that might have been obtained had fixed values of either parameter been used. Figures 23 through 28 illustrate the results of these calculations for six of the subjects.

In the top panel of each figure, the number of pulses required to support half-maximal response rate has been calculated by interpolation from the trade-off functions at several arbitrary levels of current greater than I_{min} (again in the logarithmic domain). These values are listed in the graph key below each plot. The lower panel of each figure illustrates the converse. That is, the required current has been calculated for several arbitrarily chosen values of pulse number (shown in the graph key). By comparing within and between the various sets of depth profiles it is possible to assess what biases may be introduced by determining a single reward-summation function at a fixed value of either parameter, and then generalizing from this across a range of values. The histological representation to the right of the graphs shows the profile of stimulation sites tested. Sites at which self-stimulation could not be obtained (open circles) are not shown on the graph. The

data have again been re-scaled in the same manner as in the previous section.

Figure 23 shows the depth profiles for subject PM11. Consider first the required number calculated for different levels of current. Note that the corresponding number could not be calculated for several sites because the value(s) of current chosen do not intersect all trade-off functions. Therefore one might conclude that many sites did not support self-stimulation when in fact some data could be gathered. Overall, again reflecting the consistent pattern of the trade-off functions, the three profiles give a similar picture of changing substrate sensitivity with depth, and this is independent of the value of current chosen.

This agreement is even more striking when one considers current thresholds at different values of the pulse number (Figure 23, lower panel). Despite the fact that several of the chosen values again did not intersect all functions, the overlap of the various profiles indicates that regardless of which level of the fixed parameter that is chosen, the same result would be obtained.

Figure 24 shows the depth profiles for subject F3. Again, as was the case in the previous comparison, the overlap between the depth profiles is striking. First, consider the top panel, where the required number has been

Figure 23.

Depth profiles derived from the trade-off data of Subject PM11 which simulate the results that might have been obtained had fixed values of either current or pulse number been used to assess the sensitivity of the substrate at each site. In the top panel, profiles of changes to substrate sensitivity as measured by changes in the required number are shown. Each profile was calculated by interpolation from the trade-off functions at a different arbitrarily-chosen value of current (shown in the graph key below the plot). In the lower panel, profiles of changes to substrate sensitivity as measured by changes in the required current are shown. Each profile was again calculated by interpolation from the trade-off curves using a different arbitrarily-chosen value of pulse number (shown in the graph key). A histological reconstruction showing the tested sites again accompanies the two graphs.

PM11

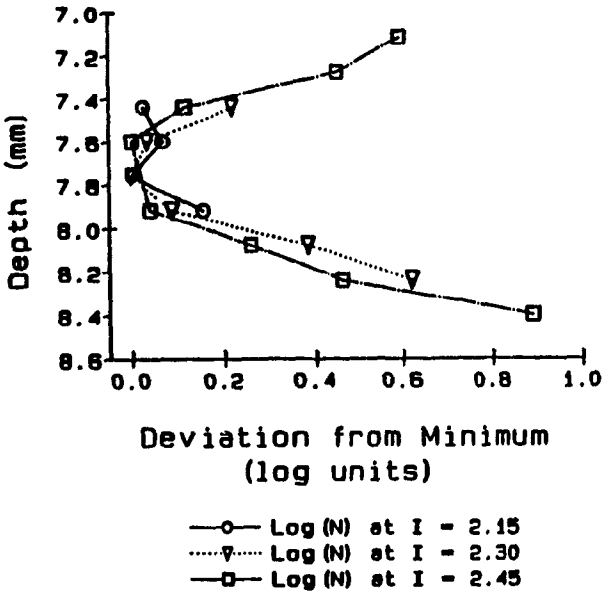
Depth (mm)
7.0
7.2
7.4
7.6
7.8
8.0
8.2
8.4
8.6
0.0
0.2
0.4
0.6
0.8
1.0
Deviation from Minimum
(log units)
Log (N) at I = 2.15
Log (N) at I = 2.30
Log (N) at I = 2.45

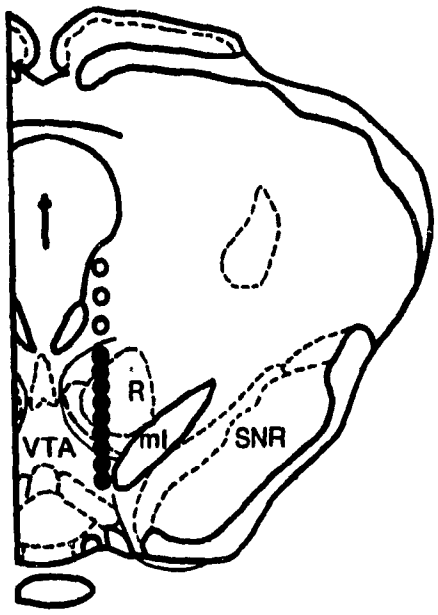
R
VTA
ml
SNR

-5.60

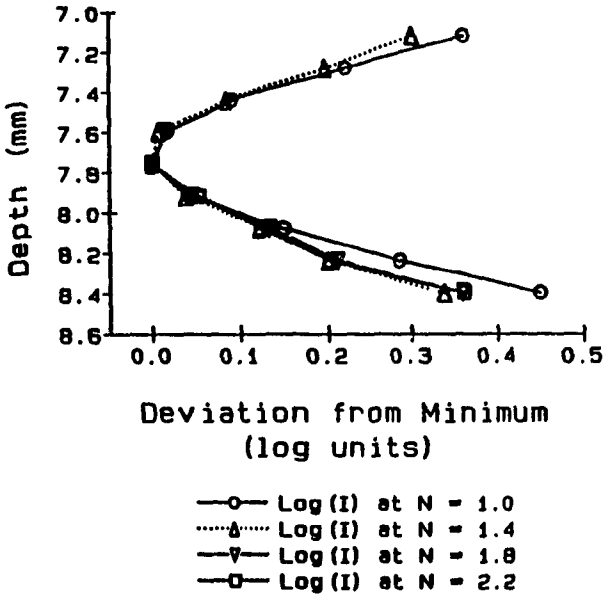
Depth (mm)
7.0
7.2
7.4
7.6
7.8
8.0
8.2
8.4
8.6
0.0
0.1
0.2
0.3
0.4
0.5
Deviation from Minimum
(log units)
Log (I) at N = 1.0
Log (I) at N = 1.4
Log (I) at N = 1.8
Log (I) at N = 2.2

Figure 24.

Depth profiles derived from the trade-off data of Subject F3 which simulate the results that might have been obtained had fixed values of either current or pulse number been used to assess the sensitivity of the substrate at each site.

F3

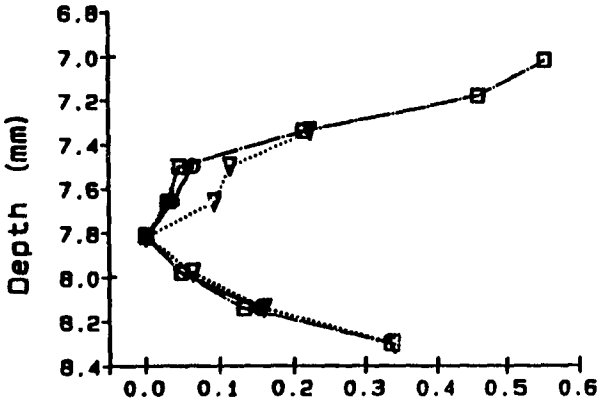

Deviations from Minimum
(log units)

—o— Log (N) at I = 2.15
·····▽····· Log (N) at I = 2.30
—□— Log (N) at I = 2.45

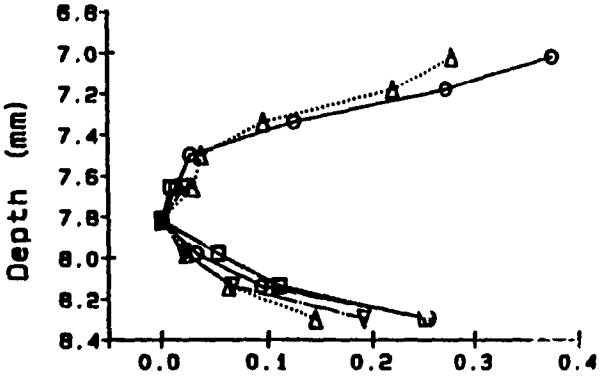

Deviation from Minimum
(log units)

—o— Log (I) at N = 1.0
·····Δ····· Log (I) at N = 1.4
—▽— Log (I) at N = 1.8
—□— Log (I) at N = 2.2

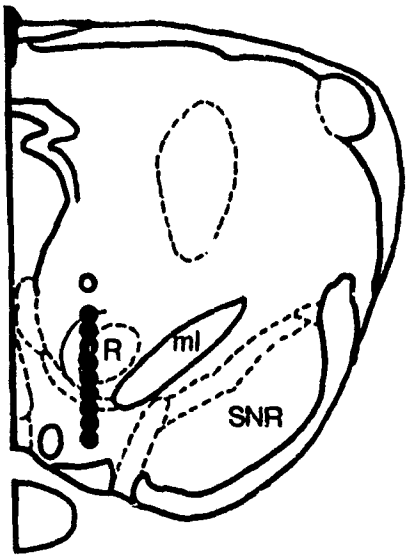

-5.30

calculated for different values of current. Again, note that not all values of current intersect each function. Despite this problem, the profiles all yield the same estimate of the site of maximum sensitivity. This same agreement can be seen when considering the lower panel in which the trade-off functions are sectioned at different values of pulse number.

As was the case when comparing $Log_{10}(I)$ at 10 pulses with I_{min}, the use of either fixed current or fixed number yields relatively similar depth profiles for these two subjects. Regardless of the plane of sectioning (i.e. using number or current as the arbitrarily chosen independent variable), similar estimates of the site of maximum sensitivity are obtained. Furthermore, the form of the profiles is roughly parabolic regardless of which set is considered, indicating that the relationship of the dependent variable to depth of electrode penetration is independent of the value chosen for the fixed parameter.

This parabolic form and close agreement were not obtained for all subjects. Figure 25 shows the data for subject PM8. While there is agreement between the profiles obtained at current of $antilog_{10}$ 2.30 (200 μA) and $antilog_{10}$ 2.45 (282 μA), the profile obtained using the lowest current ($antilog_{10}$ 2.15 or 141 μA) gives an opposite picture of how substrate sensitivity changes with depth.

Figure 25.

Depth profiles derived from the trade-off data of Subject PM8 which simulate the results that might have been obtained had fixed values of either current or pulse number been used to assess the sensitivity of the substrate at each site.

PM8

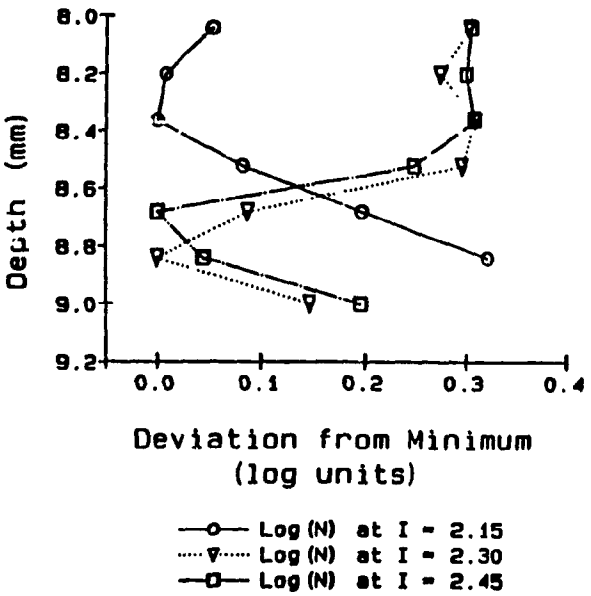
8.0
8.2
8.4
8.6
8.8
9.0
9.2
Depth (mm)
0.0
0.1
0.2
0.3
0.4
Deviation from Minimum
(log units)
Log (N) at I = 2.15
Log (N) at I = 2.30
Log (N) at I = 2.45

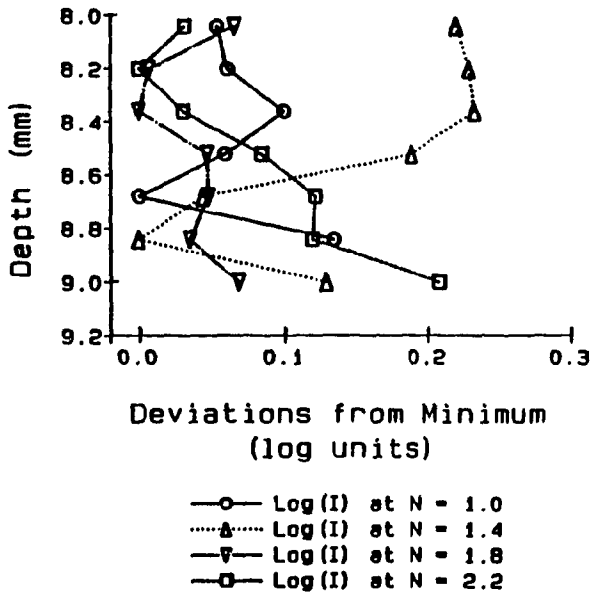
8.0
8.2
8.4
8.6
8.8
9.0
9.2
Depth (mm)
0.0
0.1
0.2
0.3
Deviations from Minimum
(log units)
Log (I) at N = 1.0
Log (I) at N = 1.4
Log (I) at N = 1.8
Log (I) at N = 2.2

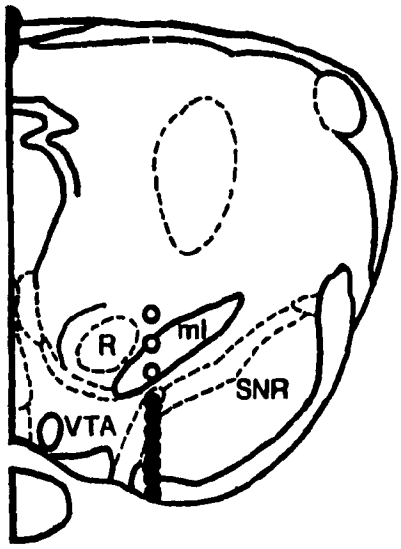
R
ml
SNR
VTA

-5.30

Furthermore, the site of maximum sensitivity differs depending on the value chosen for the independent parameter. In this case, the apparent changes in substrate sensitivity with respect to depth depend strongly on the choice of current (See Figure 12).

In the lower panel a similar result is yielded by sectioning the trade-off functions at fixed values of number. Again, choosing to section at high numbers produces a profile indicating that the more dorsal sites are the most sensitive. Profiles at the lower numbers give opposite results, indicating that sites near the base of the brain have greater sensitivity. Again, the changes in substrate sensitivity with respect to depth depend strongly on the value one selects for the fixed stimulation parameter.

Figure 26 shows the data for subject PM1. Consider first the top panel, where the trade-off functions have been sectioned with fixed values of current. As expected from the form of the trade-off functions, there is good agreement between the depth profiles taken at the three current values used for the previous subjects. However, when the trade-off functions are sectioned at a fourth, low level of current (antilog$_{10}$ 2.00 or 100 μA), an opposite picture is obtained. As with subject PM8, sectioning at different levels of pulse number (lower panel) produces four different profiles of changing substrate sensitivity.

Figure 26.

Depth profiles derived from the trade-off data of Subject PM1 which simulate the results that might have been obtained had fixed values of either current or pulse number been used to assess the sensitivity of the substrate at each site.

PM1

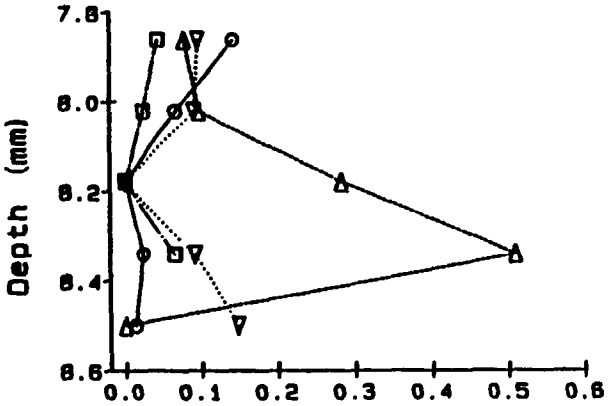

Deviation from Minimum
(log units)

—Δ— Log (N) at I = 2.00
—○— Log (N) at I = 2.15
·····▽····· Log (N) at I = 2.30
—□— Log (N) at I = 2.45

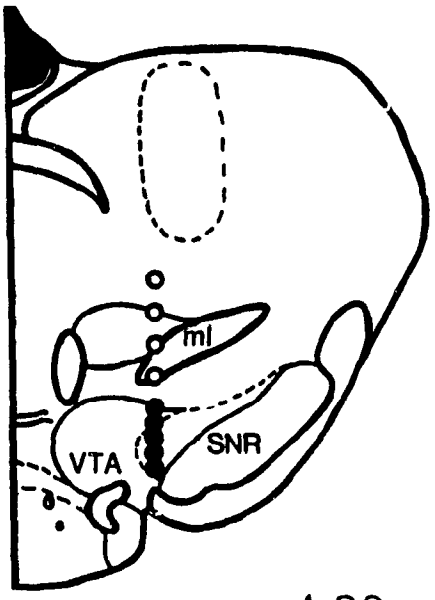

-4.80

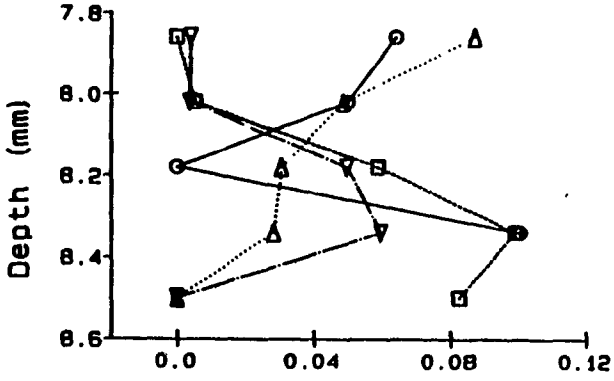

Deviation from Minimum
(log units)

—○— Log (I) at N = 1.0
·····Δ····· Log (I) at N = 1.4
—▽— Log (I) at N = 1.8
—□— Log (I) at N = 2.2

The data from these two subjects most clearly indicates the danger of using arbitrarily chosen fixed stimulation parameters. When the trade-off functions derived over a series of sites are not parallel, they cannot be adequately represented by a single point.

Figure 27 shows the data for subject F1. Although there is reasonable agreement between the various profiles, the fact that the trade-off functions span a large range of currents yields profiles that are missing some data regardless of which fixed value is chosen. Furthermore, the depth at which the stimulation was most effective differs from profile to profile. Without having collected a full range at each site some of this data would have been lost, and a biased profile would have emerged.

A similar situation can be seen when considering the data from subject F4 (Figure 28). Because of the presence of motor interference at most of the sites tested, the depth profiles are incomplete. It is possible that given the choice of a low current, all sites would have been negative.

From examining the various sets of depth profiles, it would seem that those which represent the required current at different fixed levels of pulse number provide the best overall summary of changes to substrate sensitivity with depth. This is due to the difference in the range of

Figure 27.

Depth profiles derived from the trade-off data of Subject F1 which simulate the results that might have been obtained had fixed values of either current or pulse number been used to assess the sensitivity of the substrate at each site.

F1

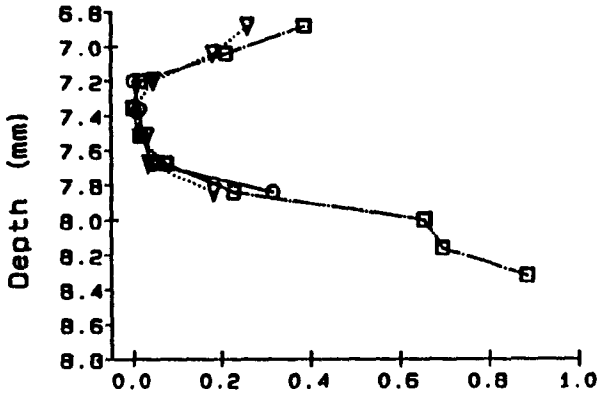
Depth (mm)
6.8
7.0
7.2
7.4
7.6
7.8
8.0
8.2
8.4
8.6
8.8
0.0
0.2
0.4
0.6
0.8
1.0
Deviation from Minimum
(log units)
Log (N) at I = 2.15
Log (N) at I = 2.30
Log (N) at I = 2.45

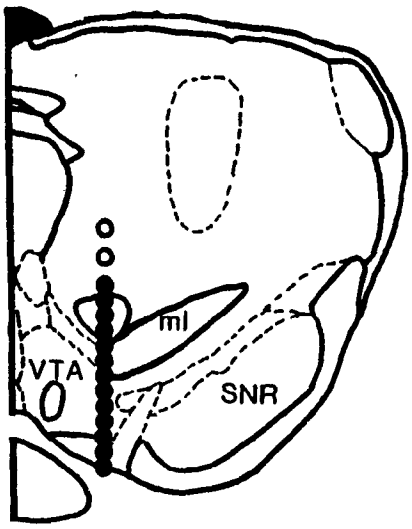
ml
VTA
SNR

-5.20

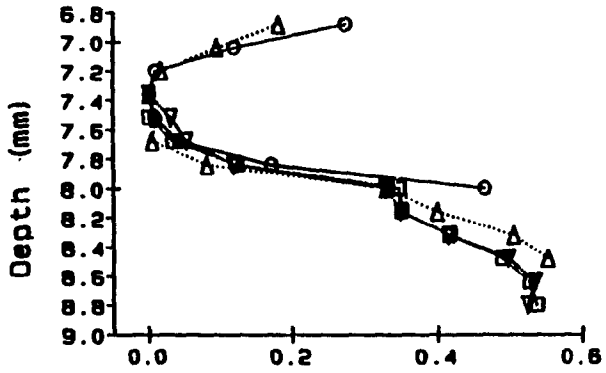
Depth (mm)
6.8
7.0
7.2
7.4
7.6
7.8
8.0
8.2
8.4
8.6
8.8
9.0
0.0
0.2
0.4
0.6
Deviation from Minimum
(log units)
Log (I) at N = 1.0
Log (I) at N = 1.4
Log (I) at N = 1.8
Log (I) at N = 2.2

Figure 28.

Depth profiles derived from the trade-off data of Subject F4 which simulate the results that might have been obtained had fixed values of either current or pulse number been used to assess the sensitivity of the substrate at each site.

F4

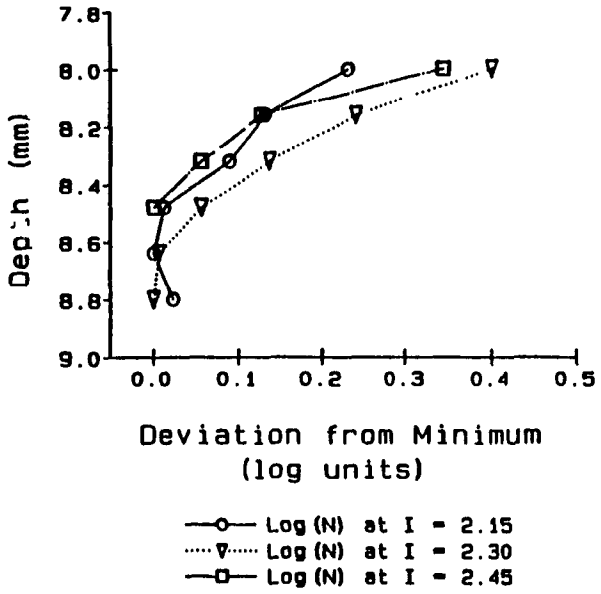
7.8
8.0
8.2
8.4
8.6
8.8
9.0
Depth (mm)
0.0
0.1
0.2
0.3
0.4
0.5
Deviation from Minimum
(log units)
Log (N) at I = 2.15
Log (N) at I = 2.30
Log (N) at I = 2.45

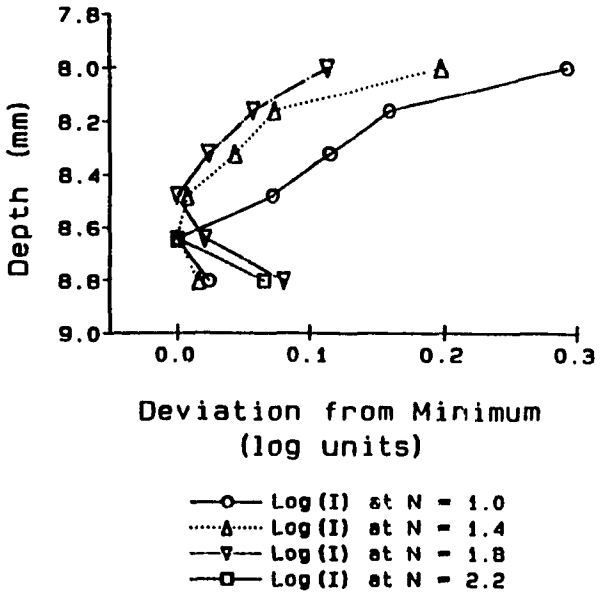
7.8
8.0
8.2
8.4
8.6
8.8
9.0
Depth (mm)
0.0
0.1
0.2
0.3
Deviation from Minimum
(log units)
Log (I) at N = 1.0
Log (I) at N = 1.4
Log (I) at N = 1.8
Log (I) at N = 2.2

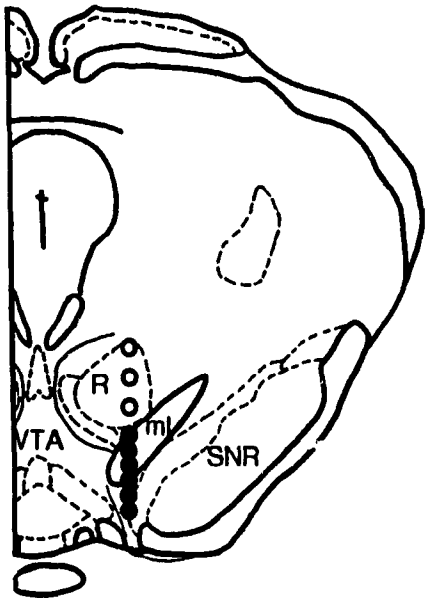
R
ml
VTA
SNR

-5.60

of values of each parameter that the trade-off functions span (e.g. an eight-fold range of pulse number).

Effects of Varying the Pulse Duration

To this point the discussion has focused on the results obtained using a pulse duration of 100 μs. With the exception of one subject (F1), trade-off functions were also collected at a second pulse-duration of 1000 μs. For subject F1, the long pulse duration could not be tested at sites below 8.00 mm. Evidence of charge build-up at the electrode/brain interface was seen at even the lowest pulse numbers, perhaps due to the high values of current required to elicit self-stimulation (see page 47).

Comparing the current-number trade-off functions. The manipulation of pulse duration did not produce a large difference between the trade-off functions for any animal. Data from four subjects have been chosen to illustrate the general trend of the results seen. Figures 29 through 32 show the two sets of trade-off functions collected at both pulse durations. The curves collected at 1000 μs lie below those collected at 100 μs due to the decrease in required current when pulse duration is lengthened. Depth is again given in the graph key, and the colour of the curve is matched to the coloured circles on the histological reconstruction on the right hand side.

Figure 29 shows the data for subject PM10. Overall, the curves at the long pulse duration have a similar shape to those at the shorter duration, but note that for last site, the curve taken at 1000 μs overlaps that of the first site, whereas the curve taken from the last site in the 100 μs condition lies below that of the first site.

Figure 30 shows the data for subject PM11. Again, with a few minor differences, the curves taken at 1000 μs have a similar relationship to each other and are of a similar shape to those taken at 100 μs.

The largest discrepancy between the two data sets was observed in the case of subject PM8 (Figure 31). At 8.84 mm, proportionately higher current intensities are required in the 1000 μs condition over the low-range of pulse numbers. Note that the curve lies above those of the more dorsal sites in the 1000 μs condition, opposite to its position when the pulse duration was set to 100 μs. Note also that the curves are much closer together at the dorsal sites in the 1000 μs condition, and exhibit a different shape than in the 100 μs set.

The data of subject PM1 (Figure 32) also show that higher currents were required at the more ventral sites in the 1000 μs condition, indicating that the stimulation was less effective than at the more dorsal sites. The functions collected from these ventral sites at 1000 μs are deflected upwards at the low pulse numbers, and lie above

Figure 29.

Comparison of current-number trade-off data for the two pulse duration conditions for Subject PM10. Curves on the upper part of the graph (e.g. higher values of current) were obtained at 100 µs, while those below were obtained at 1000 µs. Values in the graph key again correspond to the depth of electrode penetration at which each pair (100 µs and 1000 µs) curves was determined. Each curve in the pair have the same symbol, line-type and colour (which is matched to the coloured circles on the histological profile above the graph key). Open circles refer to sites where self-stimulation could not be elicited. The number below the histological section refers to the distance posterior to bregma (in mm).

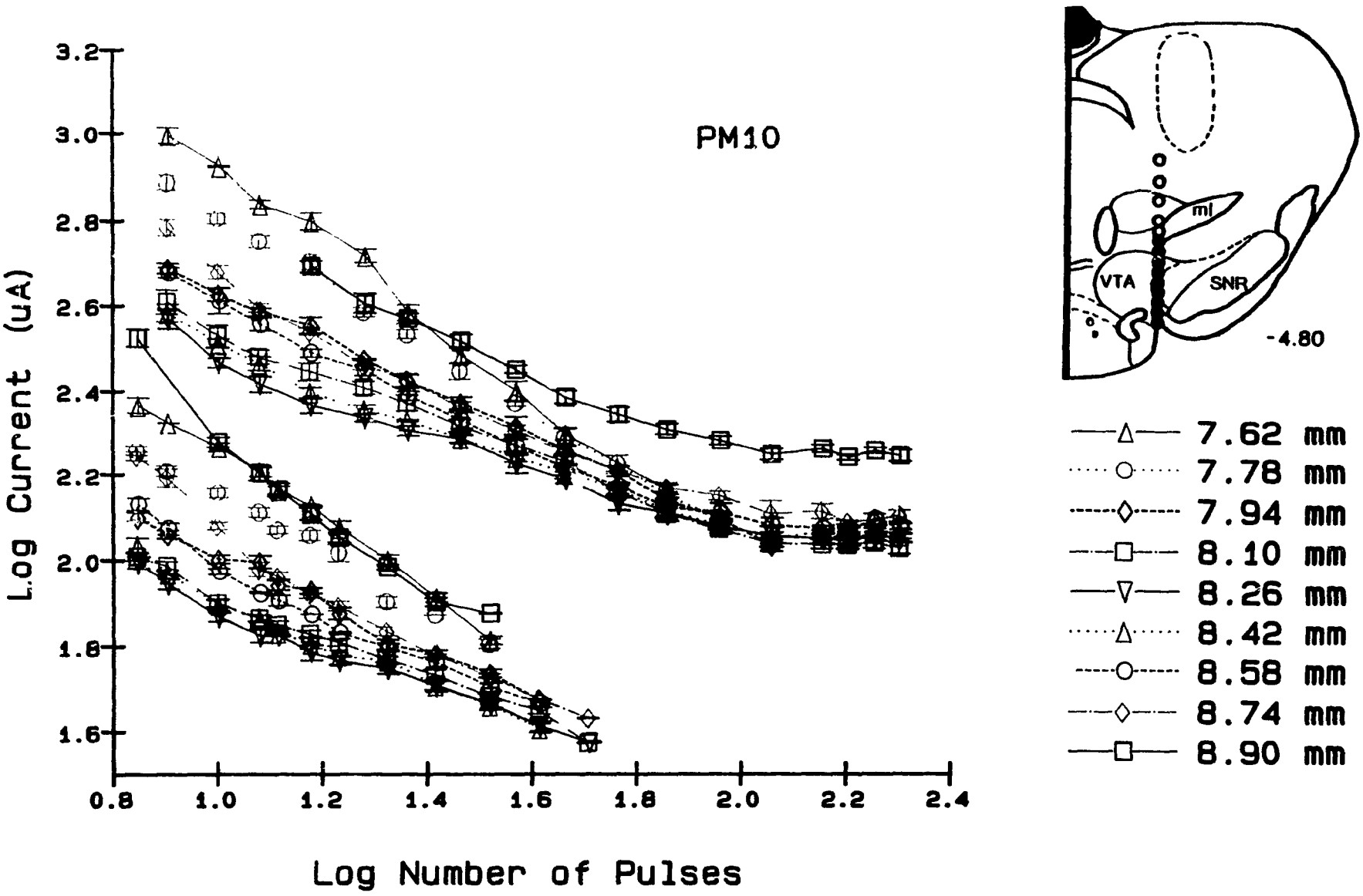
PM10
Log Current (uA)
3.2
3.0
2.8
2.6
2.4
2.2
2.0
1.8
1.6
0.8
1.0
1.2
1.4
1.6
1.8
2.0
2.2
2.4
Log Number of Pulses
ml
VTA
SNR
-4.80
7.62 mm
7.78 mm
7.94 mm
8.10 mm
8.26 mm
8.42 mm
8.58 mm
8.74 mm
8.90 mm

Figure 30.

Comparison of current-number trade-off data for the two pulse duration conditions for Subject PM11.

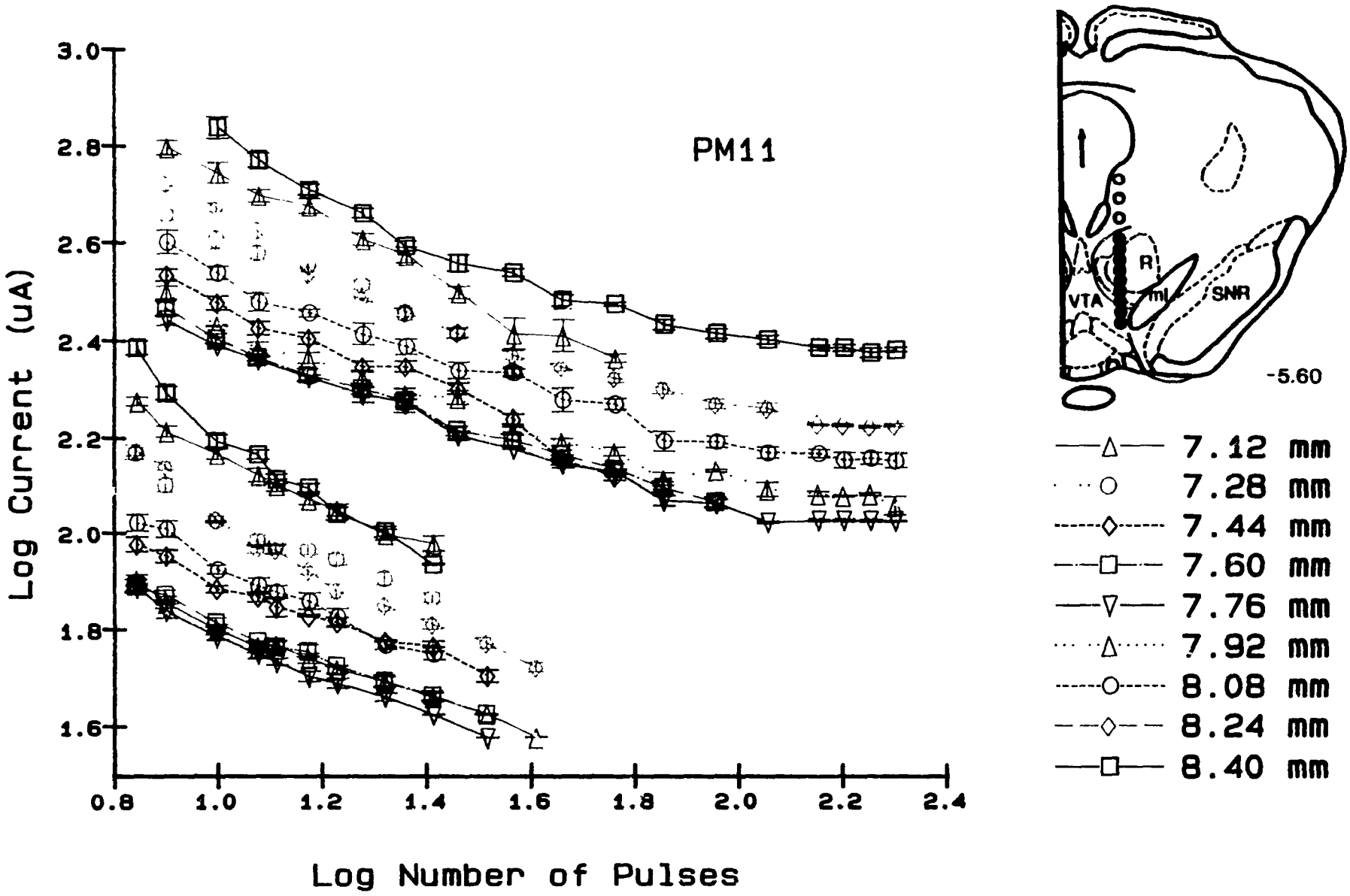
PM11
Log Current (uA)
3.0
2.8
2.6
2.4
2.2
2.0
1.8
1.6
0.8
1.0
1.2
1.4
1.6
1.8
2.0
2.2
2.4
Log Number of Pulses
R
VTA
ml
SNR
-5.60
7.12 mm
7.28 mm
7.44 mm
7.60 mm
7.76 mm
7.92 mm
8.08 mm
8.24 mm
8.40 mm

Figure 31.

Comparison of current-number trade-off data for the two pulse duration conditions for Subject PM8.

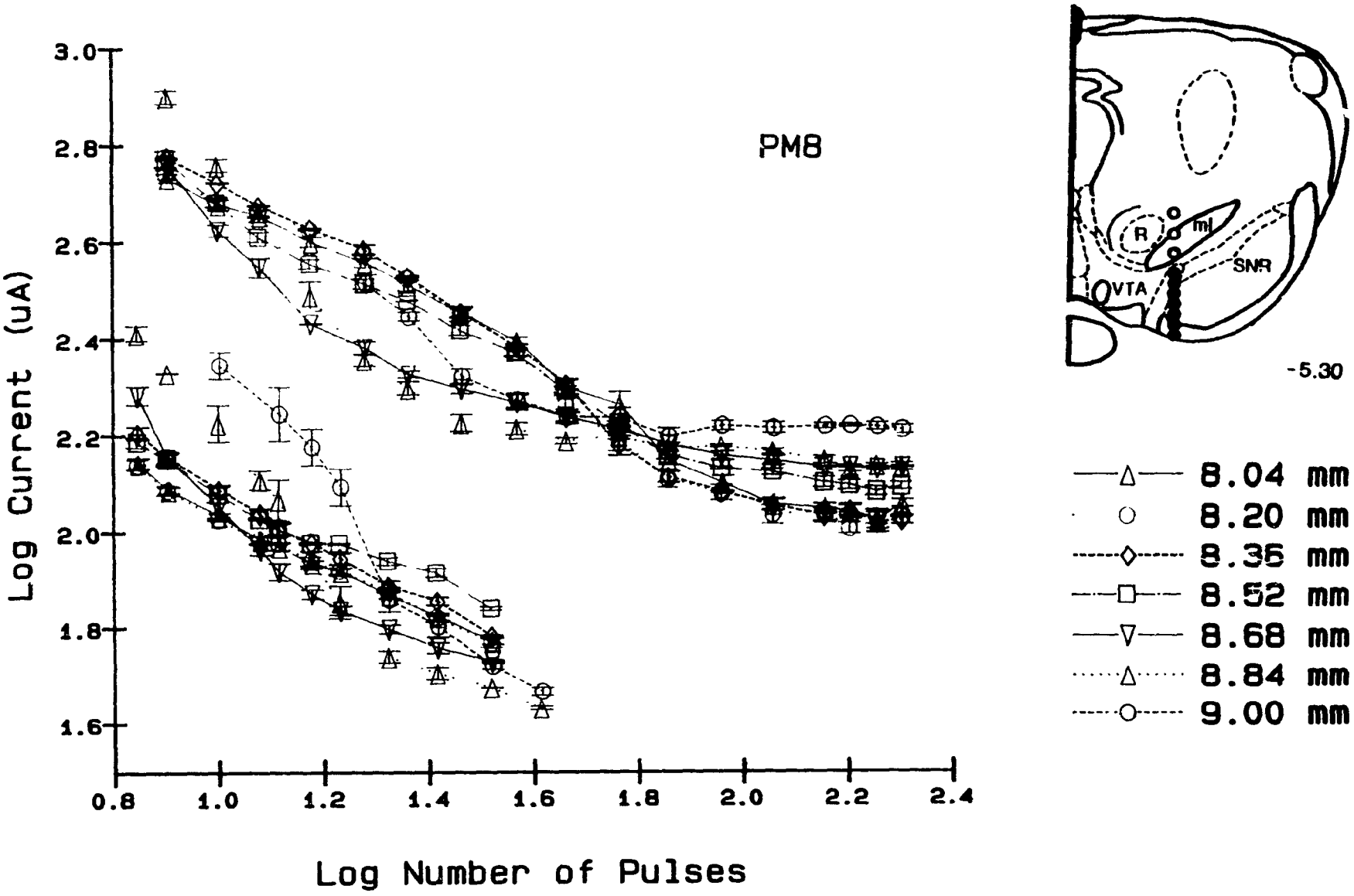
PM8
Log Current (uA)
3.0
2.8
2.6
2.4
2.2
2.0
1.8
1.6
0.8
1.0
1.2
1.4
1.6
1.8
2.0
2.2
2.4
Log Number of Pulses
R
ml
SNR
VTA
-5.30
8.04 mm
8.20 mm
8.36 mm
8.52 mm
8.68 mm
8.84 mm
9.00 mm

Figure 32.

Comparison of current-number trade-off data for the two pulse duration conditions for Subject PM1.

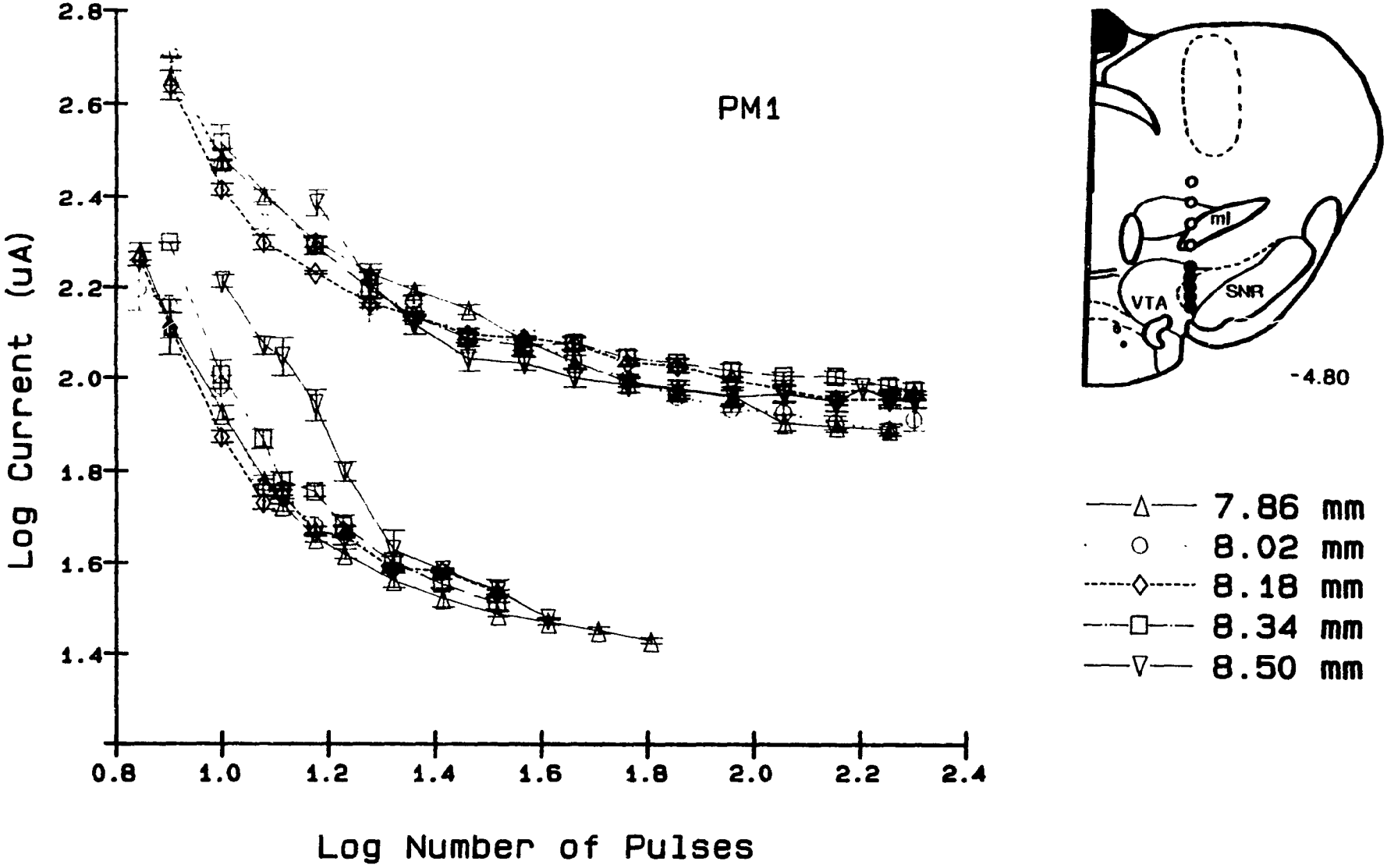
PM1
Log Current (uA)
2.8
2.6
2.4
2.2
2.0
1.8
1.6
1.4
0.8
1.0
1.2
1.4
1.6
1.8
2.0
2.2
2.4
Log Number of Pulses
ml
VTA
SNR
-4.80
7.86 mm
8.02 mm
8.18 mm
8.34 mm
8.50 mm

those collected at the more dorsal sites.

Effects of varying pulse duration within sites. In order to objectively assess any differences between the trade-off functions gathered for the two pulse durations at the same site, a comparison of their shapes was undertaken. The fact that the two functions lie at different positions along the ordinate (because lower current intensities are required at a longer pulse duration) renders such a comparison difficult. Therefore, the trade-off curve taken at a pulse duration of 1000 μs was transformed by the addition of a constant (in the logarithmic domain) to each data point. This has the effect of "sliding" the curve along the ordinate (towards higher current intensities), where it will overlap with the 100 μs data from the same site. Thus, a comparison of their shapes is facilitated. The value of this additive constant was determined by the curve-fitting procedure described previously (see page 71).

In general, large differences between the two functions were not observed for any of the subjects, and this situation is illustrated in Figure 33a. The graph shows a comparison of the trade-off data collected at 100 μs and 1000 μs for subject PM10 at a depth of 8.74 mm. The 1000 μs data (denoted by open, inverted triangles) have been transformed by the additive constant, and the solid line reflects the function that best fit the 100 μs data.

Figure 33.

Comparison of the shapes of the trade-off curves collected at a pulse duration of 100 μs (filled triangles) and 1000 μs (open, inverted triangles) for the same site. The 1000 μs data have been transformed by the addition of a constant so that the curve is shifted along the ordinate towards higher values of current, thus rendering the two sets of data comparable. The two curves are also shown with the function which best fits the 100 μs data (solid line).

a

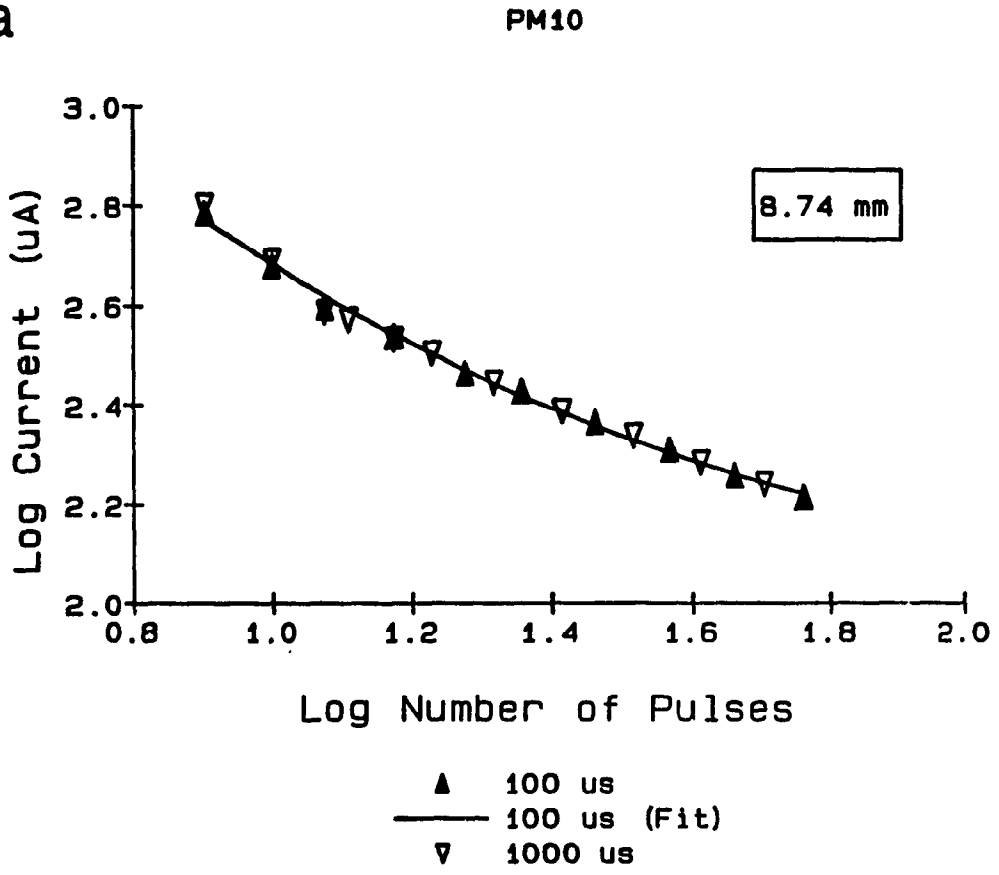
PM10
8.74 mm
Log Current (uA)
3.0
2.8
2.6
2.4
2.2
2.0
0.8
1.0
1.2
1.4
1.6
1.8
2.0
Log Number of Pulses
100 us
100 us (Fit)
1000 us

b

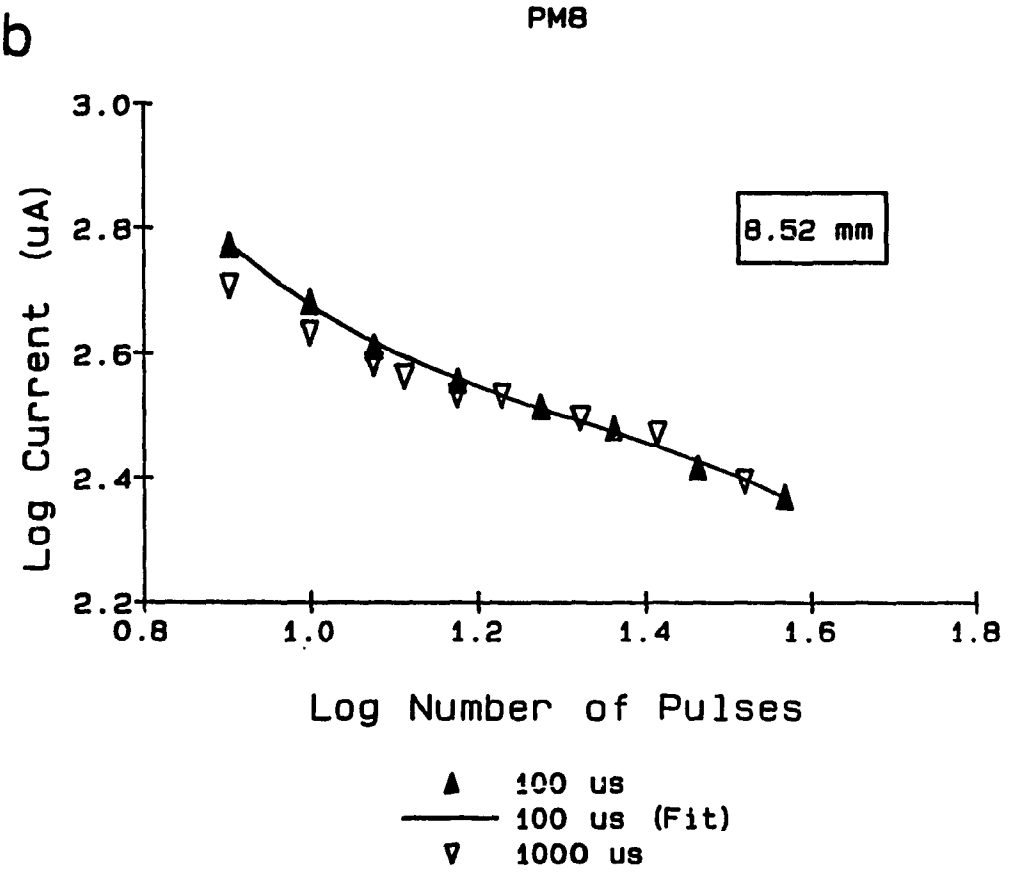
PM8
8.52 mm
Log Current (uA)
3.0
2.8
2.6
2.4
2.2
0.8
1.0
1.2
1.4
1.6
1.8
Log Number of Pulses
100 us
100 us (Fit)
1000 us

Note the proximity of each of the points from the 100 μs and 1000 μs data (at each value of pulse number), and how well the function, originally fitted to the 100 μs data, also describes the 1000 μs data.

Figure 33b shows this comparison for subject PM8 at a depth of 8.52 mm. Again, the 1000 μs data have been transformed by the addition of the constant determined by the previously described curve-fitting procedure. In this case, the 1000 μs curve does not exhibit the same shape as the 100 μs curve. Furthermore, unlike the data from PM10, the function which best describes the 100 μs data does not provide a good description of the shape of the trade-off curve determined at 1000 μs. Note that at the low pulse numbers, the 1000 μs curve lies below that determined at 100 μs, while at the higher pulse numbers, the opposite is true.

Effects of varying pulse duration between sites. In order to assess changes in the effect of lengthening the pulse duration as the electrode was lowered from site to site, depth profiles were constructed for both data sets. In the same manner as for the 100 μs data described previously, the required current was calculated by interpolation from the trade-off curves for three different arbitrarily-selected values of pulse number. The results of these calculations for the four subjects shown above are illustrated in Figures 34 to 37. The data have again been

re-scaled as in the previous sections. The message to the right of each profile indicates the log value of pulse number at which the profiles were calculated (filled circles = 100 μs, open circles = 1000 μs.

As was expected from a visual inspection of the two sets of trade-off functions, these comparisons for subject PM10 (Figure 34) and PM11 (Figure 35) show that changing the pulse duration did not yield a different depth profile. Although there are minor differences for both animals, the depth profiles have the same shape and are all overlapping.

This does not seem to have been the case for all subjects. For subject PM8, the depth profiles indicate that the substrate was relatively more sensitive at 1000 μs than at 100 μs at the most dorsal sites tested, regardless of the value of pulse number chosen (Figure 36). This can be seen by noting that the two profiles diverge at these more dorsal sites, with the 1000 μs profile lying in a region of relatively lower current than that taken at 100 μs.

The data for subject PM1 are shown in Figure 37. Note, that the shape of the profiles differs across the values of pulse number at which they were calculated. Furthermore, at $\text{antilog}_{10}(N) = 1.2$ and 1.4, the profiles taken at the two pulse durations cross each other. At the most dorsal sites, the 1000 μs profile lies in a region of relatively lower current than that calculated at 100 μs,

Figure 34.

Depth profiles representing changes in required current with depth of electrode penetration are compared for the two different pulse duration conditions for Subject PM10. Each profile was taken at a different value of pulse number (indicated to the right of each profile). Filled circles = 100 μs data; Open circles = 1000 μs data. A histological reconstruction of the stimulation sites tested again accompanies the graph.

PM10

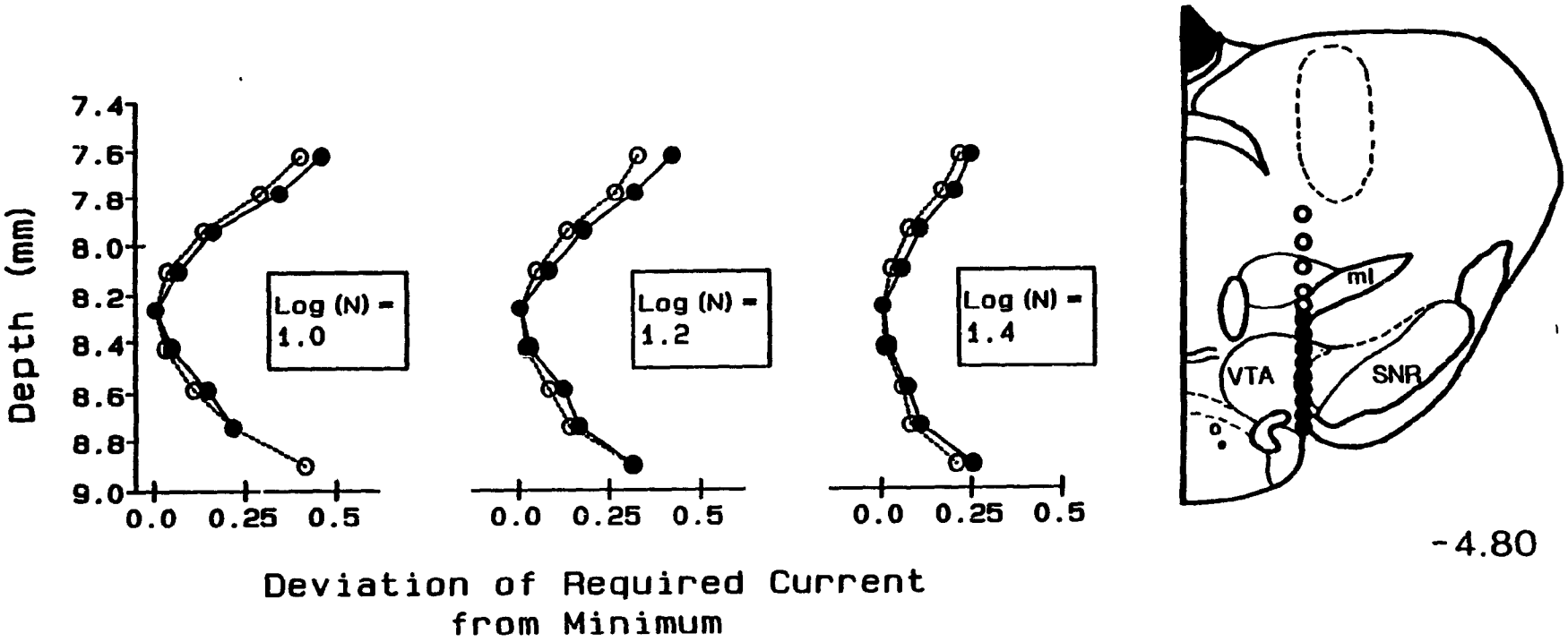
Depth (mm)
7.4
7.6
7.8
8.0
8.2
8.4
8.6
8.8
9.0
Log (N) = 1.0
Log (N) = 1.2
Log (N) = 1.4
0.0 0.25 0.5
0.0 0.25 0.5
0.0 0.25 0.5
Deviation of Required Current from Minimum
ml
VTA
SNR
-4.80

Figure 35.

Depth profiles representing changes to the required current with depth of electrode penetration are compared for the two different pulse duration conditions for Subject PM11. Filled circles = 100 μs data; Open circles = 1000 μs data.

PM11

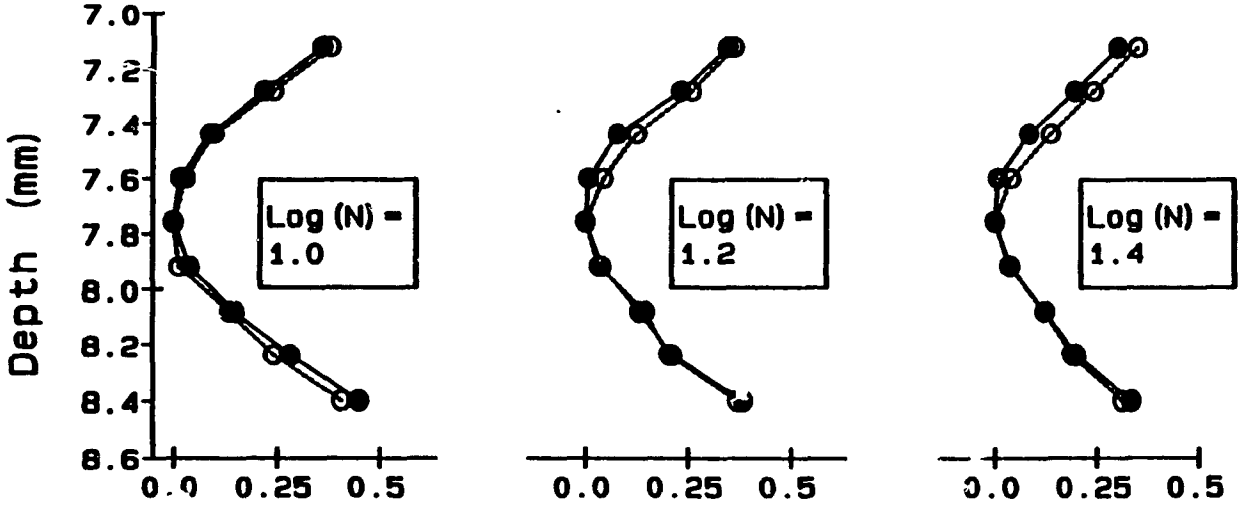
Depth (mm)
7.0
7.2
7.4
7.6
7.8
8.0
8.2
8.4
8.6
Log (N) = 1.0
Log (N) = 1.2
Log (N) = 1.4
0.0 0.25 0.5
0.0 0.25 0.5
0.0 0.25 0.5
Deviation of Required Current from Minimum

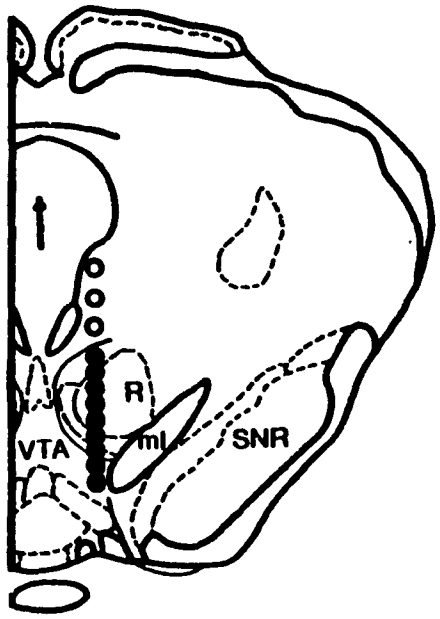
R
VTA
ml
SNR

-5.60

Figure 36.

Depth profiles representing changes to the required current with depth of electrode penetration are compared for the two different pulse duration conditions for Subject PM8. Filled circles = 100 μs data; Open circles = 1000 μs data.

PM8

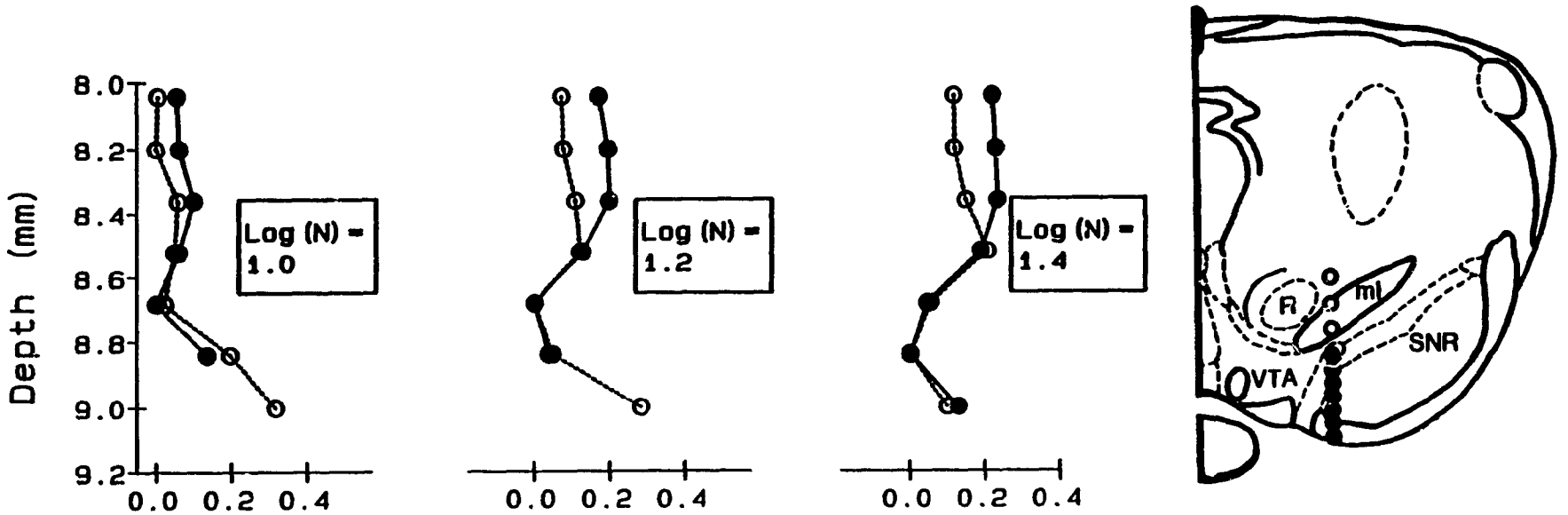
Depth (mm)
8.0
8.2
8.4
8.6
8.8
9.0
9.2
Log (N) = 1.0
Log (N) = 1.2
Log (N) = 1.4
0.0 0.2 0.4
0.0 0.2 0.4
0.0 0.2 0.4
R
ml
SNR
VTA
Deviation of Required Current from Minimum

-5.30

Figure 37.

Depth profiles representing changes to the required current with depth of electrode penetration are compared for the two different pulse duration conditions for Subject PM1. Filled circles = 100 μs data; Open circles = 1000 μs data.

PM1

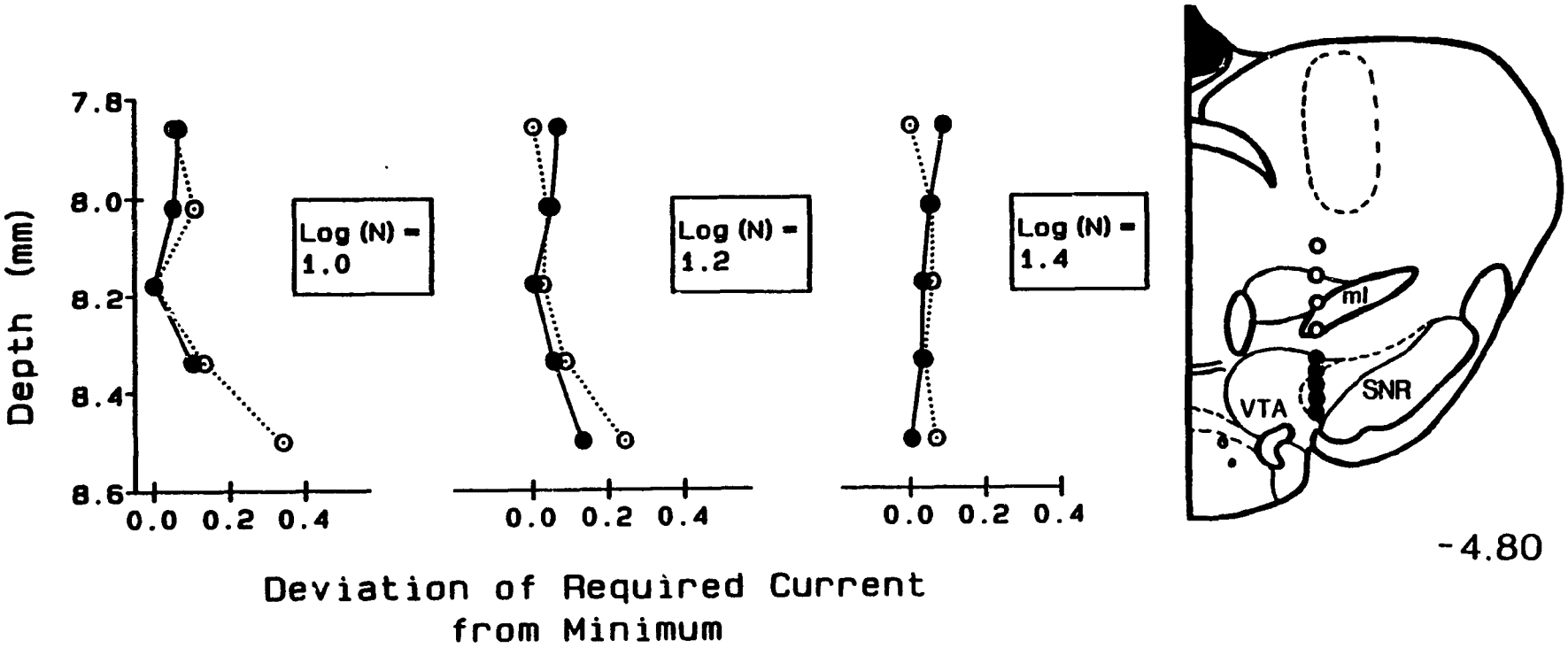
Depth (mm)
7.8
8.0
8.2
8.4
8.6
Log (N) = 1.0
Log (N) = 1.2
Log (N) = 1.4
0.0 0.2 0.4
0.0 0.2 0.4
0.0 0.2 0.4
Deviation of Required Current from Minimum
ml
SNR
VTA
-4.80

whereas the opposite situation is observed for the more ventral sites.

Comparing Behavioural Criteria

In order to determine whether the trade-off functions had been biased by calculating the current corresponding to the half-maximal rate of response rather than the current corresponding to the locus of rise of the rate-intensity function, a comparison of the two criteria was made for two subjects.

As discussed previously (see page 53), it is possible that changes to the required current that suggest changes to the rewarding impact of the stimulation, may in fact, have been artifactually produced. This might be anticipated in cases where a change in the asymptotic rate of response was accompanied by a change in the slope of the rate-intensity function. Such changes can be produced when the animals' ability to perform the operant task is hampered in some way. Miliaressis et al. (1986) have shown that in these cases, the required current calculated at threshold is less subject to such bias. Therefore, because many of the subjects tested in this experiment exhibited some form of stimulation-induced movement, and because the trade-off curves were derived based on the value of current required to sustain half-maximal responding, a comparison

of the trade-off functions calculated using both criteria was undertaken.

Figures 38 and 39 show the data from two sites for subject F3 (7.66 mm and 7.82 mm). These data were chosen for this comparison because large decreases in maximum rate were observed as the pulse number was increased. In Figure 38a the trade-off functions calculated using the two criteria at depth 7.66 mm are compared. Note that the curve calculated using the locus of rise measure (L.O.R.--open circles) lies below that calculated using half-maximal response rate (open triangles). This is because L.O.R. is calculated from a different part of the rate-intensity curves. Figure 38b depicts the trade-off function derived at the following site (7.82 mm), where a large decrease in maximum rate was also observed at high pulse numbers. In both cases the two trade-off functions are very similar and their shapes do not appear to depend on the choice of criterion.

Figure 39 shows the comparison between the two sites based upon either the half-maximal rate (a) or the L.O.R. (b). Regardless of the criterion used to estimate the required current, the relationship of the two functions is the same.

Figure 38.

Comparison of two methods of calculating the required current and the effect on the resulting trade-off function: (a) two trade-off curves with required current calculated to correspond to either 50% of maximum rate or to the locus of rise of the rate-intensity function for Subject F3 (at a depth of 7.66 mm), and (b) the same comparison at a depth of 7.82 mm.

F3

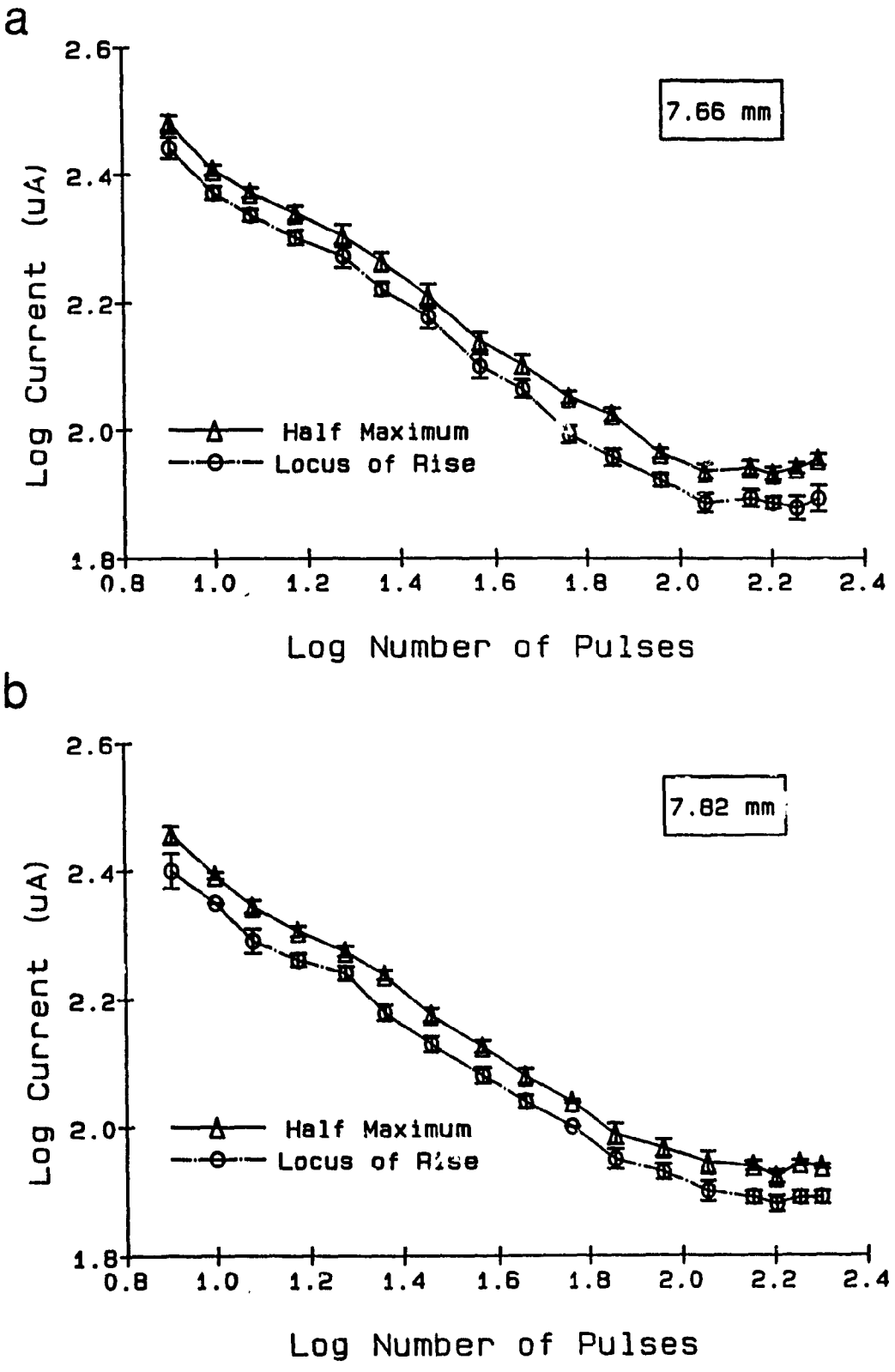
a
7.66 mm
Log Current (uA)
2.6
2.4
2.2
2.0
1.8
Half Maximum
Locus of Rise
0.8
1.0
1.2
1.4
1.6
1.8
2.0
2.2
2.4
Log Number of Pulses
b
7.82 mm
Log Current (uA)
2.6
2.4
2.2
2.0
1.8
Half Maximum
Locus of Rise
0.8
1.0
1.2
1.4
1.6
1.8
2.0
2.2
2.4
Log Number of Pulses

Figure 39.

Comparison of the effect of using two different methods of calculating the required current on the relationship between current-number trade-off functions obtained at two stimulation sites as inferred from the relationship between the resulting trade-off functions: (a) two trade-off curves with required current calculated to correspond to 50% of maximum rate for Subject F3 (at depths 7.66 mm and 7.82 mm), and (b) the same comparison with required current calculated to correspond to the locus of rise of the rate-intensity function.

F3

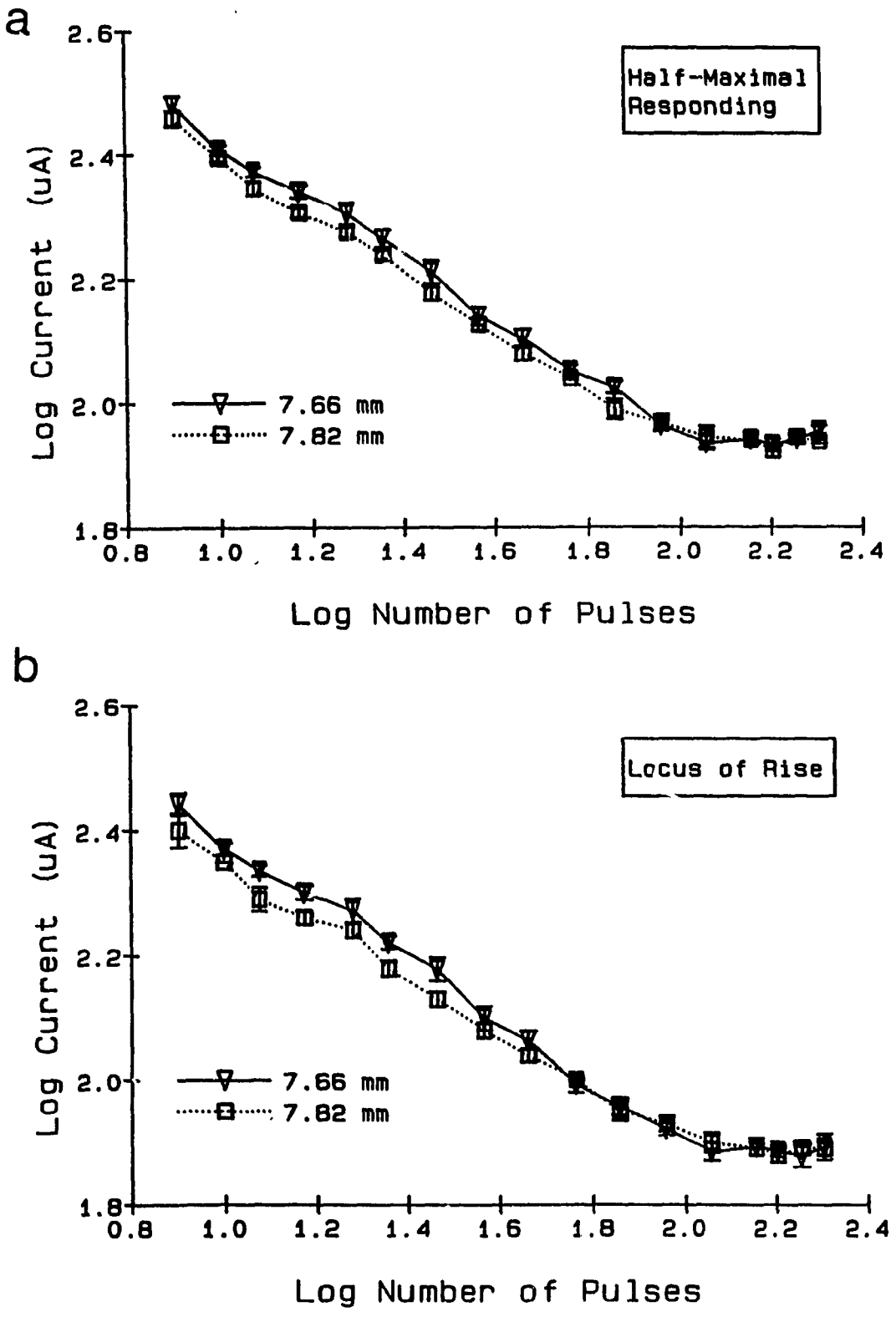
a
Half-Maximal Responding
Log Current (uA)
2.6
2.4
2.2
2.0
1.8
7.66 mm
7.82 mm
0.8
1.0
1.2
1.4
1.6
1.8
2.0
2.2
2.4
Log Number of Pulses
b
Locus of Rise
Log Current (uA)
2.6
2.4
2.2
2.0
1.8
7.66 mm
7.82 mm
0.8
1.0
1.2
1.4
1.6
1.8
2.0
2.2
2.4
Log Number of Pulses

Figures 40 and 41 show the analogous data for subject PM8. This animal was chosen for this analysis to ensure that the double-crossing of the trade-off functions was not an artifact of differences between the rate-intensity functions obtained at the most dorsal and ventral sites. In Figure 40 (a & b) the trade-off functions calculated using each criterion are shown for depths of 8.36 mm and 8.84 mm. Again, while the curve using L.O.R. lies below that calculated using half-maximal responding, the two are virtually identical in shape. Furthermore, the trade-off functions obtained at the two sites cross twice, regardless of which criterion is used (Figure 41--a & b).

Figure 40.

Comparison of two methods of calculating the required current and the effect on the resulting trade-off function: (a) two trade-off curves with required current calculated to correspond to either 50% of maximum rate or to the locus of rise of the rate-intensity function for Subject PM8 (at a depth of 8.36 mm), and (b) the same comparison at a depth of 8.84 mm.

PM8

a

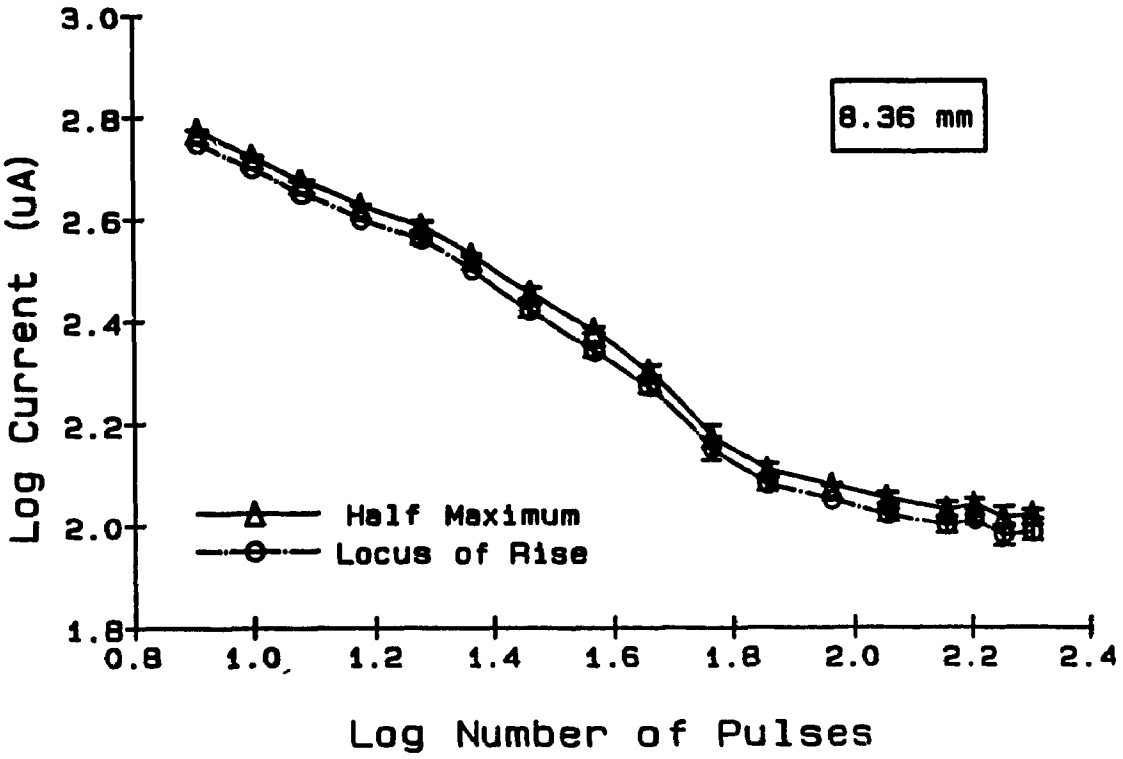
8.36 mm
Half Maximum
Locus of Rise
Log Current (uA)
Log Number of Pulses
3.0
2.8
2.6
2.4
2.2
2.0
1.8
0.8
1.0
1.2
1.4
1.6
1.8
2.0
2.2
2.4

b

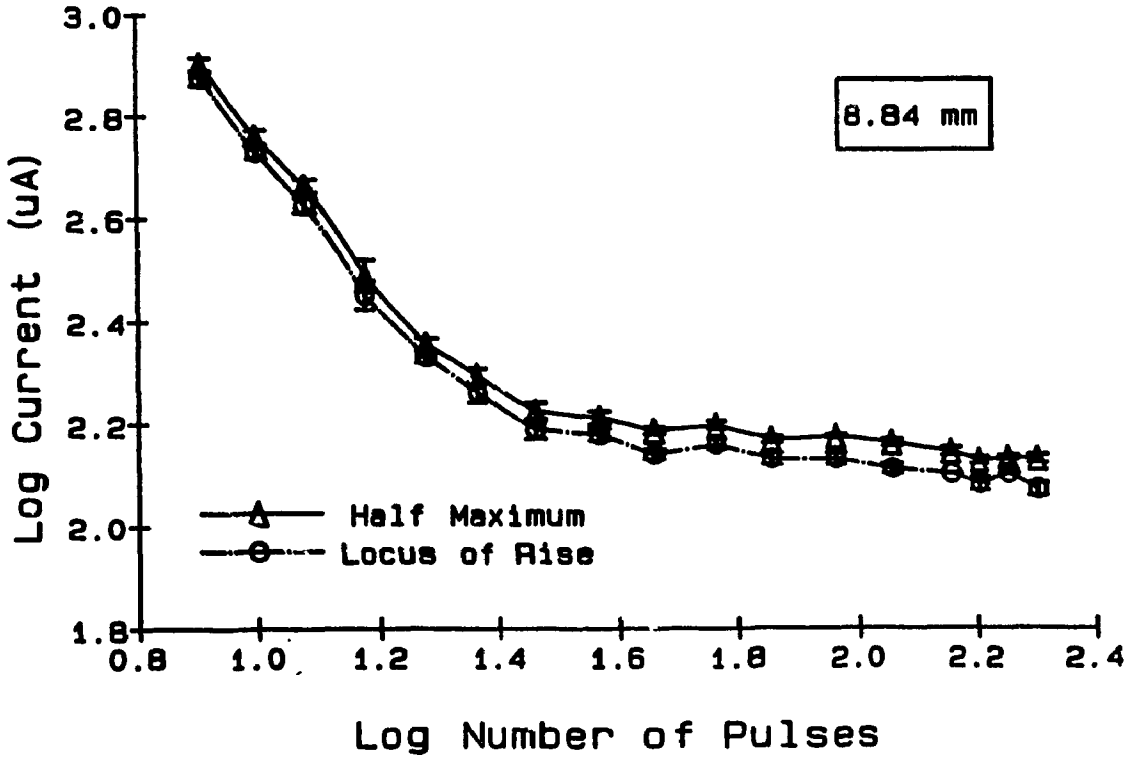
8.84 mm
Half Maximum
Locus of Rise
Log Current (uA)
Log Number of Pulses
3.0
2.8
2.6
2.4
2.2
2.0
1.8
0.8
1.0
1.2
1.4
1.6
1.8
2.0
2.2
2.4

Figure 41.

Comparison of the effect of using two different methods of calculating the required current on the relationship between the current-number trade-off functions obtained at two stimulation sites: (a) two trade-off curves with required current calculated to correspond to 50% of maximum rate for Subject PM8 (at depths 8.36 mm and 8.84 mm), and (b) the same comparison with required current calculated to correspond to the locus of rise of the rate-intensity function.

PM8

a

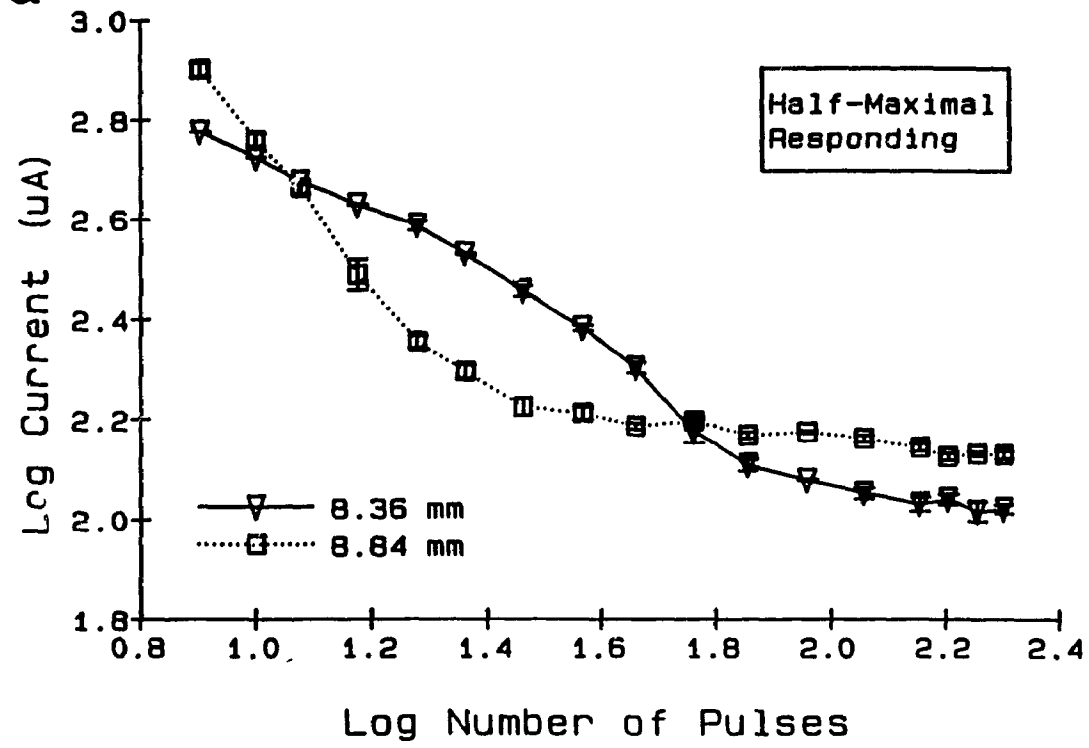
Half-Maximal
Responding
8.36 mm
8.84 mm
Log Current (uA)
3.0
2.8
2.6
2.4
2.2
2.0
1.8
0.8
1.0
1.2
1.4
1.6
1.8
2.0
2.2
2.4
Log Number of Pulses

b

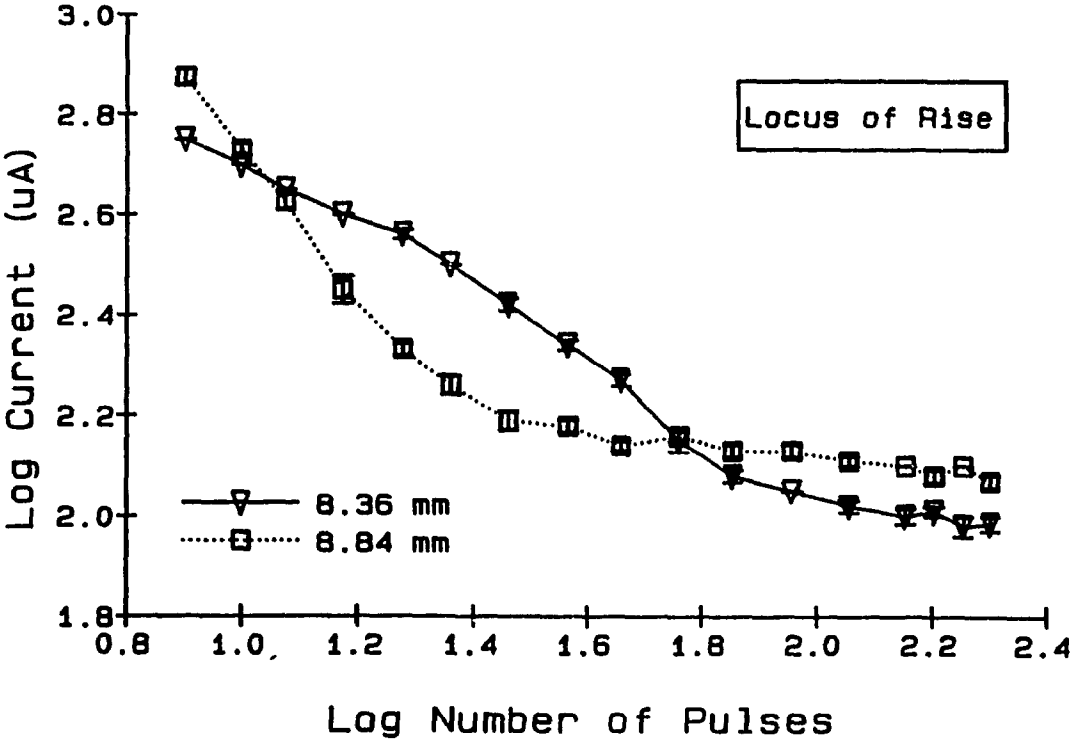
Locus of Rise
8.36 mm
8.84 mm
Log Current (uA)
3.0
2.8
2.6
2.4
2.2
2.0
1.8
0.8
1.0
1.2
1.4
1.6
1.8
2.0
2.2
2.4
Log Number of Pulses

Discussion

The primary goal of the present experiment was to provide an empirical evaluation and extension of the topographical method developed by Miliaressis, Rompré and their colleagues. Because their method consisted of determining a single rate-frequency function at a fixed value of current, it was proposed that manipulating both current and frequency for the purposes of deriving a current-number trade-off function would provide a method by which this evaluation could be made, and in addition, the use of this method would extend the amount of topographical information gathered for each site.

In proposing that the current-number trade-off function be used as a method for collecting topographical information about the reward substrate, it was predicted that this approach would make four contributions. First, it was reasoned that the shape and position of the function could provide clues to changes in substrate sensitivity along the axis of electrode movement. Second, because both stimulation frequency and current are varied in collecting the trade-off data, an evaluation of the use of fixed parameters would be possible. The larger data set provided by the current-number function would allow one to simulate the results which might have been obtained at any combination of current and pulse number. Third, based on

previous experiments, it was proposed that the minimum current required to elicit behaviour at each site (estimated as the point where the trade-off function approaches asymptote) would yield the highest resolution in measuring the local sensitivity of the substrate, and would be useful in comparing self-stimulation sites. Finally, it was proposed that by collecting the trade-off data at two different pulse durations, a preliminary assessment of the contribution of reward-relevant neurons of different chronaxie might be made.

Before taking up each of these contributions in turn, the question of the reliability of the method employed to calculate the trade-off functions is discussed.

Current-Number Trade-Off Data

Choice of Behavioural Criterion. The usefulness of the current-number trade-off function as a means of collecting topographical data relies on the validity of the method used for its derivation. This validity hinges on the assumption that the choice of the behavioural criterion at which the required current is calculated does not bias the trade-off functions. Moreover, it is important to assure that differences in the slope or upper asymptote of the rate-intensity curves between sites are not responsible for changes in the shape of the trade-off functions.

Based on the analysis of selected data from five subjects (two of which have been presented here), it can be concluded that at least in the mesencephalic region examined in this study, the form of the trade-off functions appears to be relatively independent of the constant behavioural criterion chosen. Regardless of whether the required current was calculated to correspond to 50% of the maximum response rate or to the locus of rise of the rate-intensity function, the trade-off functions maintain the same form. Furthermore, the relationship between sites as measured by the relationship between two trade-off functions is not altered. Because of this, one can be confident that any subsequent analyses based on the trade-off data that were calculated using 50% of maximum response rate are not biased by this choice of behavioural criterion.

Topographical Data. From an examination of the sets of trade-off curves derived across subjects, three different factors can be used to describe the manner in which the functions change with respect to depth. These are: (a) changes in the position of the functions with respect to the scaling variable (i.e. the function is shifted across its length towards higher or lower currents); (b) changes to the functional form which best describes the trade-off curve; and, (c) changes to the

slope of the descending portion of the function (in cases where this portion is reasonably linear). These factors are discussed with respect to the trade-off data obtained in the various subjects.

Trade-off curves taken at the more medial placements (particularly subjects F1, F3 and PM11--Figures 9, 10 and 13, respectively) are very orderly, and in general, show changes to the position of the functions with respect to the scaling variable as the electrode is advanced. The overall pattern is consistent with a gradual approach along a gradient of increasing and then decreasing sensitivity. As the electrode passes through the more dorsal sites, the curves shift towards lower values of current (across the range of frequencies tested) until a depth of approximately 7.75 to 8.00 mm, in the area just ventral to the red nucleus. As the electrode moves out of this region and into the VTA, the curves are shifted, across their length, toward values of higher current again. Furthermore, note the similarity in the last curve taken for both F3 and PM11. The site is located within the centre of the VTA, it shows the lowest effectiveness of any site, and the function is very curved.

At the other extreme, consider the two most lateral placements (subjects PM1 and PM8--Figures 8 and 12, respectively). For these subjects, there is a much more complex relationship between the depth of the electrode

penetration and the shape and position of the entire trade-off curve. Any assessment of the effectiveness of the stimulation is dependent upon which part of the curve one considers.

For these data, the factor which best describes the differences between the curves with respect to electrode position is a change of shape. The effect of this change is to cause the curves to cross one another, and this crossing is particularly striking in the data set gathered from subject PM8. At the most dorsal sites, the descending portion of the function is convex, with the low to mid-range values of frequency being relatively less effective than those at the high values. This might suggest that at these mid-range values, an increase in the number of pulses does not permit a large reduction in the required current, perhaps because few reward-relevant neurons are present at the border of the field, or because the reward-relevant neurons have limited frequency-following capacity. Both of these factors would have the effect of "bowing" the curve upwards (because the size of the stimulation field could not be reduced in large increments). Note however, that as the curve approaches asymptote, it declines more steeply, and these dorsal sites show the lowest I_{min} values collected for this subject. This would suggest that the substrate in the immediate vicinity of the electrode tip at these sites was more sensitive than that farther away. The neurons

near the tip might be more densely packed and would have to follow frequencies up to roughly 300 Hz.

At the more ventral sites, an opposite result is obtained, and the curves are now deeply concave. At the lowest frequencies the curves obtained at these more ventral sites cross those taken at the upper sites. The concave shape of the curves is due to an increase in the effectiveness of the mid-range of frequencies; a large decrease in the current is now required to offset a given increment in the number of pulses. Finally, at the higher frequencies, the curves from the more ventral sites again cross those of the more dorsal sites, levelling off at approximately 40 pulses ($\log_{10}(N) = 1.6$).

One possible scenario that is consistent with these shape changes is that the tip of the electrode moves through a region of high sensitivity as the electrode progresses ventrally. At the most dorsal sites (8.04 mm to 8.36 mm--Figure 12), the stimulation field at the very low currents impinges on an area of high sensitivity, whereas the higher currents impinge on an additional region in which the substrate is much less sensitive. As the electrode is moved (8.52 mm to 8.84 mm), the low currents become less and less effective (relative to the preceding sites), suggesting that the tip of the electrode has passed through and beyond the highly sensitive region. At the same time, because of the movement of the electrode, high

currents now impinge either upon the region that was previously at the tip of the electrode or upon another high sensitivity region.

It is interesting to note that the putative area of maximum sensitivity encountered at the dorsal sites coincides with the electrode moving into the substantia nigra, pars reticulata (SNR), while the levelling off of the more ventral trade-off functions coincides with the electrode moving into the cerebral peduncle.

The hypothesis that the crossing of the trade-off curves at these ventral sites is a function of topography and not of motor contamination of the rat's performance by stimulation in the cerebral peduncle is supported by considering the results of the locus of rise analysis (Figures 40 & 41).

In comparing the data collected from rat PM8 to those obtained from rat PM1 (Figure 8), one notes that the trade-off curves exhibit a similar pattern, but unfortunately, because the number of sites from which data could be collected was less than for rat PM8, one does not know whether the functions at the more ventral sites would have become even more concave. Although the electrode was located more anteriorly than that of PM8, the two tracks are located at the same lateral coordinate (at the edge of the substantia nigra), and the functions taken at the most

ventral site are more concave and again cross over those curves taken at the more dorsal sites.

The third factor which can cause differences to the curves with depth of electrode position is a change in the overall slope of the descending portion. The curves obtained from rat PM10 (Figure 7), show a convergence at I_{min}. That is, at the low frequencies, there is a consistent change in the required current, suggesting that as the electrode was advanced, an area of high sensitivity was approached, and then passed through. At high frequencies, with the exception of the last site tested, the functions all converge. Therefore, the slope of the functions has changed with the movement of the electrode.

At sites within the substantia nigra, pars compacta, the curves are flatter and less steep than at the more dorsal sites. The higher current intensities seem to be more effective (i.e. the curves lie below those of the dorsal sites), but the minimum current required does not differ greatly. This is consistent with the interpretation that in the region that the electrode traverses, the substrate is of similar sensitivity at the immediate area around the tip of the electrode. Farther away from the tip, in the region which higher currents impinge upon, the substrate appears to vary in sensitivity as the electrode is moved.

Changes in the overall slope of the descending portion of the curves were also observed in the data obtained from rat R1 (Figure 11). With the exception of the last site tested, the trade-off curves lie close together at high current intensities, but diverge at I_{min}. Note that the curves also cross one another, although not as dramatically as the data obtained from subject PM8. The curves taken at 8.22 mm and 8.38 mm lie below those obtained at the more dorsal and ventral sites at the low frequencies, and yet at the highest frequencies, they lie between these other curves.

The trade-off curves obtained from subject F4 (Figure 14) show both a change in slope and in shape with changes to electrode position. Note that the curves taken from the last two sites at the border of the SNC cross those taken at the more dorsal sites. It is interesting to compare these data with those of PM10 and R1, where the electrodes are similarly located with respect to the lateral coordinate, and where the curves show a mixture of effects. That is, there is evidence of crossing, shape change, and changes to the slope.

From this discussion, it is readily apparent that the trade-off data gathered in the present experiment offer far greater topographical detail than would be obtained if the sensitivity of the reward substrate had been assessed by a single value of required frequency or current. Moreover,

the anatomical arrangement of the reward-relevant neurons is constrained by the trade-off data. For example, while one might hypothesize many topographical arrangements other than a gradient of changing sensitivity that could yield the orderly pattern of functions obtained from subjects PM11 and F3, there are many which are inconsistent with the results obtained (e.g. a discrete bundle of fibres). Similarly, the pattern of functions collected in rats PM8 and PM1 are inconsistent with a smooth gradient of changing sensitivity, and appear to be due to an abrupt transition through a zone where the substrate is locally very sensitive.

Evaluating Fixed Parameter Methodologies

Perhaps the most important contribution of the present study is that it casts new light on the data collected by previous mapping methods. The method used by Rompré and Miliaressis (1985) consists of estimating the required number at a fixed value of current at each site tested. As discussed previously, the rationale for their method hinges on two basic assumptions concerning the use of a fixed value of current. First, they reason that by holding the current constant, the same size stimulation field will be produced. Therefore, determining the number of times the neurons have to fire to produce a criterion level of behaviour will allow one to make an estimate of the density

of reward-relevant neurons at each site (providing the substrate is homogeneous in all other aspects). Second, frequency was chosen as the scaling variable in order to avoid false negative findings.

In order to be able to generalize from topographical data consisting of a single reward-summation function gathered at a fixed, low value of current, this measure must yield a profile similar to that obtained using other values of current. Such a generalization would rest on the assumption that only the position of the curves changes with the depth of electrode penetration; that is, one would have to assume that the current-number trade-off functions which characterize each site are reasonably parallel to each other. In some cases this assumption is supported by data collected in this study. In general, the depth profiles constructed for subjects with more medial placements (e.g. F3, F1, and PM11) show relatively good agreement over the area traversed by the electrode regardless of whether the trade-off functions are sectioned by current or by pulse number. This finding reflects the observation that only the position of the trade-off functions changes systematically with depth of penetration. Therefore, fixing the value of either the stimulation frequency or intensity need not always yield unrepresentative data; in particular, where the relationship between the scaling variable and the depth of

electrode penetration is not dependent on the choice of the arbitrary fixed value of the independent parameter, then individual reward-summation functions provide an adequate representation.

This conclusion is supported by comparing our data to those of Rompré and Miliaressis (1985). Our data confirm their finding that at the medial placements, the site of maximum sensitivity appears to lie just ventral to the red nucleus in the region of the tip of the medial lemniscus and dorsal to the VTA. Furthermore, in both studies, effectiveness of the stimulation is reduced as the electrode penetrates more ventrally into the region of the VTA proper. The high required current as the electrode tip nears the base of the brain is also consistent with their findings that these sites did not, in general, support self-stimulation at a current of 200 μA.

The similarities in our results can be readily seen by consulting Figures 42 and 43. In these figures, data from the two studies are directly compared. Before discussing this comparison, the format of the figures, and the differences between our methods are briefly discussed. The histological profile on the left hand side of each figure illustrates the profile of sites tested by Rompré and Miliaressis (1985). This data was collected using a double moveable electrode, and therefore, the two subjects selected (824 and 826) each have a medial and a lateral

placement. In Figures 42 and 43, because the comparison concerns only the medial placement, the lateral placement has been removed for clarity. Note that the Rompré and Miliaressis reconstructions are based on the first edition of the Paxinos and Watson stereotaxic atlas (1982), rather than on the second edition which I used. Note also that the increment between the tested sites in the Rompré and Miliaressis study was 0.13 mm.

The histological reconstruction on the right hand side of the figure illustrates the profile of tested sites for a subject in the present experiment. In both reconstructions, sites at which self-stimulation could not be elicited are indicated by open symbols, and are not shown on the accompanying graph.

The graph relates the logarithm of the number of pulses required at 200 μA to the depth, and the data have been transformed as in previous sections. Data from the Rompré and Miliaressis study are approximate and were calculated from their published depth profiles which relate inter-pulse interval to depth.

In Figure 42, a comparison of the results obtained at the medial placement of subject 824 (located at 5.30 mm posterior to bregma) is made with that obtained from subject F3. Although, the placement of the electrode for subject F3 is slightly more lateral than that of subject 824 (medial track), the two profiles are very similar in

Figure 42.

Comparison of topographical data collected by Rompré and Miliaressis (1985) (Subject 824), with that taken from a similar placement in this study (Subject F3). The histological profile on the left side of the figure is used with the permission of Rompré. Note that this reconstruction is based on the first edition of the Paxinos and Watson atlas (1982). On right hand side the histological profile of Subject F3 is shown. Numbers below both profiles refer to the distance posterior to bregma (in mm). The name of each subject appears above each profile, and in the graph key. The graph shows a comparison of the depth profiles obtained in the two studies. The data from F3 consist of the required number at 200 μA calculated by interpolation from the trade-off functions. The data from 824 consist of the inter-pulse interval (train duration = 400 ms, current = 200 μA) at threshold (theta 0) recorded at each site by Rompré and Miliaressis. This has been transformed to the same scale (deviation from minimum value) by approximation from the depth profiles shown in their 1985 publication. Depth measures are based on the scale of the 1982 edition of the Paxinos and Watson atlas.

824

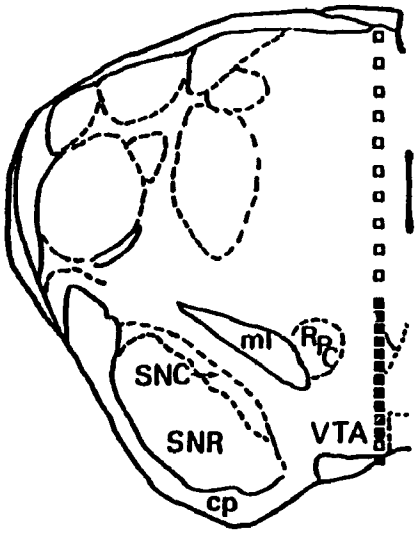

-5.30

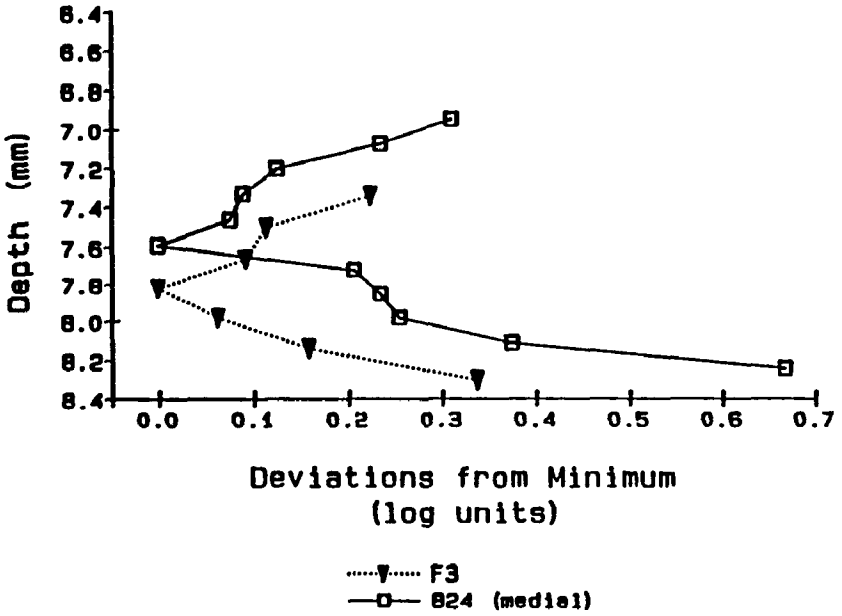

F3

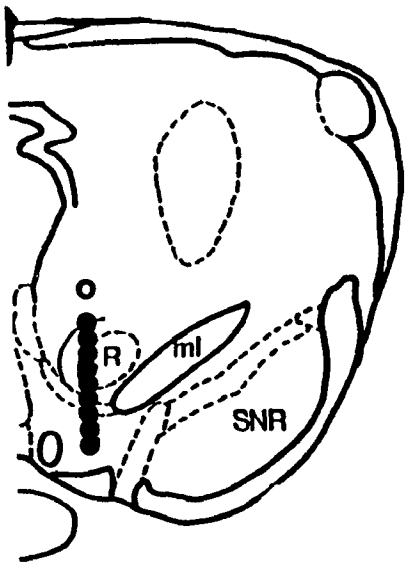

-5.30

shape. Given the differences between the two studies (particularly differences in the reconstruction of the histological profiles), and the likelihood of small histological errors, they show good agreement.

Figure 43 shows a comparison of the results obtained at the medial placement of subject 826 (at 5.80 mm posterior to bregma) with that obtained from subject PM11. Again the electrode track of PM11 is slightly lateral to that of subject 826 (medial track). It should also be noted that the version of the atlas used by Rompré and Miliaressis does not contain a plate corresponding to 5.60 mm posterior to bregma, and it was therefore not available to them when making their histological decisions. Given these histological differences, the two profiles are very similar.

The data from both the present study, and that of Rompré and Miliaressis, contradict the earlier findings of Corbett and Wise (1980) who concluded that self-stimulation in this mesencephalic region was confined to the area of the dopaminergic cell bodies. In this study, self-stimulation was observed at low currents when the electrode was within the red nucleus and the medial lemniscus, as well as in areas both dorsal and ventral to these structures. How much of this discrepancy is due to Corbett and Wise's use of a fixed value of frequency, or to their use of sine-wave stimulation is not known. It is

Figure 43.

Comparison of topographical data collected by Rompré and Miliaressis (1985) (Subject 826), with that taken from a similar placement in this study (Subject PM11). The histological profile on the left side of the figure is used with the permission of Rompré. On the right hand side the histological profile of Subject PM11 is shown. Numbers below both profiles refer to the distance posterior to bregma (in mm). The name of each subject appears above each profile, and in the graph key. The graph shows a comparison of the depth profiles obtained in the two studies. The data from PM11 consist of the required number at 200 μA calculated by interpolation from the trade-off functions. The data from 826 consist of the inter-pulse interval (train duration = 400 ms, current = 200 μA) at threshold (theta 0) recorded at each site by Rompré and Miliaressis. This has been transformed to the same scale (deviation from minimum value) by approximation from the depth profiles shown in their 1985 publication. Depth measures are based on the scale of the 1982 edition of the Paxinos and Watson atlas.

826

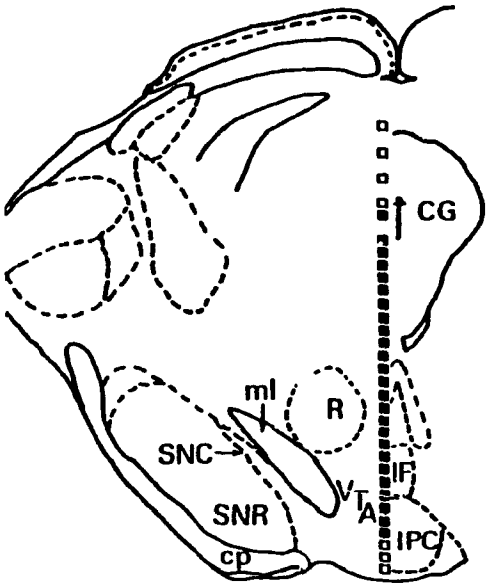

-5.80

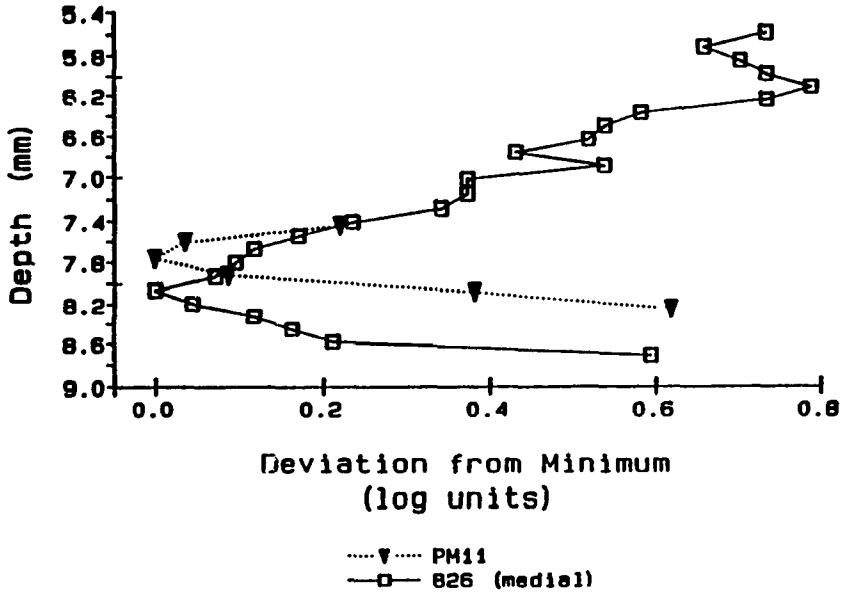

PM11

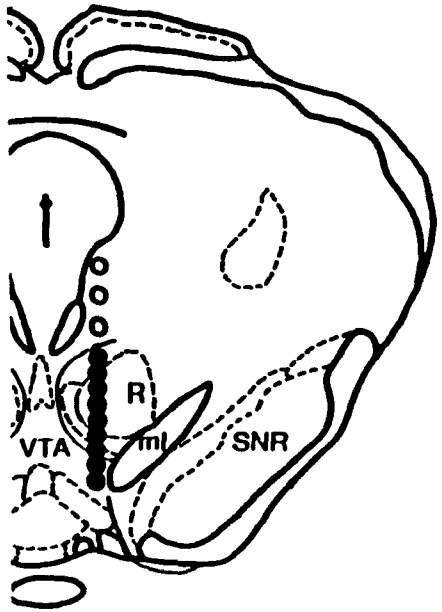

-5.60

interesting to note, however, that our findings support those of Rompré and Miliaressis who like Corbett and Wise, used a fixed stimulation parameter, but employed cathodal square-wave pulses. This same discrepancy between methods which employ the two different wave-forms and curve-shift methodology has also been encountered elsewhere (e.g. for the locus coeruleus--Corbett & Wise, 1979; Rompré & Boye, in press).

The use of fixed currents and pulse numbers is not adequate when the relationship between the curves is more complex. That is, changes in depth are reflected by a change in shape or slope of the functions. When the data of the more lateral placements are considered (Subjects PM1, PM8, R1, and F4), such agreement between depth profiles taken at different levels of the fixed parameter (either current or frequency) is not obtained, particularly for those electrode penetrations that border the substantia nigra (PM8 and PM1). Here, any profile which is purported to represent the relationship between the trade-off functions is dependent on which part of the function is sampled at each site. Thus, depending on the value of the fixed parameter chosen (either current or frequency), different profiles of changing substrate sensitivity with depth are obtained.

Our results from these lateral placements again disagree with those of Corbett and Wise (1980) and Wise

(1981). Self-stimulation was obtained from the SNR in one subject, in contrast to these previous studies which concluded that this structure did not support BSR.

Although Rompré and Miliaressis did not test as lateral a placement as in this study (e.g. PM1 and PM8), two of their most lateral placements are similar to those of subjects R1 and F4, and these are compared in Figures 44 and 45. These figures are of the same format as the previous comparisons for F3 and PM11, but here the lateral placements of subjects 824 and 826 are used. The medial placements have been removed for clarity.

In Figure 44 the depth profile calculated from the trade-off functions obtained from subject R1 is shown. Note that although the curves are displaced from each other, they have the same shape. The displacement could be a function of histological error, as the two atlases differ on the exact depth at which certain structures are located (e.g. the medial lemniscus).

In Figure 45 the depth profile for subject F4 is shown. Note the extremely close overlap in both position and shape between the two studies.

These comparisons support the notion that current-number trade-off data can be used to reliably simulate the results that might have been obtained with fixed parameters. Furthermore, they highlight the contention that anatomical generalizations may be dangerous when based

Figure 44.

Comparison of topographical data collected by Rompré and Miliaressis (1985) (Subject 824), with that taken from a similar placement in this study (Subject R1). The graph shows a comparison of the depth profiles obtained in the two studies. The data from R1 consists of the required number at 200 μA calculated by interpolation from the trade-off functions. The data from 824 consists of the inter-pulse interval (train duration = 400 ms, current = 200 μA) at threshold (theta 0) recorded at each site by Rompré and Miliaressis. This has been transformed to the same scale (deviation from minimum value) by approximation from the depth profiles shown in their 1985 publication. Depth measures are based on the scale of the 1982 edition of the Paxinos and Watson atlas.

824

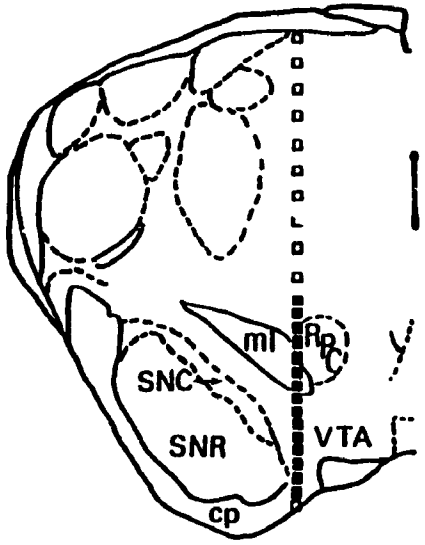

-5.30

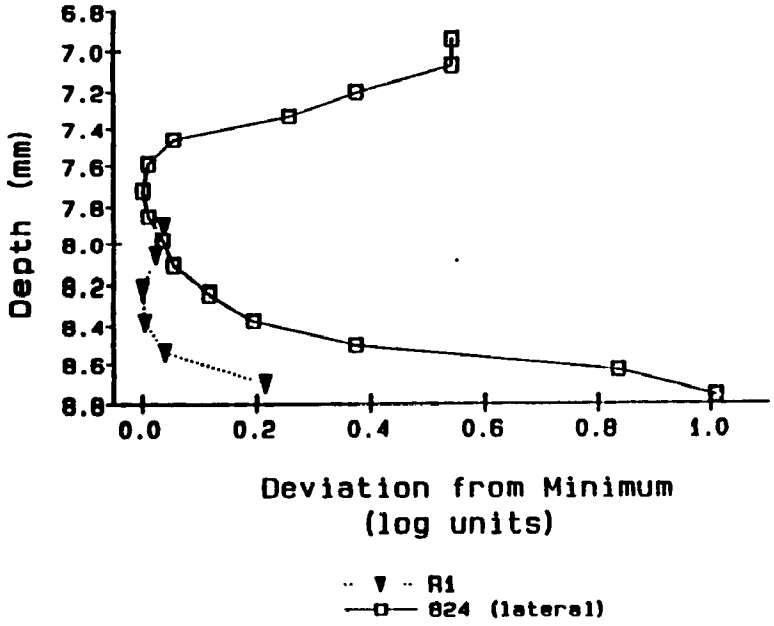

R1

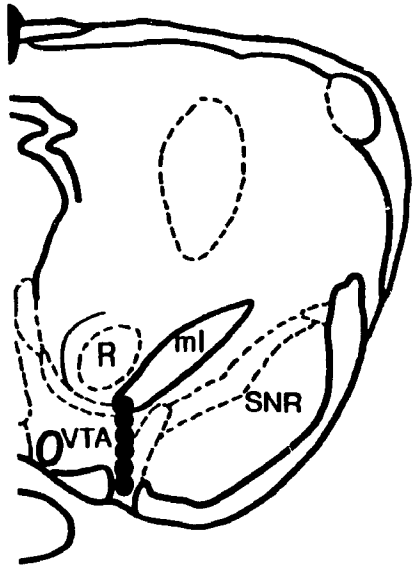

-5.30

Figure 45.

Comparison of topographical data collected by Rompré and Miliaressis (1985) (Subject 826), with that taken from a similar placement in this study (Subject F4). The graph shows a comparison of the depth profiles obtained in the two studies. The data from R1 consists of the required number at 200 μA calculated by interpolation from the trade-off functions. The data from 826 consists of the inter-pulse interval (train duration = 400 ms, current = 200 μA) at threshold (theta 0) recorded at each site by Rompré and Miliaressis. This has been transformed to the same scale (deviation from minimum value) by approximation from the depth profiles shown in their 1985 publication. Depth measures are based on the scale of the 1982 edition of the Paxinos and Watson atlas.

826

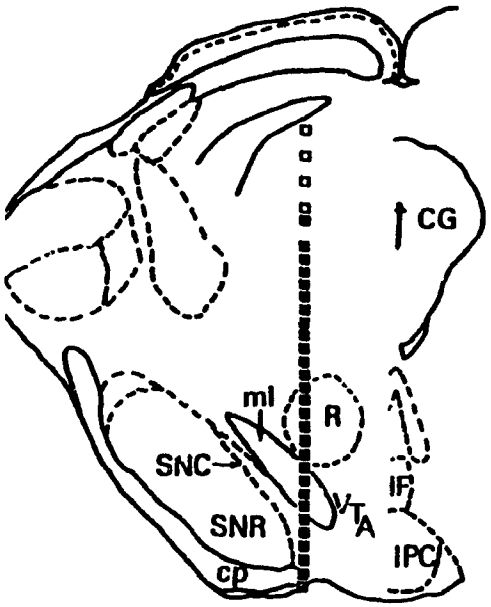

-5.80

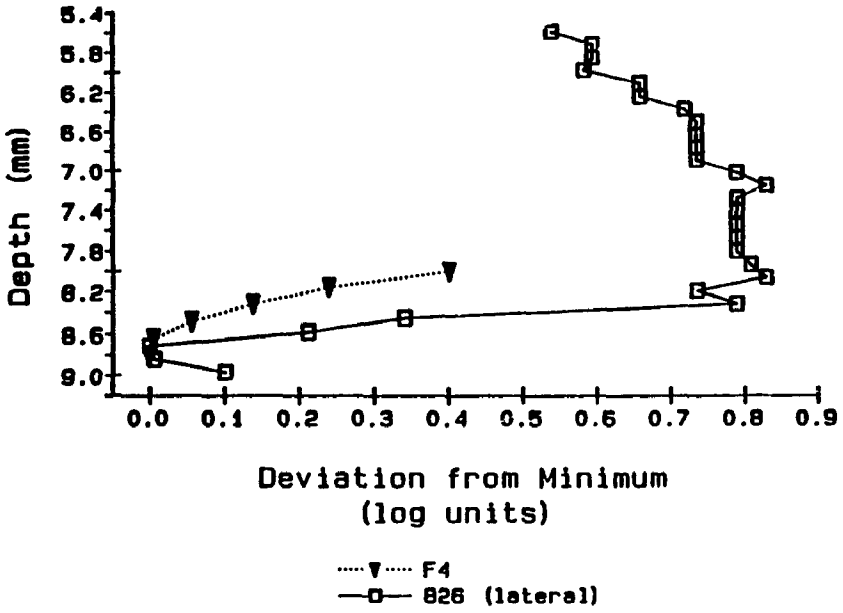

F4

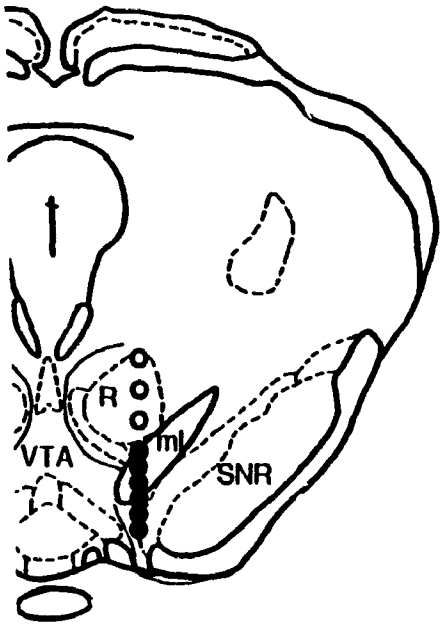

-5.60

on fixed stimulation parameters. In the latter two comparisons, although the trade-off functions change slope and shape with depth of electrode penetration, the depth profiles calculated at 200 μA in the two different studies yield similar conclusions. Therefore, had the present study used a different, but fixed value of current, results very different from those obtained by Rompré and Miliaressis would have been obtained.

Because the purpose of topographical studies is to explore regions in which the substrate for BSR is relatively unknown, there is no way of assessing a priori whether or not one's results will be representative if the value of one of the parameters is fixed. In light of this, it would seem wise to employ trade-off functions, rather than single reward-summation functions, when undertaking topographical investigations.

The Minimum Required Current

Miliaressis et al. (1982) have also proposed that the value chosen for the fixed current should be low so as to achieve high spatial resolution. Following this rationale, the minimum current required to support half-maximal responding at each stimulation site (I_{min}) should theoretically provide the optimal measure of spatial resolution. Indeed, results obtained using I_{min} as the criterion sometimes differed from results obtained at lower

pulse numbers (higher current). One would expect such differences to arise whenever there is an abrupt change in substrate sensitivity over space.

It follows that one may not always be able to generalize from the anatomical profile obtained at a small current. As with the depth profiles calculated for various arbitrarily chosen values of pulse number, the ability to generalize the results obtained at I_{min} to other, higher values of current intensity depends upon how the trade-off functions change with depth (and therefore on the topographical arrangement of the reward-relevant neurons within a region). For those subjects in which the trade-off functions are roughly parallel, the depth profiles constructed using minimum current agree with those calculated for a much higher value of current. However, where the trade-off functions change in slope or functional form with depth, this is not the case.

The ability to generalize from a small value of current addresses the question of why one undertakes a topographical study in the first place. If the goal is to characterize the distribution of the substrate in order to contribute to the application of more powerful psychophysical techniques, then the portion of the curve at high values of current is often at least as interesting as the low current portion. For example, in order to maximize the probability of stimulating common fibres at two sites,

collision studies often employ current intensities well in excess of 200 μA and frequencies as low as 20 Hz. If the topographical data taken at a very low current do not always represent those taken at higher intensities, then they cannot necessarily fulfil the goal of facilitating the application of more powerful techniques.

Although one might be tempted to forego the extended testing required to estimate I_{min} in favour of an abbreviated trade-off function, it should be noted that topographical data which include estimates of I_{min} are crucial to testing any hypothesis of the identity of the reward-relevant neurons in which the spatial distribution of the neurons changes abruptly. Thus, trade-off data which include I_{min} place further constraints upon the possible topographical arrangements of the reward-relevant neurons in a region.

A second, minor point in favour of estimating I_{min}, particularly in the case of rat PM8, is that the double-crossing of the trade-off functions may not have been observed had the very high pulse numbers not been tested in the course of estimating this quantity.

It is important to note however, that although I_{min} may have much value in certain applications, there is one drawback to its use as a general measure of substrate sensitivity; the required current cannot always be obtained at the very high pulse numbers. At sites where decrements

to performance accompany high frequency stimulation, the point at which the trade-off function approaches asymptote cannot be measured.

Practical Considerations of Using the Trade-off Function

Because one purpose of this experiment was to evaluate the effect of fixed parameters on the assessment of substrate sensitivity, I chose to use as many values of pulse number as was necessary to describe the shape of the trade-off function and its asymptote. However, from a visual inspection of the trade-off functions, it is apparent that the number of pulse numbers used could have been considerably reduced while still maintaining an adequate description of the function's form. By reducing the number of rate-intensity functions that are taken, one could also reduce the length of time needed to complete testing on any one site and thus any one subject.

After implantation of an electrode, there are identifiable physiological changes to the tissue surrounding the electrode tip (see Schultz & Willey, 1976, for example). It is possible that if such changes occur each time the electrode is descended, they may contribute to the observed differences between stimulation sites. This problem is inherent to all experiments in which a chronic stimulating electrode is used, however it may pose particular difficulty with moveable electrodes, where new

tissue damage is created with each new movement. In principal, the best solution would be to wait a lengthy period after each movement of the electrode before testing takes place, in order for the tissue to accommodate. Unfortunately, this is impractically time-consuming. Therefore, the best one can do is to try to hold the period of testing at each site as constant as possible.

That testing was terminated for three subjects (F3, F4, and R1), and some data discarded (F4 and R1), demonstrates that current-number functions can change significantly over time, when that time-period exceeds the usual testing period for a single site (i.e. the electrode was not advanced). The hypothesis that such tissue changes may have contributed to the significant changes to the trade-off functions observed for subjects F3, F4, and R1 is supported by the observation that current thresholds taken using the fixed electrode (LH placement) for F3 and F4 remain unchanged two months after the initial training period.

The Effects of Varying Pulse Duration

In determining the current-number trade-off function for each of two different pulse durations, it was predicted that the results might reveal the contribution of reward-relevant neurons of different chronaxie. It has been shown (West & Wolstencroft, 1982) that chronaxie is loosely

correlated with fibre size (e.g. small fibres tend to have longer chronaxies). If so, then differences in the chronaxie of the reward-relevant neurons (reflected in changes to the trade-off functions) may also yield data about the distribution of reward-relevant neurons of different size.

As previously discussed, because the current required to produce a given radius of excitation is reduced when the pulse duration is lengthened, a trade-off function determined at a long pulse duration will be shifted down the ordinate from one determined at a short pulse duration. If the neurons in the region surrounding the electrode tip all have the same chronaxie, or if neurons of different chronaxie are equally distributed in the region, the two trade-off functions will also be parallel to one another (i.e. the function determined at the longer pulse duration will be shifted by the same proportion at all values of frequency). However, the magnitude of the shift may be different for the latter case, where neurons of more than one chronaxie are present. This difference will depend upon the proportion of fibres of long and short chronaxie that are stimulated as the pulse duration is lengthened.

Conversely, if neurons of different chronaxie are clustered in a sub-region within the stimulation field, the trade-off function determined at a longer pulse duration will be shifted down the ordinate from one obtained at a

short pulse duration and may also be of a different shape. This would occur if the proportion of neurons with long and short chronaxies that are stimulated varied with the current as well as with pulse duration.

With the exception of the two subjects with the most laterally-placed electrodes (PM1 and PM8), little difference between the functions gathered at 100 μs and 1000 μs was observed. That is, although the 1000 μs functions were shifted down the ordinate as expected, they were in general of the same functional form as those taken at 100 μs.

For subjects PM8 and PM1, the distribution of the small and large fibres does not seem to have been similar, particularly at the more dorsal sites. This conclusion is supported by the fact that the functions obtained with a pulse duration of 1000 μs are of a different functional form than those obtained at a pulse duration of 100 μs at these more dorsal sites.

When the depth profiles calculated at 100 μs and 1000 μs are examined, differences were again observed only for subjects PM8 and PM1. This would suggest that for most of the placements, the distribution of fibres of different classes did not change radically over the area traversed by the electrode.

The general lack of effect can be explained if (a) the substrate consisted of neurons of similar chronaxie, (b) if

different classes of neurons are present but they are distributed equally, or (c) if the difference between the 100 μs and the 1000 μs pulse was not sufficiently large to preferentially excite any long chronaxie fibres that were present. One option might be to increase the pulse duration at which the data are collected. It is possible that a doubling of the value to 2000 μs may have yielded more disparate results. One should note however that the longer the pulse duration, the more likely it will be that charge build-up at the brain/electrode interface will occur. This would reduce the range of pulse numbers that could be tested at the longer pulse duration even further than in the present study.

Despite the fact that large differences in pulse duration were not observed, manipulation of this variable in future mapping studies should not be abandoned. One cannot know a priori whether the distribution of fibre classes in a region will be homogeneous, nor what pulse duration would be required to fire the different classes if it were not. In some cases, there may even be reason to believe that the use of a longer duration pulse is a necessary manipulation. For example, in the anterior basal forebrain it has been suggested that the reward substrate may contain fibres which are less excitable at the short pulse durations normally used (Bielajew, Thrasher & Fouriezos, 1987; Fouriezos, Walker, Rick & Bielajew, 1987).

Any systematic topographical investigation of this region should certainly include the manipulation of this variable.

Conclusions

Based on the results of the present experiment it can be concluded that collecting current-number trade-off functions at different locations along the track of a moveable electrode provides a richer portrait of changing substrate sensitivity than do single estimates of either the required current or number. Because a range of values of both current and frequency are tested, the data provide guidance for planning future experiments in which many different levels of each parameter may be employed (e.g. collision studies). Moreover, trade-off data collected at multiple sites using a moveable electrode place tighter constraints upon the formulation of models of the topography of the BSR substrate than do data collected using single estimates of either the required current or frequency.

It would seem however, that an abbreviated form of the function taken in this study would be sufficient to capture much of the detail observed in the present study and yet reduce the time spent on data collection. In employing an abbreviated version of the method used here, it is recommended that one reduce the number of frequencies tested (the fixed variable), and continue to use current as the scaling variable. The range of frequencies at which rate-intensity functions are collected should be chosen so

as to span the largest portion of the trade-off curve as is feasible, thereby ensuring that one does not inadvertently miss important information (e.g. crossing of the trade-off function at higher frequencies).

Finally, although no dramatic differences were observed between the two pulse duration conditions, it is recommended that the manipulation of this variable be included in future mapping studies. Furthermore, although the number of frequencies that could be tested would be reduced, a pulse duration of greater than 1000 μs should be considered.

References

Bielajew, C., Jordan, C., Ferme-Enright, J., & Shizgal, P. (1981). Refractory periods and anatomical linkage of the substrates for lateral hypothalamic and periaqueductal gray self-stimulation. Physiology & Behavior, 27, 95-104.

Bielajew, C., Lapointe, M., Kiss, I., & Shizgal, P. (1982). Absolute and relative refractory periods of the substrates for lateral hypothalamic and ventral midbrain self-stimulation. Physiology & Behavior, 27, 125-132.

Bielajew, C., & Shizgal, P. (1982). Behaviorally derived measures of conduction velocity in the substrate for rewarding medial forebrain bundle stimulation. Brain Research, 237, 107-119.

Bielajew, C., & Shizgal, P. (1986). Evidence implicating descending fibers in self-stimulation of the medial forebrain bundle. The Journal of Neuroscience, 6, 919-929.

Bielajew, C., Thrasher, A., & Fouriezos, G. (1987). Self-stimulation sites in the lateral hypothalamic and lateral preoptic areas are functionally connected. Canadian Psychological Association Abstracts, 28, Abstract No. 36.

Boye, S. (1988). Anatomical and physiological characteristics of mesencephalic and pontine substrates of reward. Unpublished master's thesis, Concordia University, Montréal, Québec.

Corbett, D., & Wise, R. A. (1979). Intracranial self-stimulation in relation to the ascending noradrenergic fiber systems of the pontine tegmentum and caudal midbrain: A moveable electrode mapping study. Brain Research, 177, 423-436.

Corbett, D., & Wise, R. A. (1980). Intracranial self-stimulation in relation to the ascending dopaminergic systems of the midbrain: A moveable electrode mapping study. Brain Research, 185, 1-15.

Crow, T. J. (1972). A map of the rat mesencephalon for electrical self-st mulation. Brain Research, 36, 265-273.

Edmonds, D. E., & Gallistel, C. R. (1974). Parametric analysis of brain stimulation reward in the rat: III. Effect of performance variables on the reward summation function. Journal of Comparative and Physiological Psychology, 87, 876-883.

Edmonds, D. E., Stellar, J. R., & Gallistel, C. R. (1974). Parametric analysis of brain stimulation reward in the rat: II. Temporal summation in the reward system. Journal of Comparative and Physiological Psychology, 87, 860-869.

Fouriezos, G., & Emdin. K. (1988). Reinforcement schedules shift self-stimulation rate-frequency functions. Canadian Psychological Association Abstracts, 29, Abstract No. 259.

Fouriezos, G., Walker, S., Rick, J., & Bielajew, C. (1987). Refractoriness of neurons mediating intracranial self-stimulation in the anterior basal forebrain. Behavioural Brain Research, 24, 73-80.

Gallistel, C. R. (1975). Motivation as central organizing process: The psychophysical approach to its functional and neurophysiological analysis. In J. K. Cole & T. B. Sonderegger (Eds.), Nebraska Symposium on Motivation, Vol 22 (pp. 183-250). Lincoln: University of Nebraska Press.

Gallistel, C. R. (1978). Self-stimulation in the rat: Quantitative characteristics of the reward pathway. Journal of Comparative and Physiological Psychology, 92, 977-998.

Gallistel, C. R., Shizgal, P., & Yeomans, J. S. (1981). A portrait of the substrate for self-stimulation. Psychological Review, 88, 228-273.

Gallistel, C. R., Stellar, J. R., & Bubis, E. (1974). Parametric analysis of brain stimulation reward in the rat: I. The transient process and the memory-containing process. Journal of Comparative and Physiological Psychology, 87, 848-859.

Gratton, A., & Wise, R. A. (1983). Brain stimulation reward in the lateral hypothalamic medial forebrain bundle: Mapping boundaries and homogeneity. Brain Research, 278, 25-30.

Gratton, A., & Wise, R. A. (1988). Comparisons of connectivity and conduction velocities for medial forebrain bundle fibers subserving stimulation-induced feeding and brain stimulation reward. Brain Research, 438, 264-270.

Harris, G. W. (1948). Electrical stimulation of the hypothalamus: A mechanism of neural control of adenohypophysis. Journal of Physiology (London), 107, 418-429.

Hess, W.R. (1957). The functional organization of the diencephalon. New York: Grune & Stratton.

Hodos, W., & Valenstein, E. S. (1962). An evaluation of response rate as a measure of rewarding intracranial stimulation. Journal of Comparative and Physiological Psychology, 55, 80-84..

Liebman, J. M., Mayer, D. J., & Liebeskind, J. C. (1973). Self-stimulation loci in the midbrain central gray matter of the rat. Behavioral Biology, 9, 299-306.

MacMillan, C. J., Simantirakis, P., & Shizgal, P. (1985). Self-stimulation of the lateral hypothalamus and ventrolateral tegmentum: Excitability characteristics of the directly stimulated substrates. Physiology & Behavior, 35, 711-723.

Matthews, G. (1977). Neural substrate for brain stimulation reward in the rat: Cathodal and anodal strength-duration properties. Journal of Comparative and Physiological Psychology, 91, 858-874.

Miliaressis, E. (1977). Serotonergic basis of reward in median raphe of the rat. Pharmacology, Biochemistry, and Behavior, 7, 177-180.

Miliaressis, E. (1981). A miniature, moveable electrode for brain stimulation in small animals. Brain Research Bulletin, 7, 715-718.

Miliaressis, E., & Malette, J. (1987). Summation and saturation properties in the rewarding effect of brain stimulation. Physiology & Behavior, 41, 595-604.

Miliaressis, E., & Rompré, P. P. (1987). Effects of concomitant motor reactions on the measurement of rewarding efficacy of brain stimulation. Behavioral Neuroscience, 101, 827-831.

Miliaressis, E., Rompré, P. P., & Durivage, A. (1982). Psychophysical method for mapping behavioral substrates using a moveable electrode. Brain Research Bulletin, 8, 693-701.

Miliaressis, E., Rompré, P. P., Laviolette, P., Philipe, L., & Coulombe, D. (1986). The curve-shift paradigm in self-stimulation. Physiology & Behavior, 37, 85-91.

Mundl, W. J. (1980). A constant-current stimulator. Physiology & Behavior, 24, 991-993.

Mundl, W. J. (1982). Amplitude of constant-current pulses can be preset. Behavior Research Methods & Instrumentation, 14, 459-460.

Murray, B. (1988). The effects of anterior medial forebrain bundle lesions on self-stimulation of the lateral hypothalamus and ventral tegmental area. Unpublished master's thesis, Concordia University, Montréal, Québec.

Olds, J. (1956). A preliminary mapping of electrical reinforcing effects in the rat brain. Journal of Comparative and Physiological Psychology, 49, 281-285.

Olds, J., & Milner, P. (1954). Positive reinforcement produced by electrical stimulation of septal area and other regions of rat brain. Journal of Comparative and Physiological Psychology, 47, 419-427.

Paxinos, G., & Watson, C. (1982). The rat brain in stereotaxic coordinates (1st ed.). Sydney: Academic Press.

Paxinos, G., & Watson, C. (1986). The rat brain in stereotaxic coordinates (2nd ed.). Sydney: Academic Press.

Rompré, P. P. (1984). Localisation et caractéterisation fonctionelle des éléments nerveux mésencéphaliques et protubérantiels responsables du comportement d'autostimulation intracérébrale chez le rat. Doctoral dissertation, University of Ottawa, Ontario.

Rompré, P. P., & Boye, S. (in press). Localization of reward-relevant neurons in the pontine tegmentum: A moveable electrode mapping study. Brain Research.

Rompré, P. P., & Miliaressis, E. (1985). Pontine and mesencephalic substrates of self-stimulation. Brain Research, 359, 246-259.

Rompré, P. P., & Miliaressis, E. (1987). Behavioral determination of refractory periods of the brainstem substrates of self-stimulation. Behavioural Brain Research, 23, 205-219.

Routtenberg, A. (1971). Forebrain pathways of reward in Rattus norvegicus. Journal of Comparative and Physiological Psychology, 75, 269-276.

Routtenberg, A., & Malsbury, C. (1969). Brainstem pathways of reward. Journal of Comparative and Physiological Psychology, 68, 22-30.

Schenk, S., Prince, C., & Shizgal, P. (1985). Spatio-temporal integration in the substrate for self-stimulation of the prefrontal cortex. Physiology & Behavior, 35, 303-306.

Schenk, S., & Shizgal, P. (1982). The substrates for lateral hypothalamic and medial pre-frontal cortex have different refractory periods and show poor spatial summation. Physiology & Behavior, 28, 133-138.

Schenk, S., & Shizgal, P. (1985). The substrates for self-stimulation of the lateral hypothalamus and medial prefrontal cortex: A comparison of strength-duration characteristics. Physiology & Behavior, 34, 943-949.

Schindler, D. C. (1983). Spatial and temporal integration in the substrate for self-stimulation of the lateral hypothalamus in the rat. Unpublished master's thesis, Concordia University, Montréal, Québec.

Schultz, R. L., & Willey, T. J. (1976). The ultrastructure of the sheath around chronically implanted electrodes in brain. Journal of Neurocytology, 5, 621-642.

Shizgal, P. (1976). Electrical brain stimulation in the rat: differentiation of temporal integration characteristics in the substrates for the rewarding and aversive effects (Doctoral dissertation, University of Pennsylvania, 1975). Dissertation Abstracts International, 36, 6422B.

Shizgal, P. (in press). Toward a cellular analysis of intracranial self-stimulation: contributions of collision studies. Neuroscience and Biobehavioral Reviews.

Shizgal, P., Bielajew, C., Corbett, D., Skelton, S., & Yeomans, J. (1980). Behavioral methods for inferring anatomical linkage between rewarding brain stimulation sites. Journal of Comparative and Physiological Psychology, 94, 227-237.

Shizgal, P., Bielajew, C., & Rompré, P. P. (1988). Quantitative characteristics of the directly stimulated neurons subserving self-stimulation of the medial forebrain bundle: Psychophysical inference and electrophysiological measurement. In M. L. Commons, R.M. Church, J. R. Stellar, & A. R. Wagner (Eds.), Quantitative analyses of behaviour: Vol. 7. Biological determinants of reinforcement (pp. 59-85). New Jersey: Lawrence Erlbaum.

Shizgal, P., & Schindler, D. (1982). Reinterpretation of strength-duration curves for neurons mediating brain stimulation reward. Paper presented at the annual meeting of the Canadian Psychological Association.

Shizgal, P., & Murray, B. (1989). Neuronal basis of intracranial self-stimulation. In J. M. Liebman & S. J. Cooper (Eds.), The neuropharmacological basis of reward (pp. 106-163). Oxford: Clarendon Press.

von Holst, E., & von Saint Paul, U. (1962). Electrically controlled behavior. Scientific American, 206 (3), 50-59.

Waraczynski, M., Stellar, J. R., & Gallistel, C. R. (1987). Reward saturation in medial forebrain self-stimulation. Physiology & Behavior, 41, 585-593.

West, D. C., & Wolstencroft, J. H. (1982). Strength-duration characteristics and non-myelinated bulbospinal axons in the cat spinal cord. Journal of Physiology (London), 337, 37-50.

Wine, J. J., & Krasne, F. B. (1972). The organization of escape behaviour in the crayfish. Journal of Experimental Biology, 56, 1-18.

Wise, R. A. (1971). Individual differences in effects of hypothalamic stimulation: The role of stimulation locus. Physiology & Behavior, 6, 569-572.

Wise, R. A. (1972). Spread of current from monopolar stimulation of the lateral hypothalamus. American Journal of Physiology, 223, 545-548.

Wise, R. A. (1976). Moveable electrode for chronic brain stimulation in the rat. Physiology & Behavior, 16, 105-106.

Wise, R. A. (1981). Intracranial self-stimulation: mapping against the lateral boundaries of the dopaminergic cells of the substantia nigra. Brain Research, 213, 190-194.

Yeomans, J. (1979). The absolute and relative periods of self-stimulation. Pnysiology & Behavior, 22, 911-919.

Yeomans, J. S., Pearce, R., Wen, D., & Hawkins, R. D. (1984). Mapping midbrain sites for circling using current-frequency trade off data. Physiology & Behavior, 32, 287-294.

Appendix A

An example of the schedules of pulse numbers at which rate-intensity functions were taken (train duration = 400 ms; pulse duration = 100 μs) for all subjects:

Schedule 1	Schedule 2
8	10
12	15
19	23
29	37
46	58
72	91
114	143
160	180
201	201
180	160
143	114
91	72
58	46
37	29
23	19
15	12
10	8

An example of the schedules of pulse numbers at which rate-intensity functions were taken (train duration = 400 ms; pulse duration = 1000 μs) for subjects PM1, PM8, PM10, and PM11:

Schedule 1	Schedule 2
7	8
10	12
13	15
17	21
26	33
41	41
33	26
21	17
15	13
12	10
8	7

An example of the schedules of pulse numbers at which rate-intensity functions were taken (train duration = 400 ms; pulse duration = 1000 μs) for subjects F1, F3, F4, and R1:

Schedule 1	Schedule 2
7	8
10	12
15	17
19	21
23	29
37	41
41	37
29	23
21	19
17	15
12	10
8	7